ISTANBUL TECHNICAL UNIVERSITY ★ GRADUATE SCHOOL OF SCIENCE ENGINEERING AND TECHNOLOGY

CHARACTERISTICS AND WEAR PERFORMANCE OF NITRIDED TITANIUM ALLOYS

Ph.D. THESIS

Farid SIYAHJANI
(506082404)

Department of Metallurgical and Materials Engineering

Metallurgical and Materials Engineering Program

Thesis Advisor: Prof. Dr. Hüseyin ÇİMENOĞLU

NOVEMBER 2015

İSTANBUL TEKNİK ÜNİVERSİTESİ ★ FEN BİLİMLERİ ENSTİTÜSÜ

NİTRÜRLENMİŞ TİTANİYUM ALAŞIMLARIN KARAKTERİSTİĞİ VE AŞINMA DAVRANIŞLARI

DOKTORA TEZİ

Farid SIYAHJANI
(506082404)

Metalurji ve Malzeme Mühendisliği Anabilim Dalı

Metalurji ve Malzeme Mühendisliği Programı

Tez Danışmanı: Prof. Dr. Hüseyin ÇİMENOĞLU

KASIM 2015

Farid Siyahjani, a **Ph.D.** student of ITU **Graduate School of Science, Engineering and Technology** student ID **506082404**, successfully defended the **dissertation** entitled "**CHARACTERISCTICS AND WEAR PERFORMANCE OF NITRIDED TITANIUM ALLOYS**", which he prepared after fulfilling the requirements specified in the associated legislations, before the jury whose signatures are below.

Thesis Advisor :	**Prof. Dr. Hüseyin ÇİMENOĞLU** Istanbul Technical University	.....
Jury Members :	**Prof. Dr. Eyüp Sabri KAYALİ** Haliç University	.....
	Prof. Dr. Sakin ZEYTİN Sakarya University	.....
	Prof. Dr. Erdem ATAR Gebze Technical University	.....
	Prof. Dr. Murat BAYDOĞAN Istanbul Technical University	.....

Date of Submission : 14 September 2015
Date of Defense : 5 November 2015

FOREWORD

I give my sincere thanks to my supervisor, Prof. Dr. Hüseyin ÇİMENOĞLU for his encouragement, kind guidance and support throughout the whole study period.

I also would like to thank Assoc. Prof. Dr. Erdem ATAR, Asst. Prof. Dr. Hasan GÜLERYÜZ and Assoc. Prof. Dr. Murat BAYDOĞAN for their advices and help in many aspects of this research.

I would like to thank M.Sc. Amir MOTALLEBZADE and M.Sc. Faiz MUHAFFEL who as good friends were always willing to help me.

Many thanks must be made also to my parents and especially my wife, Şenay, for all their encouragements and supports which gave me endless enthusiasm and power through my hours of study and work.

September 2015

Farid Siyahjani
(M.Sc)

TABLE OF CONTENTS

Page

ABBREVIATION

BCC **:** Body-Centered Cubic
CVD **:** Chemical Vapor Deposition
CP **:** Commercial Pure
EDX **:** Energy Dispersive X-ray
FC **:** Friction Coefficient
FCC **:** Face-Centered Cubic
IZ **:** Intermediate Zone
LOM **:** Light Optic Microscopy
NDZ **:** Nitrogen Diffusion Zone
PVD **:** Physical Vapor Deposition
RWR **:** Relative Wear Resistance
SEM **:** Scanning Electron Microscopy
WT **:** Wear Track
XRD **:** X-Ray Diffractometer

LIST OF TABLES

Page

LIST OF FIGURES

Pages

CHARACTERISTICS AND WEAR PERFORMANCE OF NITRIDED TITANIUM ALLOYS

SUMMARY

Titanium and its alloys are used in the aerospace industry, chemical applications, architectural areas, sports equipment industry, biomedical applications, power plant industries, transportation, marine and automobile industry. Properties such as high strength, low density and enhanced corrosion resistance are the most important advantages of titanium alloys for these engineering applications. On the other hand, the most unfavorable feature of titanium is the poor tribological properties such as wear resistance; hence, the usage of titanium alloys is limited with wear related applications. Since gas nitriding is a very simple, economical and most used surface treatment method which has been used for many years, present study focuses on gas nitriding of titanium and its alloys conduced with the aim of improving the surface hardness and wear resistance by forming titanium nitride (TiN) layer and a nitrogen diffusion zone (NDZ) beneath it. In nitriding process, in addition to treatment time and temperature, chemical composition of titanium alloys could have significant influence on the characteristics of the nitrogen exposed surfaces. Therefore, it is needed to have further studies on different classes and grades of titanium alloys to investigate the effect of chemical composition on the characteristics of nitrided surfaces.

This study focuses on characteristics of commercial purity grade titanium (Cp-Ti Grade 4) and titanium alloys (Ti6Al4V and Ti6Al7Nb) after gas nitriding at 950, 1120 and 1250 °C for 3, 7 and 12 h. The objective of this study can be summarized as investigation of microstructural features, nitriding kinetics (based on the weight changes and thickness of the grown layers), hardness and tribological performances of nitrogen exposed surfaces.

As the result of the nitriding process, the surface appearances of the samples changed to golden color upon formation of a TiN layer. As a general trend higher nitriding temperatures and longer exposure times favored formation of thicker TiN layer. However, XRD analyses conducted on Cp-Ti revealed that nitriding temperature 950°C did not cause complete covering of the surface with TiN layer unlike titanium alloys. Microscopic examinations revealed the formation of two layers consisting of TiN and NDZ on Cp-Ti, while three layers, including TiN, Intermediate Zone (IZ) and NDZ, were developed on nitrogen-exposed surfaces of Ti6Al6V and Ti6Al7Nb alloys. Energy dispersive X-ray spectroscopy (EDX) equipped scanning electron microscopic (SEM) surveys showed that IZ has a wavy appearance and formed as a thin layer upon enrichment by aluminum. In the case of Cp-Ti, the interface between TiN layer and NDZ was straight without any evidence of changes in composition. Kinetic studies conducted on the nitrided samples revealed that presence of alloying elements in the substrate caused higher activation energy for diffusion of nitrogen. In this respect, higher nitrogen diffusion activation energy of titanium alloys as

compared to Cp-Ti can be attributed to IZ formation as the result of repelling of aluminum atoms from the growing TiN layer.

As the nitriding temperature and time increase, TiN layer tend to be more porous and exhibit poor adhesion characteristics. In general, TiN layers formed at nitriding temperature of 950 °C exhibited better adhesion performance than those formed at 1120 and 1250 °C.

Results of the cross-sectional microhardness measurements and wear tests showed that nitriding process is very beneficial to enhance the hardness and wear resistance of the examined samples as compared to their as-received states. In accordance with adhesion characteristics of the TiN layer nitriding temperature of 950°C provided excellent wear resistance for the examined titanium alloys. The best wear performance of Cp-Titanium was obtained after nitriding at 1120 ºC for 7 hours.

NİTRÜRLENMİŞ TİTANİYUM ALAŞIMLARIN KAREKTERİZASYON VE AŞINMA DAVRANIŞLARI

ÖZET

Bu tezde nitrürleme süreci, titanyum ve titanyum alaşımları üzerinden anlatılmıştır. Titanyum ve titanyum alaşımları hafif olduklarından dolayı birçok teknolojik alanda kullanılmaktadırlar. Kullanılan alanlardan bazıları kimya endüstrisi, uzay endüstrisi, biyomedikal uygulamalar, gemi inşaatı ve enerji sanayi olarak belirtilebilir. Hafif ve yüksek dayanımlı olan bu malzemelerin birçok mühendislik uygulaması, yüzey modifikasyonu ile sağlanmaktadır.

Son zamanlarda titanyum alaşımlarının mekanik özelliklerini iyileştirmek ve kullanım alanlarını arttırmak için çeşitli araştırmalar yapılmaktadır. Titanyumun öne çıkan özellikleri, yüksek mukavemeti, yüksek korozyon ve erozyon dayanımı ve biyouyumluluğudur. Titanyumun düşük aşınma dayanımı ve düşük yüzey sertliği gibi yüzey özellikleri ise dezavantaj olarak kullanım alanını kısıtlamaktadır. Bu kısıtlamaları gidermek için en basit ve ekonomik yöntem gaz nitrasyonudur. Bu yöntem uzun yıllarca demir ve demir alaşımları üzerinde kullanılmıştır ve günümüzde de titanyum üzerinde yaygın olarak kullanılan yüzey modifikasyonu yöntemlerden biridir.

Titanyum alaşımları üstün özellikleri sayesinde, birçok mühendislik alanı ve uygulamasında kullanılmaktadır fakat yeni uygulama alanları yaratılması için ileri araştırma ve çalışmalar gerekmektedir. Bu çalışma kapsamında, titanyumun farklı kompozisyonları (Cp-grade 4, Ti6Al4V ve TiAl7Nb) üzerinde gaz nitrasyonu yapılmıştır.

CP-Ti ve Ti6Al4V alaşımı, yüksek biyouyumluluğu ve sahip olduğu koruyucu pasif oksit film sayesinde yüksek korozyon direnci göstermektedir, bunun yanısıra yüksek mekanik özellikleri ile de öne çıkan bir implant malzemesidir. Son zamanlarda ise, vanadyumun toksik etkisinden dolayı, vanadyum içermeyen Ti6Al7Nb alaşımı üretilmiştir.

Titanyumun olumsuz özelliklerin iyileştirilmesi için titanyuma uygulanabilecek çeşitli yüzey modifikasyon tekniklerini ise üç grupta toplanabilir; Bunlar, kaplama yöntemleri, yüzeyin kimyasal özelliklerini değiştirmeden yapısını değiştiren yöntemler ve yüzeyin kimyasal özelliklerini değiştirerek yeni ve farklı fazlar içeren bir yüzey tabakası elde etme yöntemleridir. Bu teze konu olan yüzey modifikasyon yöntemi, üçüncü gruba dahil olan gaz nitrürleme yöntemidir.

Nitrojen difüzyonu sonucu oluşan nitrür tabakası sayesinde, titanyum ve titanyum alaşımlarının yüzey sertlikleri ve aşınma dirençleri arttırılmıştır. Nitrojenin difüzyonu ile birlikte, malzemenin yüzeyinde katı eriyik oluşmaktadır ve bundan dolayı yüzey sertliği artmaktadır.

Gaz nitrürleme yöntemi, termokimyasal bir yöntemdir. İlgili metal, yüksek sıcaklığa çıkarıldıktan sonra saf azot ya da amonyum gazı ortamında belli bir süre boyunca ısıl işleme tabi tutulur. Bu süreçte, yüzeydeki atomların mobilitesi artar, titanyum yüzeyi

arayer difüzyonuna daha müsait hale gelir ve azotun arayer difüzyonu sonucunda titanyum nitrür fazı oluşur.

Bu çalışmada, titanyum alaşımları 950, 1120 ve 1250 derece sıcaklıkta ve farklı sürelerde (3, 7 ve 12 saat) nitrürlenmiştir. Çalışma kapsamında, nitrasyon kinetiği, malzemenin ağırlık değişimi ve nitrür tabakalarının kalınlık değişimi ile hesaplanmıştır. Titanyumun yüzey özelliklerini geliştirmek için termokimyasal yöntem uygulanmıştır. Bu işlemin sonucunda titanyumun gri yüzeyi, titanyum nitrürün karakteristik özelliklerinden olan altın rengine dönüşmüştür. Ayrıca titanyum nitrürün oluşumu X-ray cihazı ile de tespit edilmiştir.

Faz dönüşüm sıcaklığı altında yapılan nitrürleme çalışmalarında ise CP-Ti yüzeyi nitrür tabakası ile tamamen kaplanmamışken, alüminyum içeren titanyum alaşımlarının yüzeyi tamamen nitrür ile kaplanmaktadır.

Bilindiği gibi titanyum ve titanyum alaşımlarının nitrojen ile reaksiyon verme eğilimi yüksektir, özellikle sıcaklık ve zamanın artması ile de bu malzemeler nitrojen atmosferinde nitrojen ile bileşik oluşturmaktadır. Önceki araştırmalarda sunulduğu üzere, titanyum ve alaşımlarının yüzeyinde oda sıcaklığında titanyum oksit bulunmaktadır. Sıcaklığın artması ile nitrojen atomları oksit atomları ile yer değiştirmektedir.

Faz dönüşüm sıcaklığının üzerinde ise tüm numuneler tamamen nitrür tabakası ile kaplanmıştır. Yüksek sıcaklıkta, titanyumun alfa yapısı beta titanyuma dönüşmektedir. Azot difüzyonunun başlaması ile birlikte faz dönüşüm sıcaklığı düşmekte ve nitrür tabakasının altında yeniden alfa tabaka özelliğine sahip NDZ tabakası oluşmaktadır. Optik mikroskop çalışmalarında, Cp-Ti yüzeyinde çift katlı bir tabaka oluştuğu görülmektedir. Üst tabakada nitrür ve alt tabakada ise nitrojenin difüzyon ettiği alfa tabakası bulunmaktadır.

Beta titanyum fazının nitrürleme yapıldığı sırada gösterdiği dönüşümler aşağıdaki şekilde özetlenebilir;

1- Azotun beta titanyumda çözünmesi ve katı çözelti oluşturması.

2- Nitrojen ile zenginleşmiş yüzeyde beta titanyumun alfa titanyuma dönüşüp NDZ (nitrojen diffusion zone) oluşması.

3- Alfa titanyumda nitrojen konsantrasyonunun yeterince artması sonucu altın renginde nitrür tabakasının oluşması ve alüminyum içeren titanyum alaşımlarında ise ara tabaka oluşması.

Alüminyum içeren titanyum alaşımları üzerinde yapılan optik mikroskop incelemelerinde, nitrür tabakası ve NDZ tabakası ortasında IZ adı verilen bir orta tabaka oluştuğu gözlemlenmektedir. Taramalı elektron mikroskobu bünyesinde bulunan enerji dağılım spektrometre analizlerinde bu tabakanın yüksek alüminyum içerdiği tespit edilmiştir. Bilindiği üzere, nitrür tabakası içinde alüminyum tutunamadığı için alüminyum alt tabakalara itilmektedir ve IZ tabakası oluşumuna sebep olmaktadır. Aktivasyon enerjisi hesaplandığında nitrür tabakasının büyümesini kontrol eden parametreler nitrojenin beta fazındaki difüzyonu ve alüminyumun alfa fazındaki difüzyon hızıdır.

Numunelerin kesitleri EDX ve EPMA yöntemleri ile incelendiğinde IZ ara tabakasının alüminyum ile zenginleşmiş olduğu, vanadyum ve niyobyum elementlerinin ise beta fazında çözünüp malzemelerin iç kısımlarına doğru nufüz edip genellikle tane sınırlarına yerleştiği gözlemlenmektedir.

Sıcaklığın ve zamanın artması ile malzemede bulunan nitrür tabakası, ara tabaka ve NDZ tabakasının büyüdüğü tespit edilmiştir. Bu büyüme ile birlikte nitrür tabakasının pürüzlülüğü de artmaktadır. Dönüşüm sıcaklığının altında nitrürlenmiş malzemelerin yüzeyinde yapılan Rockwell C yapışma testi sonucunda, nitrür tabakasının yüzeye daha iyi yapıştığı gözlemlenmektedir. Dönüşüm sıcaklığının üzerinde yapılan nitrürlemelerde nitrür tabakasının basınç ve aşınma sırasında kırılıp yüzeyden kopduğu görülmektedir.

Titanyum numunelere kesitten 50 g yük ile uygulanan sertlik testi sonucunda, titanyum nitrür tabakasının sertliğinin iç kısımdan yüzeye arttığı tespit edilmiştir. Elde edilen sonuçlara göre, sıcaklık ve işlem süresi arttıkça sertlik artmaktadır. Malzemenin yüzeye yakın kısımlarında sertliğin ise en yüksek sertliğe ulaşılmış ve 2000-2500 HV civarında olduğu tespit edilmiştir.

Nitrürleme yöntemi malzemenin aşınma direncini çok büyük ölçüde iyileştirmektedir. Yapılan aşınma testleri sonucunda, Cp-Ti 1120 derecede ve 7 saat nitrürleme sonucunda en iyi aşınma dayanımı performansı gösterdiği saptanmıştır. Alüminyum içeren titanyum alaşımlarını ise en iyi aşınma dayanımını, faz dönüşüm sıcaklığının altında yani 950 derecede 3 saat nitrürleme şartlarında göstermişlerdir. Aşınma yüzeyi incelendiğinde, çok ince bir izi ve hafif parlamış bir yüzey görülmektedir. Genel olarak aşınma için tespit edilen mekanizma abrasif aşınmadır. Aşınma testleri sonucunda, alüminyum içeren titanyum alaşımlarının malzemenin aşınma direncini 300 kata kadar arttığı gözlemlenmektedir.

1. INTRODUCTION

1.1 Classification of Titanium Alloys and Their Applications

Titanium was discovered in 1791 by William Gregor, a British chemist and mineralogist, who produced titanium from “ilmenite”. Four years after this discovery, a chemist from Berlin named Martin Heinrich Klaproth produced titanium from “rutile”. The element Ti is the fourth most abundant metal in the earth's crust. Because of its great affinity for oxygen and nitrogen, pure titanium was not produced in a commercial process until the late 1930's. Titanium is not a rare element or structural metal; rather it is the ninth most common elements. The concentration of titanium is approximately 0.6% of the earth structure, making it the fourth most prevalent structural metal [1-6]. Interest in the properties of titanium increased in the late 1940 and early 1950 after World War II. In the following decades, titanium research and application exhibited tremendous development [2].

Titanium and its alloys are used in many industrial areas. For example, about 80% of the produced titanium is used in aerospace industry. Moreover, it is used in the areas like medicine and biomaterial engineering, offshore and marine, transportation, architecture, chemical processing, power industry, military, sports industry and automotive sector [1, 2, 3-5]. Titanium is present in many different places including the moon, meteorites, the sun and the other stars. However, it cannot be found in high concentrations. Furthermore titanium ore is never found as a pure metal. Due to these factors, producing titanium is very difficult and expensive [7-11].

Titanium is a very light metal due to its low density. At the same time, its strength is very high.Therefore, it can be used in the structures requiring strength and lightness, such as needed for the aviation industry [6-12]. Moreover, the temperature capability of titanium is very high, allowing it to be used in cryogenic applications; and it can also resist to corrosion, hence one of the usage areas is marine and offshore structures. In addition to these advantageous features, the biocompatibility of titanium is very high so it can be used in medical industry widely [2, 5, 12-15].

Titanium is neutral for the human body, it does not cause any cyto-toxic reactions and hence titanium is used in bio-engineering applications such as heart valves, joints and bone plates, too. Titanium has been used as artificial body parts, especially hips and the other joints for about 35 years. Moreover, its corrosion resistance and mechanical properties are excellent for structural bioengineering applications. Because of the features of strength and biocompatibility of titanium, it is an optimum material for oral prosthetics and other dental applications [10, 13-19]. Titanium is also used for applications needing damage tolerance, high resistance against corrosion, low elastic modulus and high strength-to-weight ratios such as sports equipment [5, 8]. Like the most of other metals, titanium and its alloys also have some disadvantages. The adhesive and abrasive wear resistance of titanium is very low, its friction coefficient is very high, its fretting properties are inadequate and hardness values of titanium are low. However, these alloys have significant problems with wear. Moreover, pure titanium can disfigure and relay drastically in wear applications without lubricants [14, 20-23].

The specific strength of titanium alloys at high temperature is significantly high. Nevertheless, the maximum use temperature of titanium (about 600 ºC) is not very high because of the high reactivity of titanium with oxygen [19, 21, 23]. Above 600 ^{o}C, oxygen diffuses through the oxide layer on the surface too quickly, causing extreme growth of the oxide layer which results in oxygen embrittlement in titanium. Moreover, because of this oxidation behavior, melting processes of titanium requires extra equipment which increases the production cost and hence, titanium price. However, a thin oxide layer provides excellent corrosion resistance of titanium in several types of aggressive media such as aqueous acid [24-27].

Pure titanium has an allotropic phase transformation at 882°C from a body-centered cubic (BCC) β phase to a hexagonal close-packed crystal structure (HCP) α phase. During the transformation, titanium atoms in the BCC beta structure slightly shift to convert to the HCP alpha structure. The unit cell of hexagonal α phase and cubic β phase is shown in Figure 1.1. At room temperature, the lattice parameters of α phase are a = 0.2951 nm and c = 0.4684 nm. The resulting c/a ratio = 1.5871 is smaller than the ideal ratio of 1.633 for the HCP structure. There are several densely packed planes in these two phases. In β, it is one of the six {110} planes, while in α, there are three types of densely packed planes: (i): (0001) plane, also called basal plane;

(ii): one of the three {1010} planes, also called the prismatic planes (iii): one of the six {1011} planes, also called pyramidal planes. In β, the close-packed directions have four <111> directions.

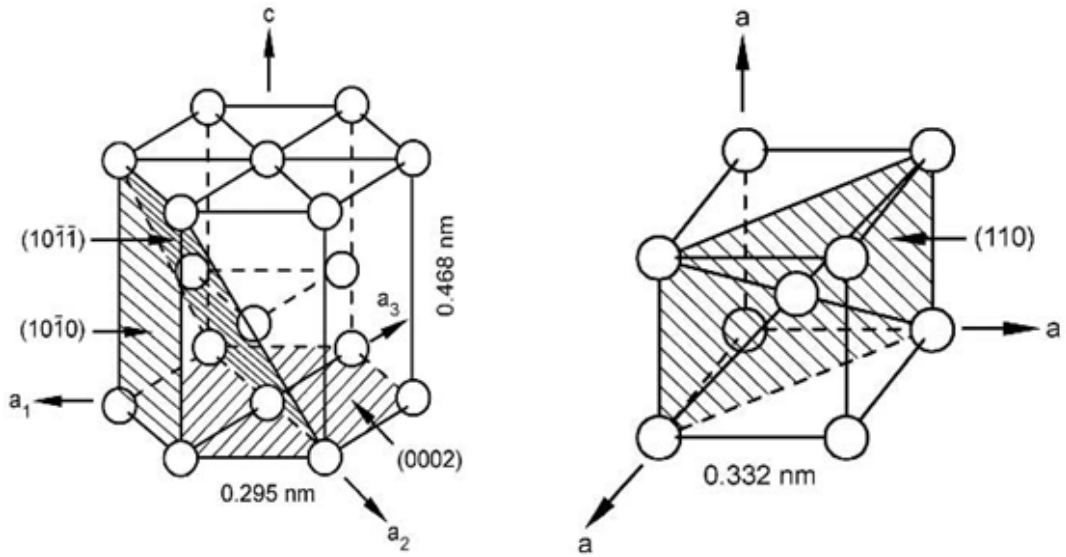

(a) α-phase unit cell of titanium (b) β-phase unit cell of titanium

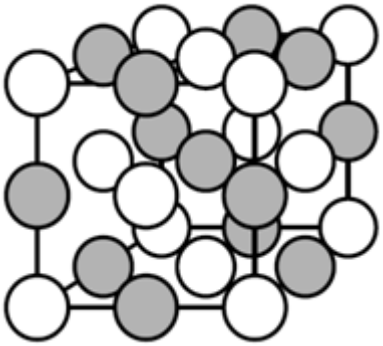

(c) TiN structure

Figure 1.1 : Crystal structures of Ti and TiN [2].

In α, there are three <1120 > directions. The α/β transformation temperature of titanium alloys is strongly influenced by interstitial and substitutional elements, and therefore depends on the purity of the metal. Alloying elements in titanium are usually classified as α or β stabilizing additions, depending on whether they increase or decrease the α/β transformation temperature [1-2, 18].

The substitutional element Al and the interstitial elements C, N, and O are all strong α stabilizers. The transus temperature from HCP to BCC increases with increasing concentrations of these alloying elements (see Figure 1.2 (a)). Aluminum is the most widely used alloying element in titanium alloys, because it is the only common metal

that can raise the transus temperature and it has a large solubility in both α and β phases. Some other α stabilizers include B, Ga, Ge and the rare earth elements, but their solid solubility are much lower as compared to aluminum and none of these elements is used commonly as an alloying element [1-5].

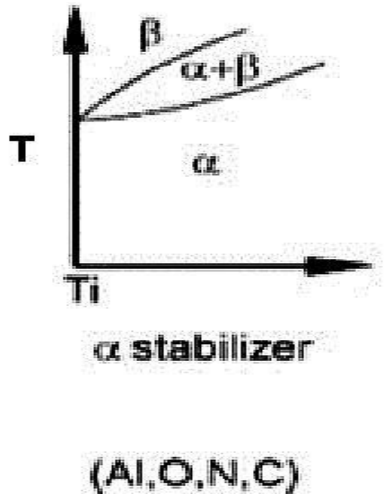

(a)

Figure 1.2 : Effect of alloying elements on phase diagrams of titanium alloys [2].

Titanium nitride has rock-salt crystal structure, c-TiN (or NaCl crystal structure, Figure 1.1 (c)), with a mass density of 5.44 mg/cm^3. As the result of different growth methods and operation conditions, it does not always exhibit composition Ti/N equal to unity [25-31], while the atomic ratio between titanium and nitrogen determines the color of titanium nitride.

Stoichiometric titanium nitride has metallic shiny gold color, making it popular as decorative coatings. It has been reported that the color of titanium coatings is gray when it suffers from nitrogen deficiency. With increasing the nitrogen content, the color becomes pale and yellowish, and finally reaches the yellow-gold color as the nitrogen content in the film close to the titanium. Over stoichiometric nitrogen turns the appearance into dark yellow and brown [24, 26-28].

Titanium alloys can be categorized depending on the development of α and β phases as α alloys, β alloys and α+β alloys. There are two subcategories of α+β alloys named near-α and near-β alloys. The compositions of the alloys belonging to these subcategories are located near to (α+β)/β or α/(α+β)-phase boundaries, so these alloys are named near-β or near-α alloys respectively [1-5, 31-33]. Table 1.1 shows most used elements to produce alloys and their stabilizing influences.

Table 1.1 : The most used alloying elements and their stabilizer influences [4].

Alloying Element	Influence on the structure	Range (wt. %)
Silicon	Enhances the resistance against creeping	0.2 to 1
Tin	Stabilizing α	2 to 6
Aluminum	Stabilizing α	2 to 7
Zirconium	Strengths α and β	2 to 8
Chromium	Stabilizing β	2 to 12
Vanadium	Stabilizing β	2 to 20
Copper	Stabilizing β	2 to 6
Molybdenum	Stabilizing β	2 to 20

1.1.1 α alloys

Alpha Alloys includes substitutional alloying elements such as tin and aluminum or interstitial elements such as N, O or C. These are α-phase stabilizing elements, and they can dissolve in the hexagonal α phase as well as raise the temperature of the phase transformation. [13]. Specific and favorable features of Alpha alloys are toughness, gratifying strength and ability to be welded. However, the most important disadvantage of these alloys is less formability in comparison to β alloys [4]. Another significant advantage of α alloy is that they have the HCP structure; hence these alloys do not have a ductile-brittle transformation making them convenient for the usage in cryogenic applications [4].

Moreover, these alloys are commonly used in the chemical applications and process engineering applications because of the super corrosion resistance and formability. In addition to this, these alloys have a very high strength [1]. Cp-Titanium is actually a α-alloy. The difference of them from the other α-alloys is their oxygen contents. Their oxygen contents range from 0.18% to 0.40% respectively from grade-1 Cp-Titanium to grade-4. The oxygen content of these four grades raises the values of the stress yield of these alloys. In addition, all Cp-Titanium grades do not obtain their strength from the substitutional alloying elements such as Ru, Fe or Pd, and hence, they form a group different from the other α alloys [13]. Cp-Titanium alloys grade 1 to 4 have a tensile strength values range from 240 to about 550 MPa at room temperature. The tensile strength values of Grade 2 range between 390 and 450 MPa. This alloy is the most used grade of CP-titanium. Grade 3 has a high strength. It can be moderately cold-formed. Table 1.2 that shows some properties of the Cp-Titanium

alloys grade-1 to 4. CP grade-4 Titanium, which is used as specimens for this thesis work, is the strongest one of the Cp-Titanium alloys. Its strength value can be up to 740 MPa [1].

Table 1.2 : Cp-Titanium alloys grade 1 to 4 with some of their features [13].

Common Name	Transus Temperature(T_β,^oC)	Composition of the Alloy
Grade 1	890	CP-Ti (0.18 O, 0.2 Fe)
Grade 2	915	CP-Ti (0.25 O, 0.3 Fe)
Grade 3	920	CP-Ti (0.35 O, 0.3 Fe)
Grade 4	950	CP-Ti (0.40 O, 0.5 Fe)

1.1.2 β alloys

These alloys include several alloying elements such as Fe, V, Cr and Mo. These alloying elements are β-stabilizer and can reduce the α→β phase transformation temperature (β Transus). Another feature of beta alloys is their tendency to transform from ductile to brittle, because the crystal structure of beta alloys is BCC and the materials formed in BCC structure tend to exhibit ductile-brittle transition. Hence these alloys-similarly to other bcc structured materials-cannot be used for the at low temperatures [4]. Figure 1.3 shows the schematic phase diagram for β stabilizers.

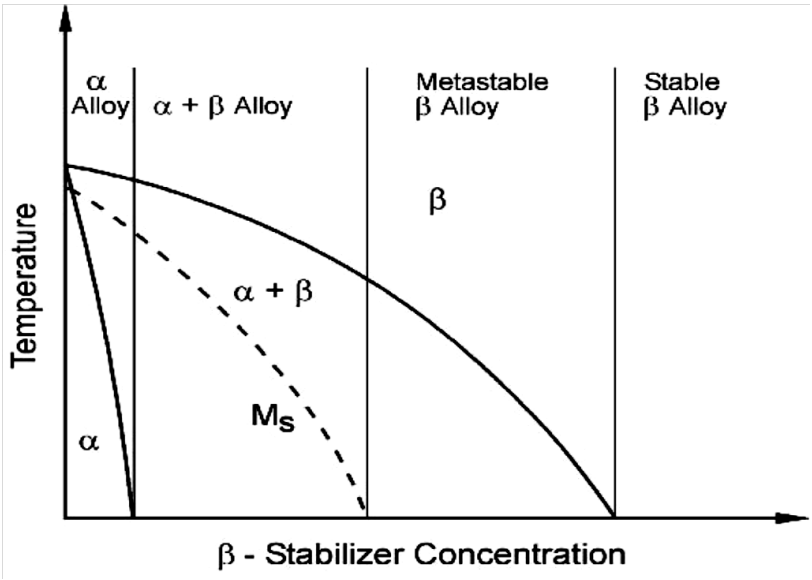

Figure 1.3 : Pseudo-binary section through a isomorphism phase diagram [2].

1.1.3 α+β alloys

These alloys have a mixed composition of α and β phases. α+β alloys include mixes of β and α stabilizing elements. The features of α+β alloys can be adjusted by heat processing, hence the existing phases' types and amounts. These alloys usually show sufficient strength at high temperature values and very good strength at room temperature values. Moreover, the machinability of these alloys is also quite good. Ti-6Al-4V is an example of the most used α+ β titanium alloy, Figure 1.4 shows Typical microstructures for α, α-β and β titanium alloys [2, 4].

The most commonly used β stabilizers in α+ β titanium alloys are V, Mo, and Nb. Sufficient concentration of these elements make it possible to stabilize the β phase at room temperature [34-36]. These elements have solubility in α and β phases of titanium.

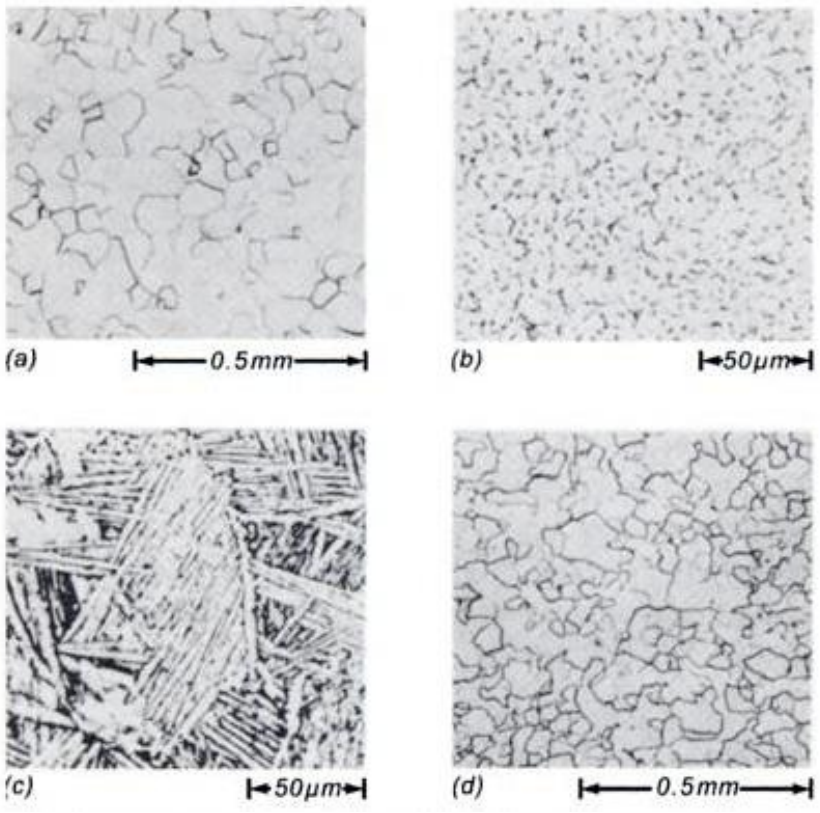

Figure 1.4 : Typical microstructures for α, α-β and β titanium alloys: (a) equiaxed α phase in unalloyed titanium (after1h/1,290 °F); (b) acicular equiaxed α+β; (c) acicular α+β in Ti-6Al-4V; (d) equiaxed β in Ti-13V-11Cr-3Al [2].

2. SURFACE MODIFICATION TECHNIQUES APPLIED TO TITANIUM AND ITS ALLOYS

As mentioned in the previous sections, the tribological properties of titanium are very poor [1-3]. The high values of coefficient of friction, low hardness and poor resistance against abrasive wear prevent the use of titanium in some applications. For improving these poor features of titanium, some surface engineering methods can be applied to commercial purity titanium and titanium alloys. With these methods, the problems of wear and hence, galling of titanium can be minimized .Generally, the surface modification techniques applied to titanium and its alloys can be categorized two major classes: deposition and thermochemical processes. A variety of surface engineering techniques, such as PVD/CVD coating, direct gas nitriding, plasma, and laser thermochemical processing, generates surface layers with considerable thickness. The improved wear resistance has a cost in mechanical properties, such as ductility and fatigue resistance [1, 2, 34].

2.1 Deposition Processes

There are many different kinds of coating methods that can be applied to titanium and its alloys. These coating methods can be categorized as physical vapor deposition (PVD), chemical vapor deposition (CVD), chemical conversion coatings, sprayed coatings or plating. All of these coatings are applied to titanium substrates in order to improve the tribological properties of titanium and its alloys [4].

PVD and CVD are coating techniques which give a completely different chemistry, structure and property to the surface compared to the substrate. Basically, PVD involves evaporating a coating metal, and then depositing that metal on the substrate. These coatings are applied at substrate temperatures of several hundred degrees celsius and are accomplished in high-vacuum chambers. The coating metal is vaporized by induction coils. Electrical resistance or electron beams heat the source and thus coating materials evaporate in the presence of reactive gases, in most cases N. Nitride compounds form and deposit on the surface of substrates [1-8].

CVD involves supplying a source of several reactant gases, and then depositing the chemical reaction products on the substrate. Gaseous compounds of the materials to be deposited are transported to a heated substrate surface where a thermal reaction/deposition occurs. The reactions of gases occur at the surface of the hot substrate to form a solid deposit. A more detailed interpretation of CVD mechanism would include chemical reactions that take place in the vapor phase prior to adsorption, as well as surface diffusion of the reactive adsorbents. The most advanced CVD systems allow control over the extent of these processes, thus allowing control of the morphology of the deposit. Chemical conversion coatings are applied on titanium to enhance lubricity. These coatings behave like a base to retain the lubricants [1-8].

2.2 Thermochemical Diffusion Treatment

As mentioned before, most surface modification techniques can be applied to titanium and its alloys. Some case hardening methods can be applied as surface modification techniques to Cp-Titanium and commercially available alloys, but as a consequence of these methods, significant alterations of the composition of the surface do not occur. These alterations are limited by the substrate composition; therefore the thermal hardening processes are not effective in many cases. The treatments, which can change the surface composition locally, can produce microstructures and related mechanical features which are different from those of the base material [2-8, 16].

Moreover, titanium alloys can react with all elements with the exception of the most stable ones at several temperature values. This property of titanium allows for the application of many different diffusion-based treatments to the surface. For developing the mechanical features of titanium and its alloys, different kinds of thermochemical processes can be implemented .In addition to these conditions, the treatments that are applied to the surfaces of titanium and its alloys have to be completed in protecting inert gas environment or in vacuum, because titanium and its alloys can react with interstitial elements, particularly oxygen easily because of the chemically activeness [34-35]. Today, the popularity of the thermochemical treatment techniques depending on diffusion saturation of the surfaces of the materials with several elements is increasing. These treatments can reduce the

coefficient of friction , enhance the corrosion resistance and the wear resistance and harden the surface of the relevant material. The most used thermochemical treatments for the enhancement of the poor tribological features of titanium and titanium alloys are carburizing processes, oxidation processes and nitriding processes [1-4].

2.2.1 Carburizing

During carburizing process, titanium and its alloys should be treated in carburizing and non-oxidizing media because of the very low solid solubility of carbon in titanium. For this reason, the phase equilibrium system of titanium-carbon is different from the titanium-nitrogen system and the titanium-oxygen system. The solid solubility of nitrogen and oxygen in titanium are higher than found with carbon. Because of this low solid solubility of carbon in titanium, although the thickness of the formed TiC compound layer varies from 1 to 10 μm, there is no remarkable diffusion zone underneath this TiC layer. The process temperature values of carburizing vary up to 1050 ^{o}C in an environment that includes carbon. After carburizing, wear-resistant surfaces can be obtained for titanium and its alloys. This modification method can be used to enhance the surfaces of engine valves [4, 10-12].

2.2.2 Oxidation

The oxidation of titanium has been studied by different research groups. However, initially, this thermochemical process has not been considered as a surface modification technique that can be applied to titanium and titanium alloys [1-2]. The poor tribological features of titanium and its alloys can be developed via oxidation process. The solid solution of oxygen and α-Ti provides a remarkable enhancement of the strength of the material. Titanium has a super resistance against corrosion under normal conditions commonly because of the development of protecting, adhesive and steady oxide films on the material surface. This oxide film grows into a tougher and thicker form during oxidation and this form provides an extra corrosion protection [1-4]. These protecting oxide layers can be created while titanium and its alloys are being heated in air at a temperature ranging from 400 ^{o}C to 800 ^{o}C. However, these oxide films are very brittle and therefore, these films can fail during mechanical applications with ease. In the end, this means the oxidation process cannot really enhance the resistance against wear [2-7].

There are some studies about the thermal oxidation to develop the wear resistance of titanium. According to these studies, the rutile surface oxide (TiO_2) is formed after the thermochemical treatment of Ti6Al4V in a gas environment of Ar/O_2. This rutile layer shows ideal values of wear resistance for Ti6Al4V and the maximum hardening depth is 250 μm at 900 ^oC and 125 μm at 850 ^oC. Another method is plasma electrolytic oxidation which is used to obtain a wear-resistance layer on the surface of titanium. With this technique, a thick and outstandingly adhesive film can be formed. The maximum thickness of this layer can reach to 500 μm. Plasma thermochemical interactions within the multiple-surface discharges eventuate in developing a coating in either direction from the surface of the substrate [1-4].

2.2.3 Nitriding

Nitriding is a method to harden the surface of titanium and its alloys and this method has been used for a long while. The poor tribological properties of titanium, such as the low resistance against wear and tending to gall, can be enhanced via this method [1]. The process of nitriding and its derivative processes are seen today as a future surface enhancement technique for many ferrous and nonferrous metals. Interest in the subject of nitriding has grown and even more recognized as a proven surface engineering process. Particularly, during the past 10 years it has been recognized as a very simple process without serious problems such as the problem of distortion. The process of nitriding, while not distortion free, is a process that can cause only minimal distortion compared to that seen on other surface treatment process techniques such as carburizing and carbonitriding, which involve higher process temperatures as well as a quench from a high austenitizing temperature [18].

The main reasons for nitriding are:

- To obtain high surface hardness.
- To increase wear resistance and anti-galling properties.
- To improve fatigue life.
- To improve corrosion resistance.
- To obtain a surface that is resistant to the softening effect of heat at temperatures up to the nitriding temperature [19].

There have been developments in the application areas of the nitriding process. The automotive industry has shown serious interest in the use surface enhanced high-

strength low-alloy to reduce material costs as well as giving a good performance. Still, the majority of the work on all of the process methods and process metallurgy is still dedicated to ferrous materials and only a small amount of research is directed to nonferrous materials such as aluminum and titanium. One of the areas of investigation with nonferrous materials is conducted on the nitriding surface treatment of titanium to form a non-brittle surface layer of titanium nitride [18].

Nowadays, some features of nitriding are being studied mainly such as saturation control, mechanism of development of layers, the form of the treatment, engineering and industrial applications of nitrided materials. With these studies, the current classification of nitriding process and nitriding based treatments will be expanded. And the classification like this can provide some advantages such as systematization of the current treatments, understanding and developing of the process parameters and mechanism of forming, to control the features of the acquired compound layer and the final structure of the specimen and the specification of the optimum application areas for the treated materials. There are four important criteria for the classification of nitriding process: the properties of the treatment, the mechanism of the development of the saturating atoms, the materials and temperature of the treatment and the composition and features of the phase.

After nitriding process, the strength of the surface layer increases remarkably, because of the high solubility of nitrogen in α-Ti. Moreover, the hardness values of titanium and its alloys increase. Especially, the longer nitriding time and the higher process temperature can cause higher values of hardness. In addition to this, nitriding process should not be carried out in air, because titanium tends to react with oxygen to form TiO_2 in preference to TiN and TiN_2. Because of this tendency, nitriding has to be applied to titanium in a vacuum furnace [1-4].

Some of the problems commonly encountered in nitriding are:

- Low case hardness or shallow case.
- Discoloration of work pieces.
- Excessive dimensional changes.
- Cracking and spalling of nitrided surfaces.
- Variations in percentage of ammonia dissociation.
- White layer deeper than permitted.
- Plugging of exhaust lines and pipette lines.

Knowing the causes of these problems should help to avoid, prevent, or correct them [19].

Although many techniques are commercially available to modify the surface properties of titanium alloys, conventional gas nitriding is still considered to be the most promising method for engineering applications because it can easily form a hardened nitrided layer on the surface of material and it is not as expensive as those newly developed technologies. The nitriding processes can be classified as:

i- Gas nitriding,

ii- Laser nitriding,

iii-Plasma nitriding and

iv-Ion beam nitriding

Gas nitriding:

Gas nitriding is a thermochemical treatment that can be applied easily to the surface of the materials to develop a harder compound layer for engineering applications. This process does not need particular equipment and is not dependent on the geometry of the specimen [1-3].

The treatment is usually conducted in a furnace with a controlled gas atmosphere. Pure nitrogen, nitrogen/argon gas mixture, nitrogen/hydrogen gas mixture, or ammonia can be used as the nitriding gas resource (Figure 2.1). The general procedure is first to create a vacuum in the furnace and then re-introduce a gas until atmospheric pressure is reached. This nitrogen gas diffuses into the specimens after it dissociates thermally during this process [1]. The disadvantage of this process is that it can take a very long time to do the nitriding. Moreover, this treatment decreases the fatigue strength of titanium and its alloys .The thickness of the surface layer and the value of the hardness depend on two parameters-temperatures and time [1-4]. In the gas nitriding practice, the oxygen contamination is very hard to control. The processing gases all have a certain level of oxygen impurities in the form of oxygen gas or water vapor. Gas leakage through heat treatment facilities also introduces the contamination. Titanium alloys with a high level of oxygen have a tendency to form the brittle α phase on the surface which has a detrimental effect on mechanical properties [1-4].

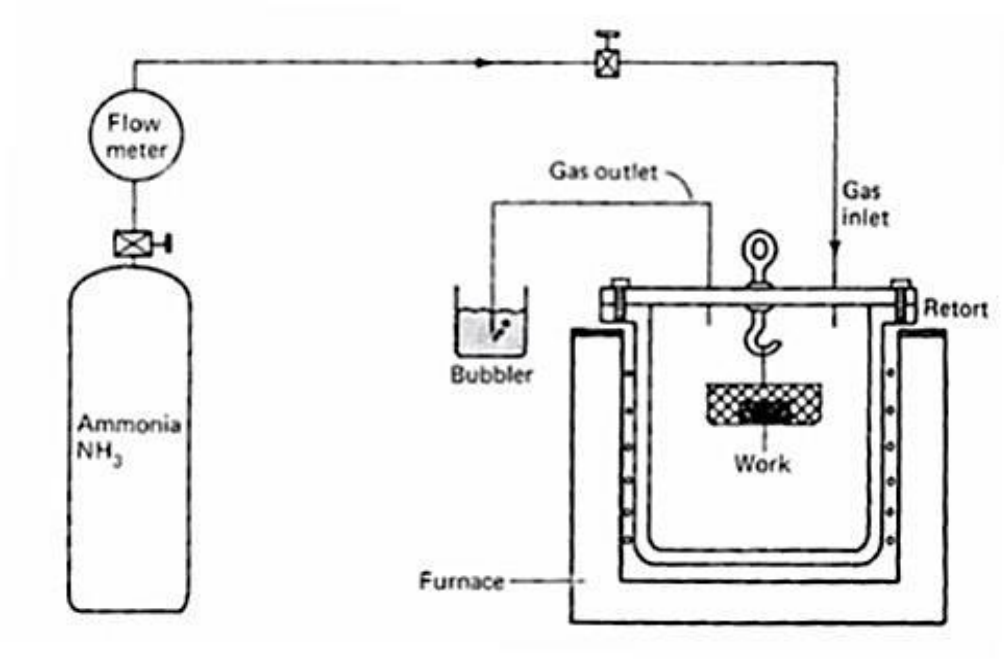

Figure 2.1 : Gas nitriding setup [4].

Nitrogen is in the periodic table of nonmetals in Group IVA, along with four other nonmetals. It will readily form gases with both hydrogen and oxygen. In addition, it is diffusible in metals especially at low temperature and it will not only diffuse, but also react with metals with which it can form nitrides (Figure 2.2). Nitrogen is generally obtained for gas nitriding from the decomposition of nitrogen and ammonia from the following reaction sequence during the gas nitriding procedure by using heat as the method of decomposition and the material as the catalyst [18]:

$2NH3 \Longrightarrow N2 + 3H2$

$N_2 \Longrightarrow 2[N]$

The nitriding process requires perhaps the lowest temperature range of all the thermochemical diffusion techniques: 315 °C to 540 °C [18].

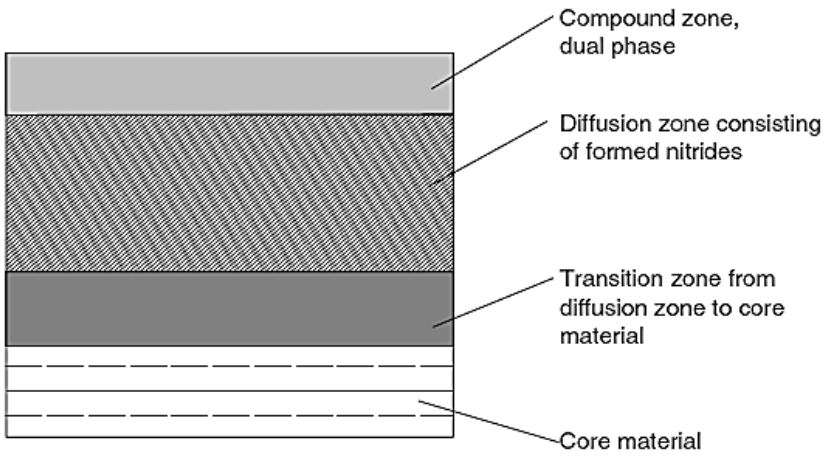

Figure 2.2 : A typical nitrided structure [18].

The control of the compound layer thickness will depend on the following process parameters:

- Process time
- Process temperature selection
- Process gas composition
- Gas dissociation

Laser nitriding:

In some applications of industry such as some mechanical parts, diffusion barriers in microelectronics, die molds, decorative stuff and cutting tools, the thin films made of TiN are the most used ones. Laser Nitriding is one of the nitriding processes applied to titanium and its alloys to produce a hard titanium nitride layer on the surface of the material. During this process, the surface is melted in depth of 1 to 1.5 μm by a focused laser beam in a nitrogen gas medium. After laser nitriding process, a super metallurgical bond between the substrate and the surface layer can be obtained and because of that, it is a very attractive method to harden titanium and its alloys [2-5]. During this process, nitrogen has to flow through a nozzle with an angle of minimum 30^{o} to the surface into the melting pool. The major problem of the laser nitriding of titanium is the surface cracking. The parameters of the laser nitriding treatment such as scanning speed, the concentration of nitrogen and laser pulse energy can be adjusted to avoid cracking. The most important disadvantages of the laser nitriding of titanium and its alloys are the importance of the geometry of the used material and the requirement of particular equipment [29, 36].

In recent years there has been widespread interest in using lasers to modify surface structures and compositions of titanium alloys (Deevi, Sikka, Swindeman, &Seals, 1997). In this case, the use of gaseous nitrogen interaction with the laser melted surface is utilized, since elemental titanium has a strong affinity for nitrogen. Very high incident power is brought by CO_2 or YAG lasers to bear on the substrate surface, producing extremely rapid heating [1, 2]. Since there is a steep temperature gradient, the bulk of the material remains unaffected and acts as a heat sink to provide self-quenching. A relatively thick and hard nitrided layer on Ti-alloys can be obtained. Primarily this will improve their tribological properties. Laser beam moving velocities, processing pressure as well as nitrogen/argon ratio, gas flow rates are major controlling factors (Figure 2.3).

Laser surface modification of Ti-6Al-4V alloy was investigated by Akgun and Inal under nitrogen gas atmosphere. The results showed that laser-treated Ti-6Al-4V alloy produced a hardened surface layer due to TiN formation [2, 8]. Laser surface melting followed by an aging treatment resulted in uniform hardness distribution in the melted zone. Ignatiev and et al. also produced a laser-nitrided surface with very small roughness, free from cracks [2]. They demonstrated that the wear properties of laser-treated surfaces improved considerably, which encouraged the use of laser nitriding as a potential surface treatment technique for the industry. Yilbas and Shuja (2000) have described that laser melting plus PVD TiN coating duplex treatment can improve the surface wear property considerably. Although laser nitriding can generate a hardened layer about hundreds of microns in a very short time and without affecting the substrate properties, the melting-solidifying process totally changes the surface microstructure. Surface roughness is comparably high and it is very hard to have a crack-free surface. Significant reduction in ductility and fatigue strength also occurs after laser melting and alloying with nitrogen. This cracked, brittle surface layer has limited the application of laser nitrided titanium alloy products.

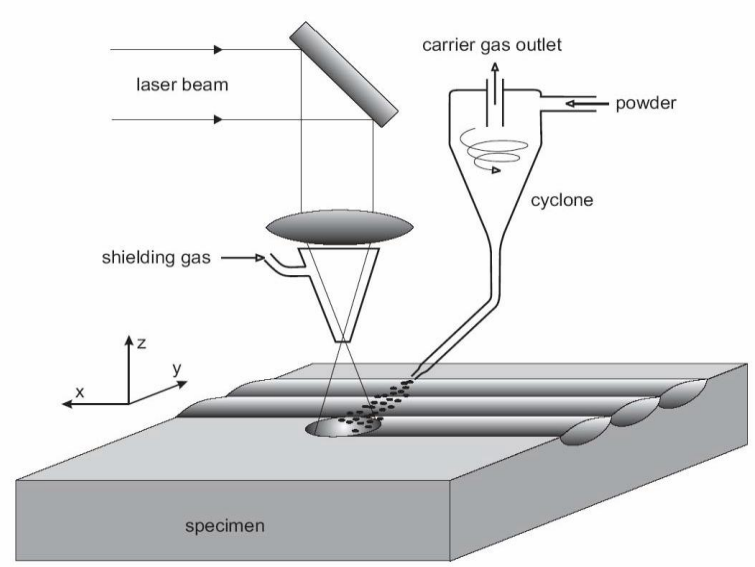

Figure 2.3 : Principle of operation of a laser nitriding furnace [21].

Plasma nitriding:

Plasma nitriding is a very advantageous thermochemical process. Controlling of the depth of the developing layer and the creation of the phase during process are the main advantages of the plasma nitriding. Moreover, the nitriding during this process lasts a short time and it prevents oxidation .There are two main plasma processes for synthesizing titanium nitride: ion nitriding and PVD. Plasma nitriding has some disadvantages. For this treatment, high ionizing energy and some particular equipment are needed. Furthermore, this process diminishes the fatigue strength of titanium and its alloys. However, if the temperature of the treatment is decreased, this issue can be solved. Plasma based technology can be used for many process applications, which include the treatments of a metal, plastic, or other surface treatment methods. Plasma nitriding is a method of surface hardening that uses glow discharge technology to introduce elemental nitrogen to the surface of a material which then diffuses [4, 20].

Plasma nitriding uses voltage applied between two electrodes in a sealed chamber to ionize gas under low pressure. Positive ions are accelerated toward the work pieces which act as a cathode (Figure 2.4). Therefore the potential drop emits visible radiation (popularly called “glow”). The process gas contains nitrogen and its positive ions hit the treated surface when a potential of several hundred volts is applied. In this way, the plasma completely covers the cathode, exposing the surface

of the whole work piece to a flux of ions .This ion bombardment process heats the work piece and cleans the surface providing active nitrogen, which under the influence of the glow discharge, forms the nitrided case. The addition of diffusive atoms improves the hardness of work pieces .The inner wall of the chamber is the anode. A gas mixture containing nitrogen (usually nitrogen and hydrogen) is introduced into the chamber. During the process a pump continuously evacuates the gas to maintain a soft vacuum of between 0.1 and 10 mbar. The pressure during the plasma process is measured by a pressure transducer [35-38].

During these last years, the pulsed plasma generation technique has been preferred for the plasma nitriding process. This technique is based on the ability to interrupt the continuous DC power at specific and variable time intervals. Through this pulse system used in combination with additional heating, high temperature uniformity is obtained over all the work pieces in the furnace [20-22].

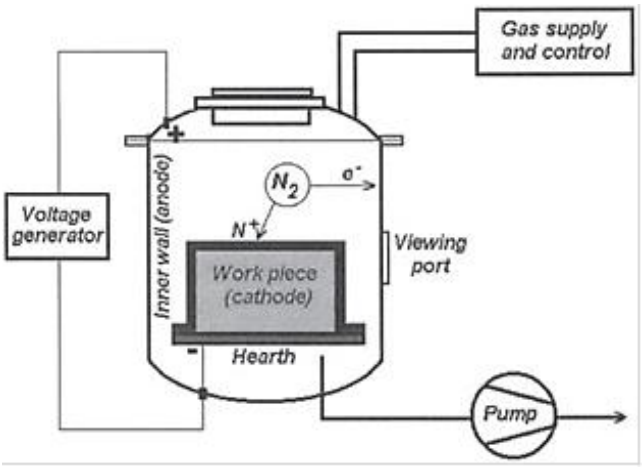

Figure 2.4 : Principle of operation of a plasma nitriding furnace [21].

Most of the thickness of the nitride case is the diffusion zone where fine metal/alloy nitride precipitates produce increased hardness and strength. Compressive stresses are also developed, as in other nitriding processes. The hardness resulting from ion nitriding is similar to ammonia-gas nitriding, but due to a lower processing temperature, the near-surface is usually harder. The hardness of the nitride case is determined by the concentration and size of the alloy nitride precipitates formed and the hardness of the parent materials. The thickness of the nitrided case and the compound layer are determined by process gas ratios, process time and temperature and material composition. To obtain a uniform surface properties with consistent and

repeatable results, all the following process parameters must be carefully and precisely controlled during the plasma nitriding process [18-19]:

- Time
- Temperature of the work piece
- Temperature of the process chamber
- Process gas flow (nitrogen, hydrogen, methane, and argon)
- Surface working area
- Support fixturing surface area
- Process power voltage
- Current density
- Operation time
- Process amperage
- Rate of temperature rise
- Process pressure (vacuum level)

Plasma nitriding typically offers engineers and metallurgists a number of advantages including total absence of pollution, very good process control and reproducibility , total process automation , precise phase control of the nitrided surface layers and improved control of case thickness, possibility of selective nitriding by simple masking techniques, reduced nitriding time , lower surface treatment temperatures , lower distortion , process span that encompasses all subcritical nitriding, wide range of process gas composition possibilities , relatively low energy, gas consumption and operating costs and cleaning and activation of surfaces by initial sputtering [10,19].

Ion-beam nitriding:

Ion-beam nitriding is one of the hardening processes applied to the surface of titanium. During this process, the surface of the material is treated by an ion beam via using Ar and N_2. The surface of the sample is bombed by nitrogen and as a result of this, the atoms of the impurities are desorbed and sputtered [4].

The surface modification of titanium and its alloys by ion implantation with N or C has been studied as a means to improve the wear, fatigue, or fretting fatigue behavior of the alloys. During ion implantation, accelerated ions are driven into a substrate surface. An ion source is bombarded with electrons that ionize the molecules by

striking an arc discharge between an anode and a cathode. The ions are extracted by an electrostatic field, which then are magnetically accelerated, separated and detected on a substrate. If the implantation is under a suitable level, it will correspond to the formation of a stoichiometric or near-stoichiometric balance between the implanted species (N or C) and the host lattice. The ion implantation process is carried out at room temperature, however, the surface temperature increases dramatically. The high energy ions enter the lattice and produce vacancy-interstitial point defects [1, 3-6].

2.2.3.1 Mechanism of nitriding in gas atmosphere

During nitriding process, many reactions occur at the gas-metal interface and in the base material. A simplified physical model of the development of consisted layers during gas nitriding process of titanium is proposed. This physical model is attributed to reaction-diffusion laws and can be applied for the nitriding process temperatures that are below $\alpha \rightarrow \beta$ transformation temperature [36-40]. In order to optimize the nitriding effects, the thermodynamics and kinetics of Ti-N system should be investigated more thoroughly. The nitriding process can be divided into the following steps [37, 39-42]:

1. Nitrogen is supplied or generated from sources such as NH_3, nitrogen gas or decomposition from nitrogen-containing compounds.
2. Nitrogen moves towards the surface of titanium by gas diffusion.
3. Nitrogen molecules impinge the titanium surface and then adsorb to the surface (physisorption).

4. The nitrogen is absorbed by the substrate at the surface, and then nitrogen diffuses inside of the substrate and makes an interstitial solution with hcp α-titanium. This layer is named as the diffusion zone (α (N)).
5. The diffusion process proceeds until the α-titanium saturates with nitrogen atoms. When the concentration of nitrogen at the boundary between the gas media and the substrate becomes higher than the α-titanium phase, this phase cannot maintain itself and a new reaction occurs to compose a new phase called Ti_2N. Accordingly, there are two layers: on the top, a compound layer named Ti_2N and a diffusion zone beneath.
6. After the formation of Ti_2N, this layer continues to develop until the nitrogen concentration at the boundary between gas environment and the surface of the

substrate becomes higher than the Ti_2N, Ti_2N phase transforms to TiN phase. So, the consisted layers are TiN on the top, Ti_2N underneath it and the diffusion zone (α (N)) is at the bottom [4-6].

Reactions may happen on the surface to form Ti_2N and TiN compounds when the nitrogen concentration becomes high enough. The reactions, which take place during nitriding, are:

$$\alpha\text{–Ti} \Rightarrow \alpha\ (N)\ \text{–Ti} \Rightarrow Ti_2N \Rightarrow TiN$$

Figure 2.5 shows the development kinetics of consisted layers during nitriding process of Titanium specimen.

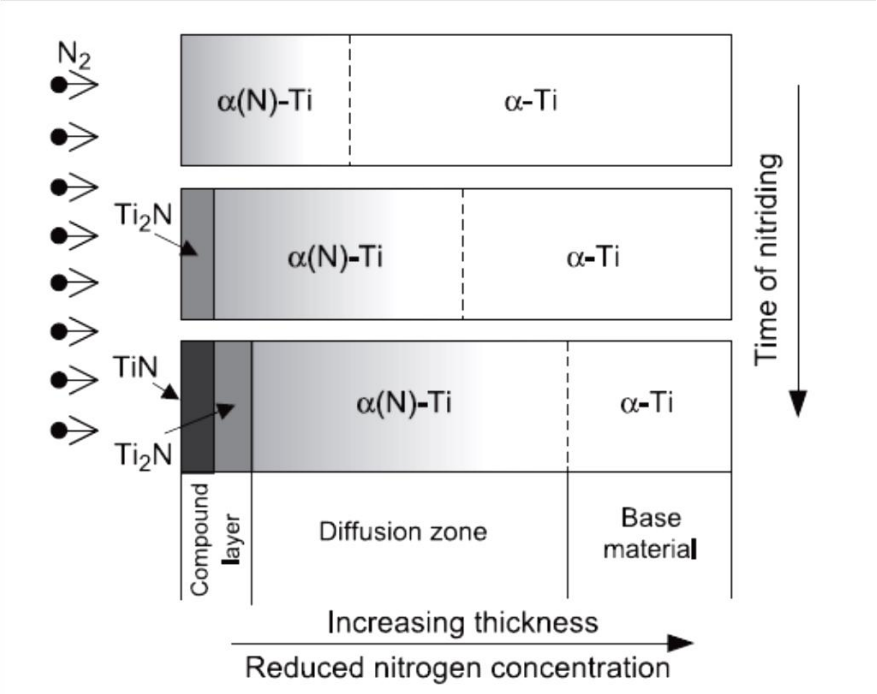

Figure 2.5 : A schematic drawing of consisted layers during nitriding [4].

Some β-stabilizer elements, such as vanadium, affect the nitrogen diffusion in titanium and its alloys negatively [2, 3]. The proportion of α to β phases varies in several alloys at the same temperature values. The strengthened surface layer consists of nitride and gas-saturated area. It is the result of the high-temperature interaction of titanium with nitrogen. This interaction is accompanied with the redistribution of alloying elements in alloy's surface layers. The general regularities of alloying elements redistribution at nitriding of titanium alloys can be considered here. The alloying elements of titanium alloys are categorized as α- (Al), β- (Mn, V, Mo, Cr, Fe,Nb, Si, W) - stabilizers and neutral reinforcing (Zr, Sn). [1-3].

The increase of electron concentration during the nitrogen dissolution leads to decrease of solubility of alloying elements in titanium due to the limited solubility and also the formation of continuous series of solid solutions. It assists in redistribution of alloying elements in the surface layers of titanium alloys: their separation from solid solution and diffusion into titanium matrix [43-45]. Thus, after thermodiffusion saturation by nitrogen there is diffusion of elements separated from solid solution into the alloy, Figure 2.6. The intensity of this diffusion is determined by the solubility and diffusion mobility of alloying elements.

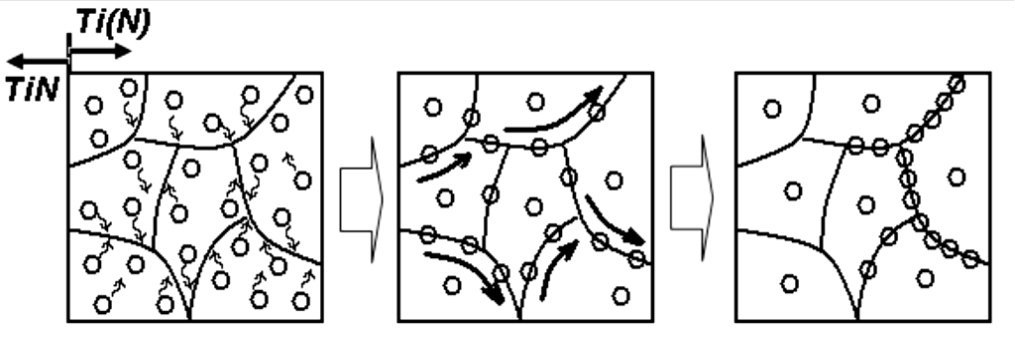

Figure 2.6 : Scheme of redistribution of alloying elements in the gas-saturated layer of titanium alloys at nitriding [23, 43].

The thickness and the microstructure of the nitride layer are related to the nitriding temperature and the nitriding time. The nitriding temperature above and below β-transus affect the specimens differently. According to this, different features, different morphologies of the microstructure and the different process kinetics for various phase compositions can be obtained after nitriding .In addition, the effect of the nitrogen to the temperature of α-β transformation should be considered. For example, a very low concentration of nitrogen can change the β-transus significantly. Hence, the phases can form at different ratios at the equilibrium phase diagram of α- and β-phases according to Figure 2.7 .The effect of the process temperature to the nitrided layer is directly proportional. For example, the growth of TiN increases with the increasing temperature of nitriding. The whole depth of nitrided layers increased with ascending process time [21-23]. Nitriding temperature also affects the surface microstructures. Low treatment temperatures such as 950 ^{o}C cause homogenous and fine microstructure. However, increased temperatures (such as 1050 ^{o}C) result in an inhomogeneous and coarse non-uniform microstructure in the surface layers.

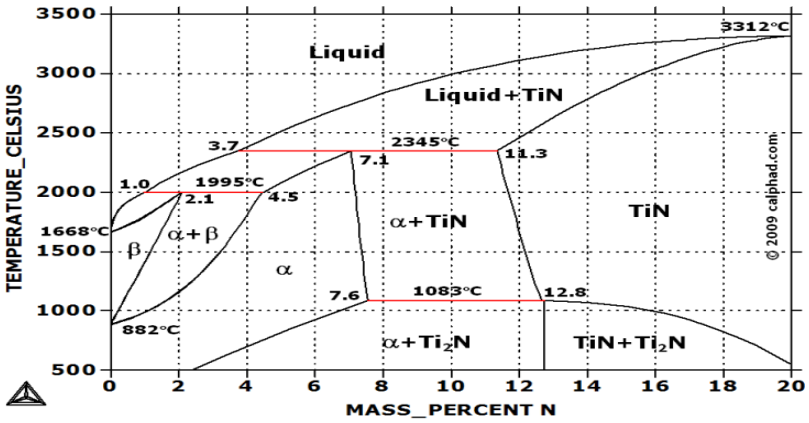

Figure 2.7 : Binary phase diagram of Ti and N.

The alloying elements have different solubility and diffusion coefficients in α- and β-phases of titanium. According to studies in reporting the diffusion constants, the diffusion mobility of alloying elements is decreased in a sequence Fe>Mn>Zr>Cr>Al>Sn>Nb>V>Mo. With regard to solubility, the solubility of zirconium is unlimited, and tin and aluminum are characterized by high solubility in α- titanium [23]. Vanadium, molybdenum and niobium are less soluble in α-titanium but dissolve indefinitely in β-titanium. Iron, chromium and manganese are limitedly soluble in β-titanium and solubility in α-titanium is small, Figure 2.8 shows this ratio with change of temperature. Iron, manganese and chromium are more actively redistributed in surface layers because their solubility is minimal and diffusion mobility is the highest. The solubility of zirconium, aluminum and tin in α-titanium is high and diffusion mobility is low. Therefore, the substantial redistribution of these elements does not occur. Molybdenum, vanadium and niobium more actively redistribute than zirconium, aluminum and tin but weaker than iron, manganese and chromium [23]. Except for diffusion, there is the concentration of β-stabilizing elements separated from solid solution of nitrogen in α-titanium on the boundary of nitride - gas-saturated areas, even with high diffusion constants. These effects are caused by unoccupied bonds between atoms located on the phases' interface and possible anomalous value of electron concentration in these areas.

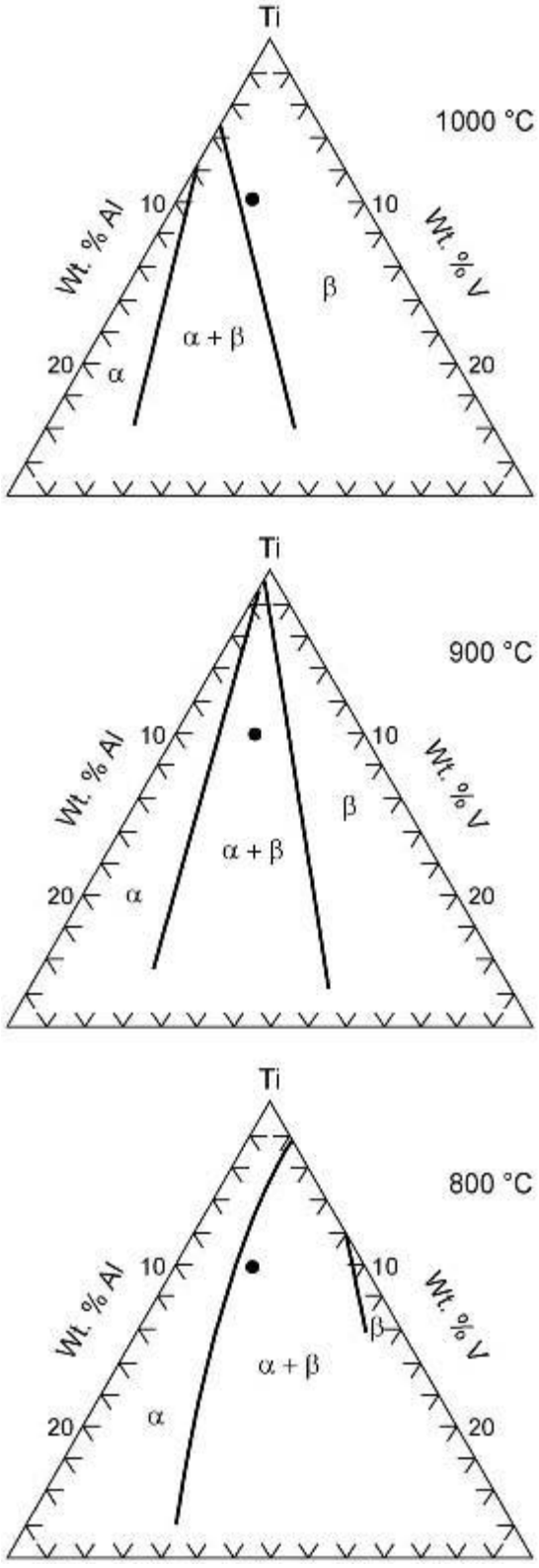

Figure 2.8 : Effect of nitriding temperature.

The difference also can be explained by whether these temperatures are above or below the β-transus and an alloy treated at these temperatures can have different microstructure because of different proportions of the phases during processing.

Thus, it can be understood that the β-transformation temperature significantly affects the microstructure .Different temperatures of nitriding influence the consisted diffusion zones, too. Moreover, diffusion kinetics and mechanism are affected by the varied treatment temperatures. As a result of this, different morphologies occur. The alterations of the mechanism and kinetics of diffusion may result in some segregations that change the morphology. Moreover some transformations occurred during cooling after nitriding at different temperatures can cause some differences in morphology of the structure. [21-23].

The nitriding temperature affects the crystal structure of the substrate as well. With increasing process temperature, the lattice parameters of α-phase increase, too. This situation shows that the concentration of nitrogen on the surface also rises with ascending temperature. This increase does not depend on the cooling rate or aging treatment .The microhardness values increase according to the increasing nitriding temperature. The reason of this enhancement is the development of an inhomogeneous structure at elevated temperature values. The nitriding temperature also influences wear resistance. Higher nitriding temperature values provide higher wear resistance values, because harder and thicker nitride layers can develop on the surface with increasing temperature [23-26].

The thickness of the nitrided layers increases with the increasing process time [21]. The total depths of these layers increase with ascending treatment time [23, 44]. However, the development rates of these layers vary according to the nitrogen diffusivities in different phases such as α- and β- phases and their different rates in the alloys [21]. Improvement of the surface hardness is mainly accomplished through gas nitriding. However, raising the hardness does not necessarily impove the wear behavior of titanium alloys considerably. The hardness values increase with increasing nitriding time and temperature. Because of the formations of the new phases such as TiN during nitriding, the surface hardness increases. [24] According to B. Zhao et al., the specimen made of TiAl based alloys had a maximum Knoop hardness value of 1629 kg/mm^2, when this specimen was processed in ammonia at 1213 K for process time prolonged to 50 h [22-25].

The nitriding time differences affect the physical appearance as well. With increasing time, the surface color of the specimen changes according to the amount of nitriding. After completing the nitriding treatment, the surface of the sample is covered with

TiN and the surface color turns into golden yellow generally. For example, β21s alloy is silver-grey colored before nitriding. After process at 850 °C, the surface color of this specimen became grey. After treatment at 950 °C for 1 and 3 h, the surface of the sample began to have a white colored appearance. After nitriding at 950 °C for 5 h, the surface of the sample became grey colored. A golden colored surface was seen after nitriding at 1050 °C [14]. The nitriding time also affects the resistance against wear. A longer process time can cause an increase in hardness and thickness of the layers on the surfaces of the samples and with this development, the wear resistance value becomes higher [18].

2.2.3.2 Kinetics of nitriding

After nitrogen atoms adsorb onto the surface layer, the high chemical potential of nitrogen constitutes the driving force for the interstitial diffusion of nitrogen into the solid bulk.

The diffusion coefficient for interstitial atoms, D, follows an Arrhenius type dependency, with an activation energy which is equal to the enthalpy barrier to atomic migration. It can be expressed as follows [1, 2]:

$$D_0 = D \exp(-Q/RT) \quad \textbf{(2.1)}$$

Where D_0 is a temperature-independent pre-exponential constant, Q is the activation energy for the diffusion of nitrogen into metal substrate, *T* is the absolute temperature in Kelvin, and *R* is the gas constant (8.314 J mol^{-1} K^{-1}).

Fick's law of diffusion can be applied in all cases, using a diffusion coefficient which depends on composition where appropriate. However, it cannot be used to calculate composition profiles in materials except under steady–state situations, i.e. when the composition at all points remains constant with time. However in the majority of cases, we are concerned with the increasing of weight profiles as a function of time. Nitriding is a non-steady state diffusion process in which the weight increases with increasing time. The weight changes (in mg) of the Titanium in different time are formulated as**:**

$$\Delta m/S = K_{\times} t^{n} \quad \textbf{(2.2)}$$

Where *t* is nitriding duration (hour) and *n* is the reaction index; It is obvious that the growth kinetic is linear if *n* = 1 and parabolic if *n* = 0.5 and *K* is the rate constant that can be obtained using following:

$$K = K_0 \exp(-Q/RT) \quad \textbf{(2.3)}$$

The constant K_0 is computed using numerical values obtained as equation **(2.3)**. The calculated constant K_0 is then used in mathematical models presented by Matychak et al. The predetermined temperature and duration of saturation process allow for the prediction of the thickness of the phases formed during the nitriding process or as a way to determine the time and temperature parameters required for nitriding. The results of investigating the kinetics of the saturation process of titanium alloys by nitrogen demonstrate the alloying influences on nitriding rate.

Higher nitriding temperature and prolonged nitriding duration elicit thicker nitride layer and the wider NDZ .The thickness variations (in μm) of the nitride layer or NDZ (X_{NL} and X_{NDZ}, respectively) are formulated as

$$X_{NL} \text{ or } X_{NDZ} = K\, t^n \quad \textbf{(2.4)}$$

Where t is nitriding duration (hour) and *n* is the reaction index; It is obvious that the growth kinetic is linear if *n* = 1 and parabolic if *n* = 0.5, and K is the rate constant that can be obtained using equation **(2.3).** Many titanium production processes, such as solution and aging heat treatments, hot working and recrystallization, are diffusion dependent. A selection of diffusivity data is shown in Figure 2.9 in the form of Arrhenius plots [2]. It can be seen that the self-diffusion of titanium in the β phase is about an order of magnitude three times faster than the self-diffusion in the α phase. The discontinuity of the Arrhenius curve at the transformation temperature is a unique phenomenon for the Group IV elements [44-48].

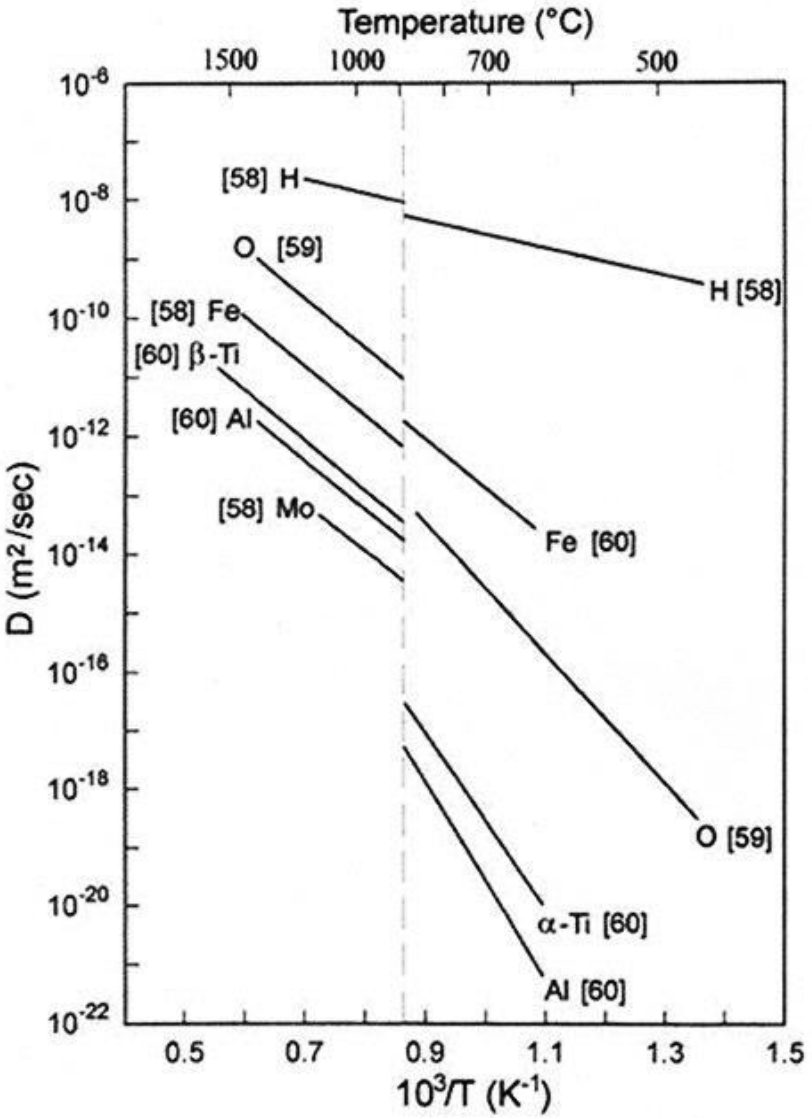

Figure 2.9 : Arrhenius diagram of various alloying elements in titanium [1].

3. EXPERIMENTAL PROCEDURES

3.1 Materials

ASTM Grade 4 (commercial purity titanium, CP) and ASTM Grade 5 (Ti-6Al-4V) and biomaterial (Ti6Al7Nb) alloys (Table 3.1) are studied in this work for nitriding experiments. Disc shaped samples of were machined from the as-received rods having 8 mm diameter with a thickness of 5 mm. Later, machined surfaces were ground with SiC abrasive papers up to 2400 mesh and polished with fine grade Al_2O_3 paste prior to gas nitriding process.

Table 3.1 : The chemical analyze of examined titanium alloy.

Component (Wt. %)	C	Fe	H	N	O	Ti	V	Nb	Al
Cp-Titanium grade-4	Max 0.10	Max 0.2	Max 0.015	Max 0.03	Max 0.18	99.5	-	-	-
Ti6Al4V	0.02	0.22	-	0.01	0.18	Re	4.02	-	6.08
Ti6Al7Nb	0.08	0.25	-	0.05	0.20	Re	-	7.30	6.01

3.2 Nitriding Process

Nitriding was conducted isothermally at temperatures of 950, 1120 and 1250 °C in an atmosphere controlled furnace (Nabertherm VHT08/22GR). After placing the samples, the chamber of the furnace was purged three times by the combination of vacuum and nitrogen gas feed. After this procedure, nitrogen gas was continuously introduced into the chamber with a flow rate of 200 m^3/h. After reaching to the preset nitriding temperature, samples were kept at this temperature for 3, 7 and 12 hour. Samples were then cooled to room temperature in the chamber of the furnace.

3.3 Microstructural Characterization of the Nitrided Samples

Structural evaluations of the nitrogen exposed surfaces were made by microscopic examinations and X-ray diffraction (XRD, Philips RV 3710 diffractometer) analysis. The XRD studies were performed by using Cu Kα radiation with the incidence beam angle of 2°. Microscopic examinations were conducted on the cross-sections of the

nitrided samples after gentle grinding, polishing and etching with the mixture of 5% HNO_3 and 10 % HF solution. Microscopic examinations were made by utilizing a light optical microscope (LOM, Leica CTR 6000) and scanning electron microscope (SEM, Philips SFG) equipped with energy dispersive X-ray spectroscopy (EDX).

3.4 Hardness and Adhesion Tests

Microhardness tests were applied by HMV Shimadzu conventional microhardness test device in HV scale under a load of 50 g. The microhardness measurements were conducted on the cross-section of the samples in order to determine the case depth profiles.

The adhesion characteristics of the TiN layers were evaluated Rockwell C adhesion test conducted according to the standard ASTM C1624-05(2015). Indentations were made on the nitride surfaces under a load of 150 kg. Afterwards imprints and their surroundings were examined by light optical microscopy at 50X magnification in order to detect the failure on the TiN layer.

3.5 Wear Tests

Wear tests applied to the nitrided specimens were conducted on a Tribotester device with reciprocating movements. Al_2O_3 balls (6 mm dia.) rubbed on the nitrided surfaces of the samples under the conditions of the temperature range of 20-30 ºC and the humidity rate between 30-40%. The testing time was approximately 330 min. The length of the wear track was 2 mm and the sliding speed of the Al_2O_3 ball was 0.303 m/s. During wear tests, the frictional force data was recorded. The load of the dry sliding wear test was 5 N. The results of the wear test were analyzed by examining the 2D profiles of the wear tracks. The horizontal and vertical distances of the wear tracks were measured by a profilometer (Veeco Dectac 6M) using a stylus under a 1 mg and the measured distance was 1000 μm. The wear tracks of the nitrided surfaces were analyzed by the SEM. The mean values of the cross sectional wear track areas (μm^2) of the each specimens were calculated according to Equation **(3.1)** and then used for determining relative wear resistance of worn samples as mentioned in Equation **(3.2)**.

$$\text{Wear track area} = \frac{\text{Width of the track} \times \text{Depth of the track} \times \pi}{4} \quad \textbf{(3.1)}$$

$$\text{Relative wear resist. of nitrided sample} = \frac{\text{Wear track area of the untreated sample}}{\text{Wear track area of the nitrided sample}} \quad \textbf{(3.2)}$$

4. RESULTS

The results of microstructural examinations, hardness and adhesion tests and finally wear tests conducted on the nitrided Cp-Titanium, Ti6Al4V and Ti6Al7Nb are sequentially presented below:

4.1 Cp-Titanium

4.1.1 Microstructural features

As a result of the nitriding process, the color of the sample surfaces changes from metallic grey to golden (which is the characteristic color of TiN). The XRD patterns of the samples nitrided at 950, 1120 and 1250 °C for durations of 3, 7 and 12 hours, respectively, are illustrated in Figure 4.1. The XRD analysis of the surface indicates that the surfaces of the samples nitrided for durations of 3 to 12 hours in 950°C are not coated with titanium nitride completely. On the XRD pattern α-Ti peaks were appeared and local dark blue zones were detected at nitrogen exposed surface. Over transus temperature at 1120 and 1250 °C the samples were completely covered with TiN layer, which matches with the golden appearance of the samples. Detection of α-Ti peaks on the XRD patterns along with the TiN peaks confirms that NDZ has α- Ti structure.

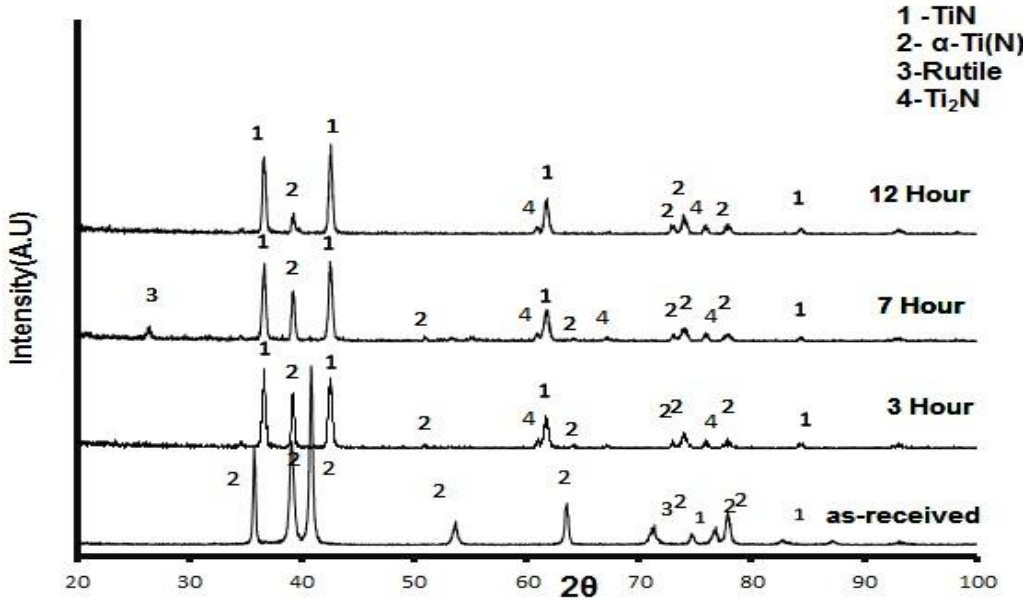

(a)

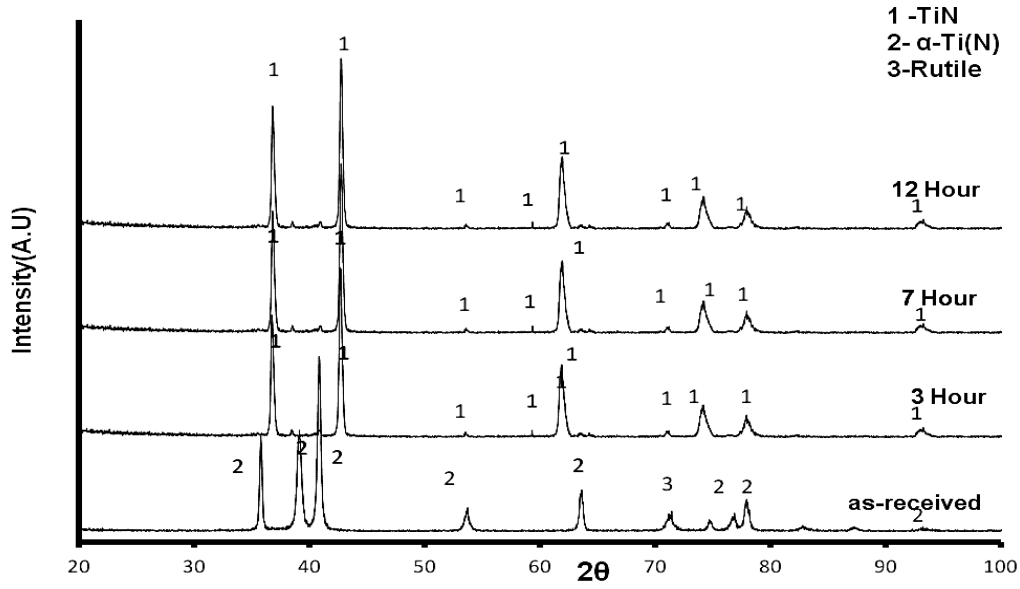

(b)

Figure 4.1 : XRD patterns of the samples nitrided a) 950 °C and b) 1120 °C and 1250 °C for Cp - titanium.

The cross-sectional SEM micrographs of Cp-Titanium samples nitrided at 950, 1120 and 1250 °C are presented in Figure 4.2. As a general trend, higher nitriding temperatures and longer exposure times encourage formation of nitride layers. Observations showed that the interface between TiN layer and the NDZ is straight. The numerical atomic percentage of nitrogen in TiN and NDZ are listed in Figure 4.2 (d). As expected, highest nitrogen concentration was obtained in the TiN

layer. In the NDZ, nitrogen concentration decreased towards the substrate. The results of line EDX analysis are shown in Figure 4.3. Decreasing titanium content and increasing nitrogen content in the nitride layer is confirmed by X-ray elemental mapping analyses presented in Figure 4.4.

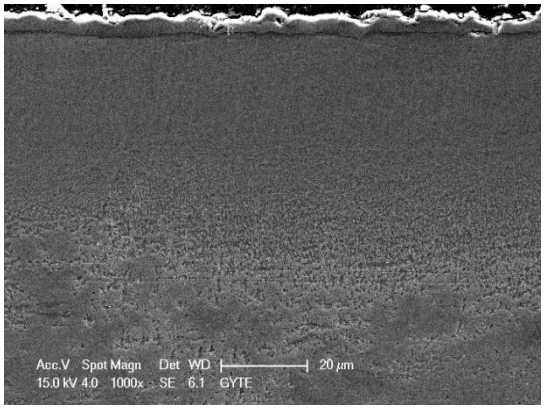

(a)

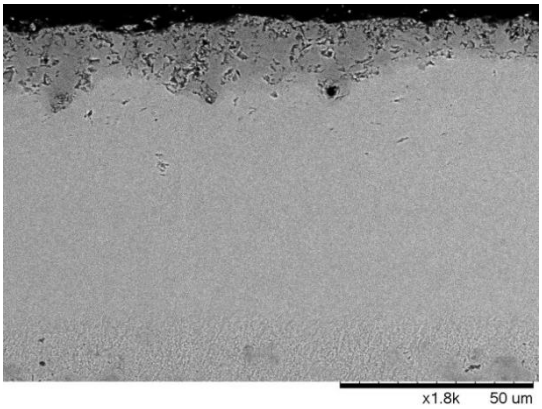

(b)

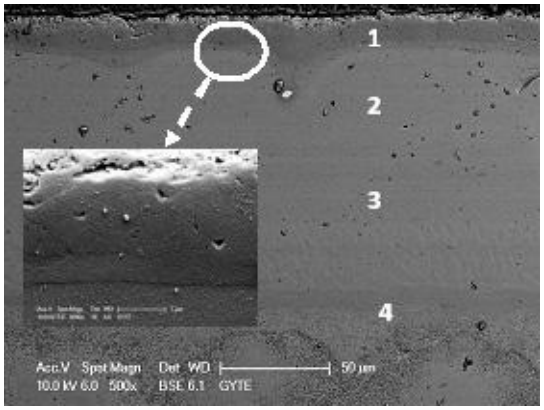

(c)

Numbers in Figure	Location in Figure	Ti	N
1	TiN	23.35	77.74
2	NDZ	84.39	15.61
3	NDZ	86.70	13.30
4	NDZ	87.07	12.93

Figure 4.2 : Cross-section SEM micrographs of the samples nitrided Cp-Titanium at a) 950 °C, b) 1120 °C, c) 1250 °C for 12 h and d) EDX spot analysis of the main elements at different locations.

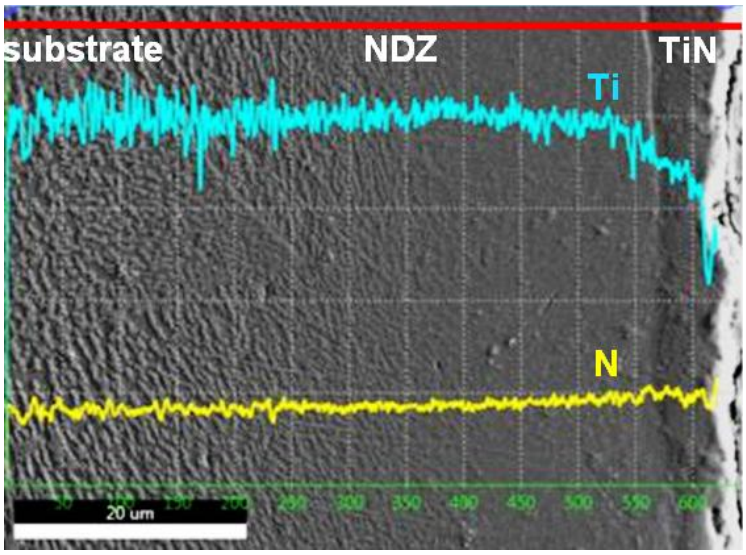

Figure 4.3 : Line scans analysis of Cp-Titanium showing distribution of the main elements after nitriding at 1250 °C for 12 hours.

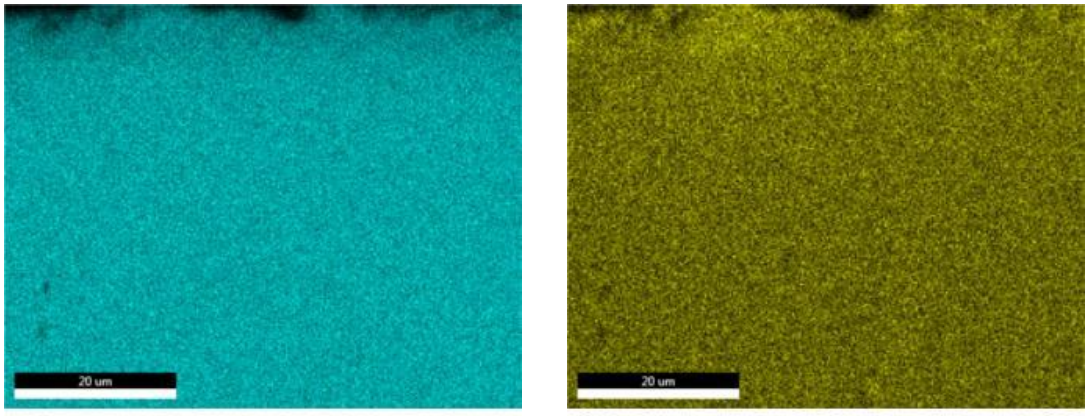

(a) (b)

Figure 4.4 : X-ray elemental map analysis of the main elements after nitriding Cp-Titanium at 1250 °C for 12 h (a) titanium (b) nitrogen.

4.1.2 Nitriding kinetics

4.1.2.1 Analyses of nitriding kinetic according to weight change

Figure 4.5 illustrates the weight change per unit surface area, with respect to time in ($\Delta m/S$), where Δm (mg) and S are weight gain and the surface area of the sample (cm^2). The weight changes of the Cp-Titanium with respect to time are formulated in Table 4.1. The equation was used for finding nitriding rate costant K and then by using Arrhenius diagram nitrogen diffusion activation energy was calculated. Table 4.1 shows the weight gain kinetics of nitriding followed parabolic path with n = 0.5 and activation energy was calculated as 113 kJ/mol.

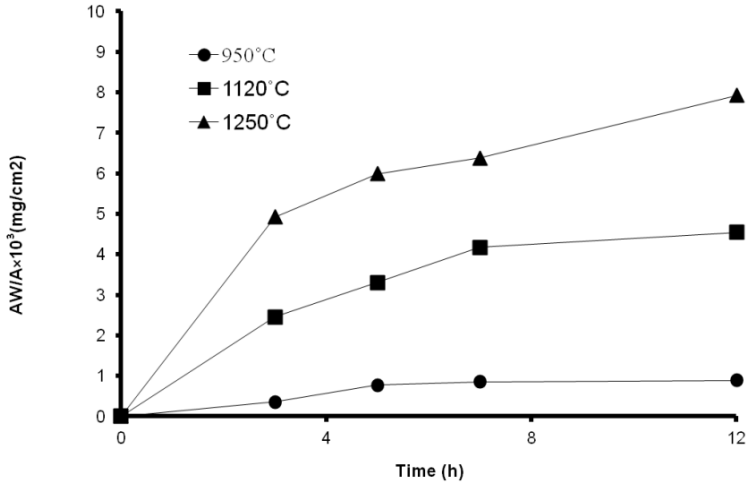

(a)

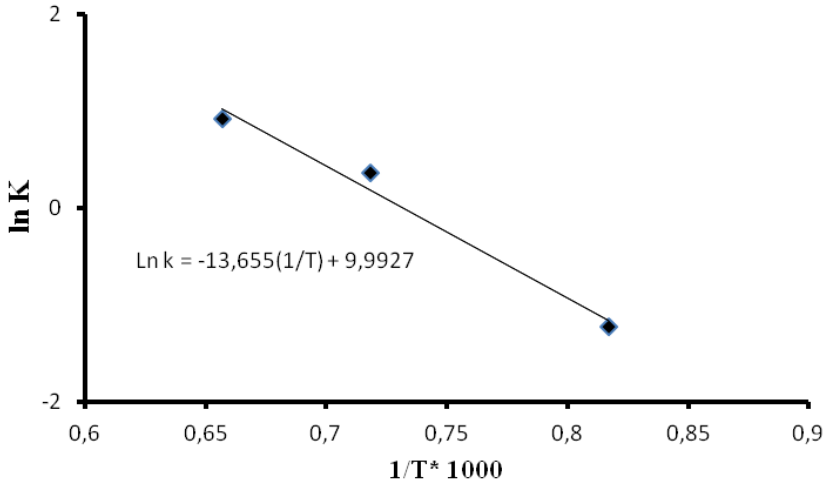

(b)

Figure 4.5 : a) Weight change rate of Cp–Titanium and b) related Arrhenius diagram.

Table 4.1 : Empirical equations derived from Figure 4.5 according to Equation (2.2).

	950 °C	1120 °C	1250 °C
Cp-Ti	$\Delta m/S = 0.29 \times \sqrt{t}$	$\Delta m/S = 1.42 \times \sqrt{t}$	$\Delta m/S = 2.46 \times \sqrt{t}$

4.1.2.2 Analyses of nitriding kinetic according to cross-sectional examination

The cross-sections of the nitrided Cp-Titanium samples were examined with LOM (Figure 4.6) to measure the thickness of the TiN layer and depth of the NDZ with respect to processing parameters. Initially, it could be observed that nitrogen exposed surfaces can be characterized with a TiN layer and an underlying NDZ. At 950 ºC titanium nitride layer became observable after 7 hours of nitriding. By increasing

nitriding operation temperature and duration, the TiN and NDZ layer tend to become thicker.

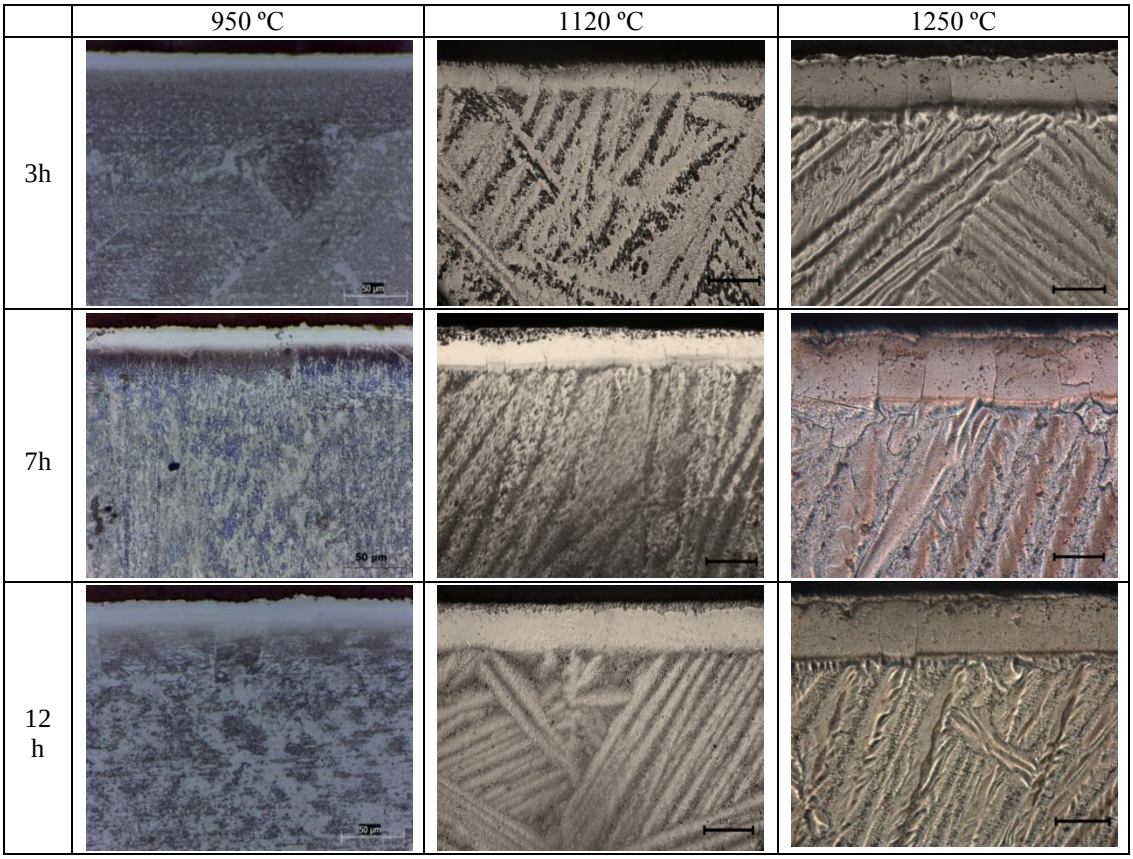

Figure 4.6 : The cross-section micrographs of the Cp-Titanium samples depending on the nitriding temperature and time.

Higher nitriding temperature and prolonged nitriding duration elicit thicker nitride layer and deeper NDZ as depicted in Figure 4.7 and Figure 4.8. The thickness variations (in μm) of the nitride layer or NDZ (X_{NL} and X_{NDZ}, respectively) are formulated in equation **(2.4)** for calculating activation energy of nitrogen diffusion similar to previous section we use thickness instead of weight change in Table 4.2. According to calculations, the growth of nitride layer was linear with n = 1 and the growth of NDZ was parabolic with n = 0.5 in Cp-Titanium.

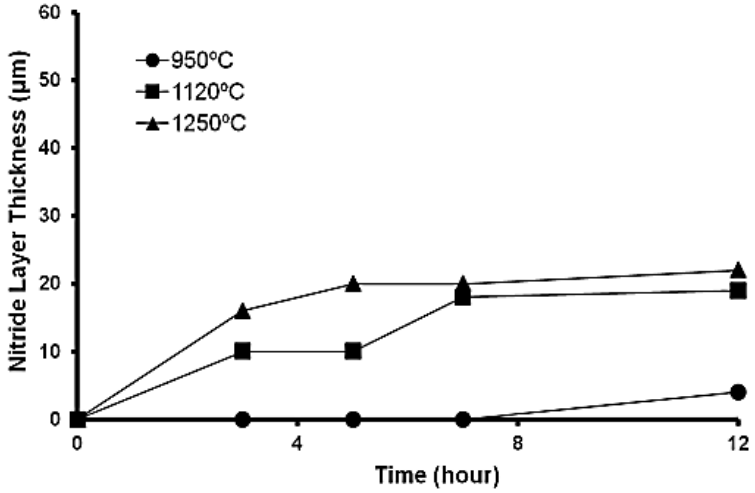

(a)

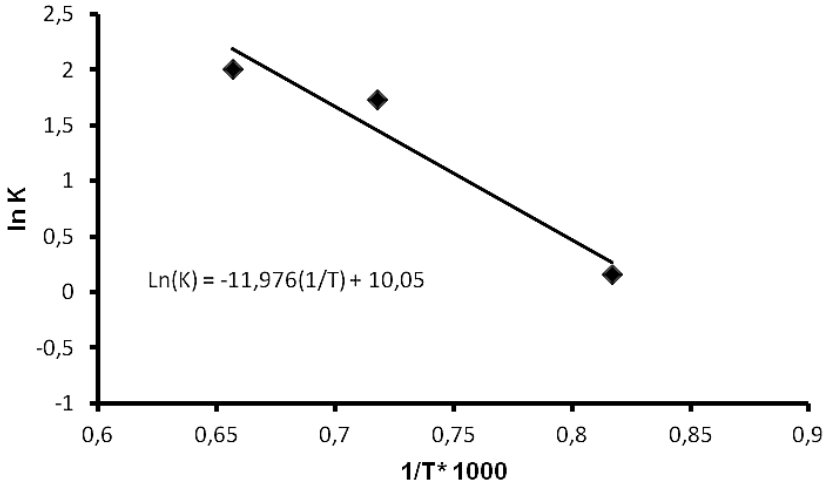

(b)

Figure 4.7 : The variation of nitride layers thicknesses of Cp-Titanium with respect to nitriding temperature and time b) and related Arrhenius diagram.

According to the data listed in Table 4.2, gas nitriding showed linear diffusion kinetics for the growth of the nitride layer on Cp-Titanium, with activation energy of 145kJ/mol. Nitrogen diffusion zone (NDZ) showed parabolic diffusion kinetics, with activation energy of 63 kJ/mol.

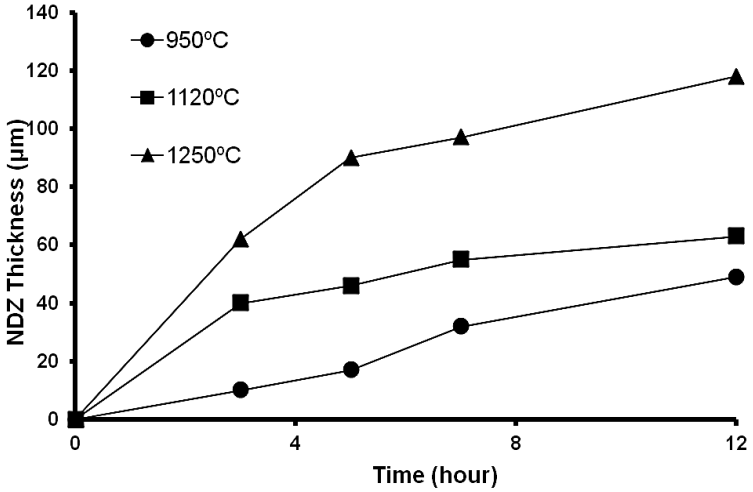

(a)

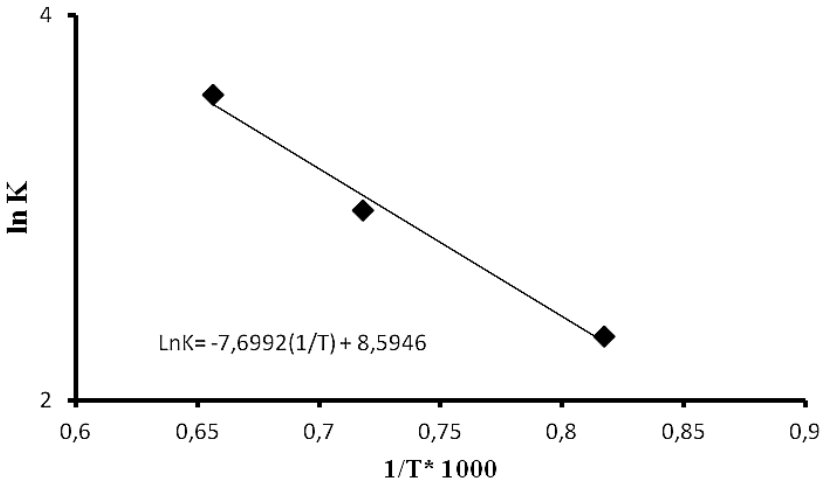

(b)

Figure 4.8 : a) The variation of NDZ layer thicknesses of Cp-Titanium with respect to nitriding temperature and time b) and related Arrhenius plot.

Table 4.2 : Empirical equations derived from Figure 4.7 and Figure 4.8 according to Equation (2.4).

Materials	Layers	950°C	1120°C	1250°C
Cp-Ti	Nitride Layer	$X= 1.17\times\sqrt{t}$	$X = 5.92\times\sqrt{t}$	$X = 7.47\times\sqrt{t}$
	Nitrogen Diffusion Zone	$X= 10.32\times\sqrt{t}$	$X= 19.88\times\sqrt{t}$	$X= 36.14\times\sqrt{t}$

4.1.3 Case Depth Analyses

Figure 4.9 shows the case depth profile as variation of micro-hardness measured on the cross-sections of the samples.The higher the nitriding temperature and time, the harder the surface layer formed. For the nitrided samples, the hardness gradually decreases from the top surface to the substrate, and there is no sharp change between the surface layer and the substrate. The total thickness of the TiN and NDZ with enhanced nitrogen concentration and hardness increased with increasing temperature and nitriding time . The higher the nitriding temperature and time, the harder and thicker TiN layer and NDZ is formed, which is in accordance with microstructural studies shown in Figure 4.6. On the cross section of the sample nitrided at 1250 °C for 12 h, hardness varied from 2810 HV at the surface to 290 HV in the core, at a maximum distance of about 142 μm from the surface. The hardness of the as-received samples was between 220-290 HV. For samples nitrided at 1120 °C for 12 h the surface hardness was 2400 HV and total TiN and NDZ layer thickness was 80 μm. After nitriding at 950 ºC for 12 h surface hardness of sample and total TiN and NDZ layer thickness were around 2020 HV and 50 μm respectively. Nitriding for 3h at 950 ºC produced a thin nitride layer with a thickness that was not measurable with LOM. Decreasing hardness within the TiN layer inward the core can be attributed to the non-stoichiometric behavior of TiN. According to the titanium–nitrogen binary phase diagram, the solubility of nitrogen in TiN varies across a broad range (max 10 wt %).

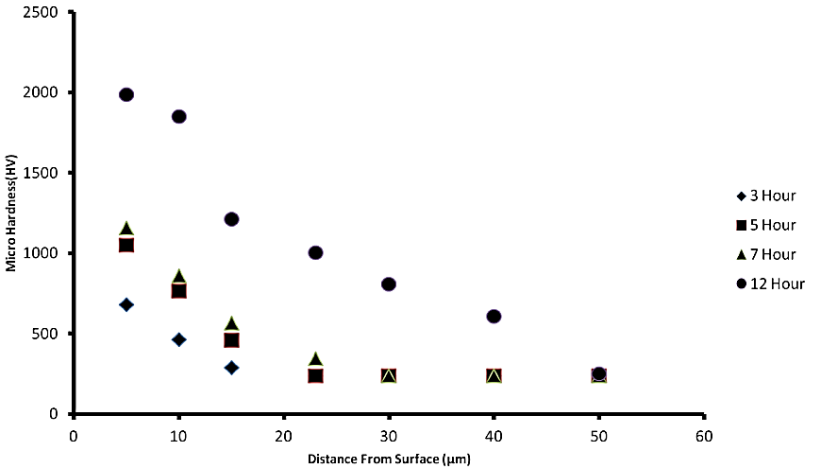

(a)

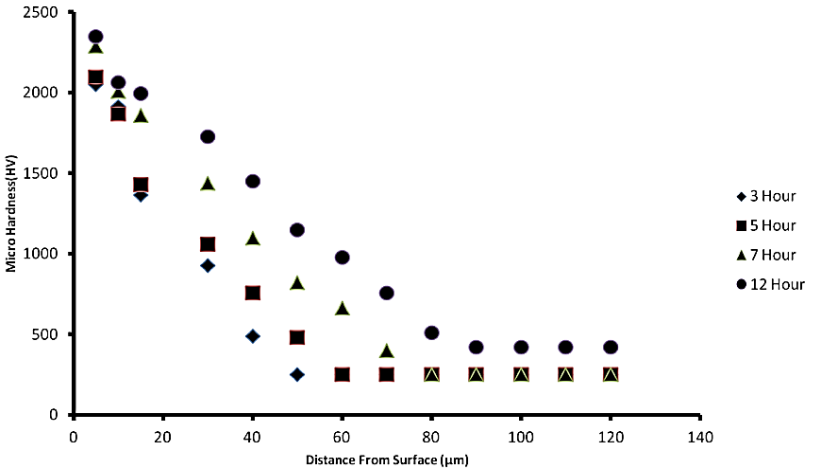

(b)

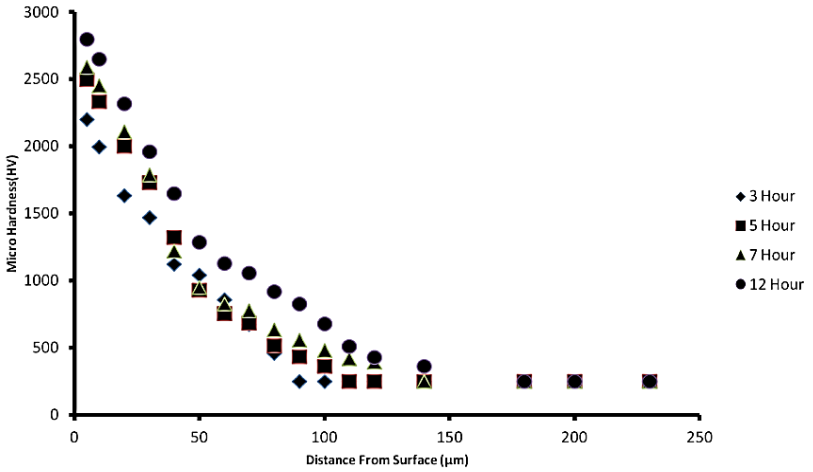

(c)

Figure 4.9 : Micro hardness tests results of nitrided samples at a) 950 °C, b) 1120 °C and c) 1250 °C.

4.1.4 Adhesion Characteristics

The nitride layer can be porous or dense, depending on the nitriding time. With increasing nitriding time , the structure of the layers becomes porous and gradually loses its adherence to substrate. Figure 4.10 shows RC test results confirming decrease in adherence of nitride layer to the substrate with increasing time and temperature . At 950 ºC, cracking and separation of nitride layers were not detected, thus, we can conclude that nitriding below transus temperature (1070 ºC) leads to a robust adherence but with increasing temperature and time nitride layer exhibits brittle behavior.

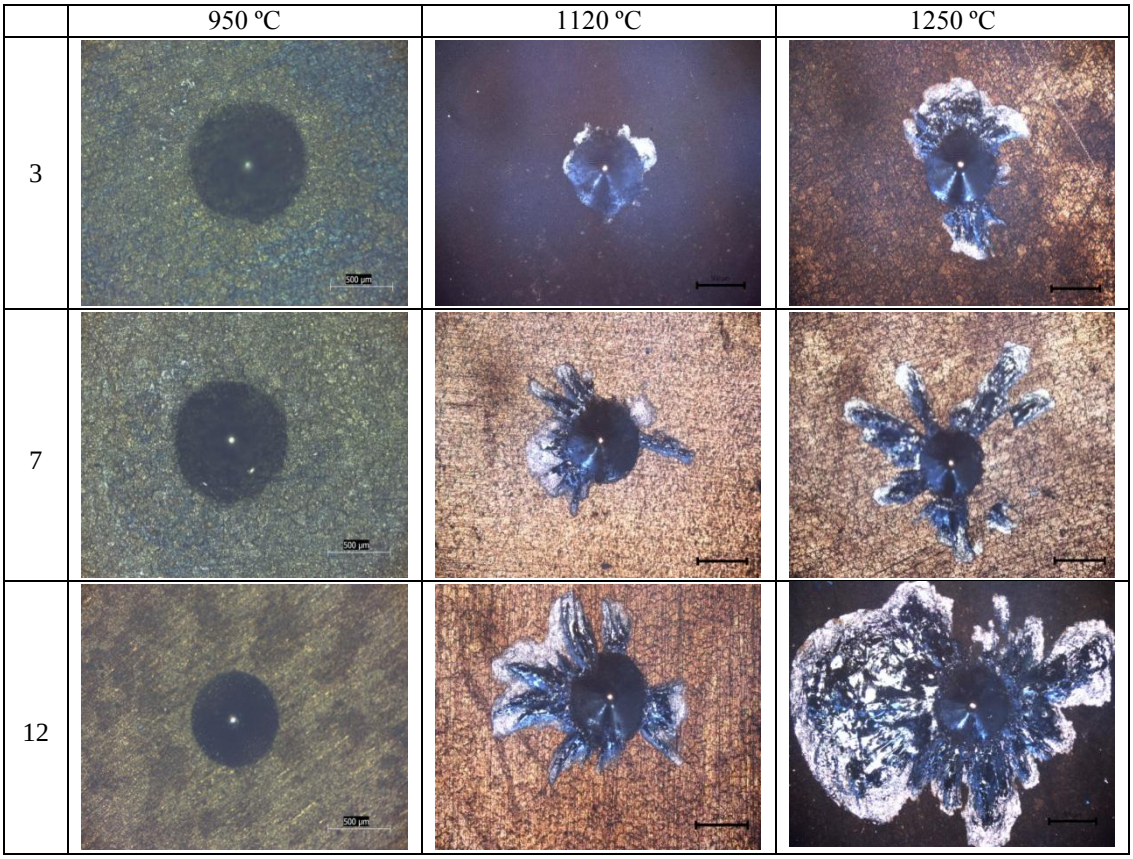

Figure 4.10 : RC test results of Cp-Titanium of nitrided samples at a) 950 °C, b) 1120 °C and c) 1250 °C.

4.1.5 Wear resistance

Figure 4.11 presents a micrograph showing the high wear rate, intemperate plastic deformation and heavy ploughing on the surface of the as-received Cp-Titanium sample subjected to dry sliding wear test. The low abrasive wear resistance was attributed to the low hardness of the Cp-Ti and also to its high ductility and chemical activity which gave rise to a strong tendency for adhesion. The morphology of the

worn surface indicated that the presence of fracture, craters and material removal were caused by tearing. The sliding wear of metal alloys can be described by the evolution of the following phenomena: surface and subsurface plastic deformation, formation of debris and materials transfer, reaction with the environment and mechanical mixing.

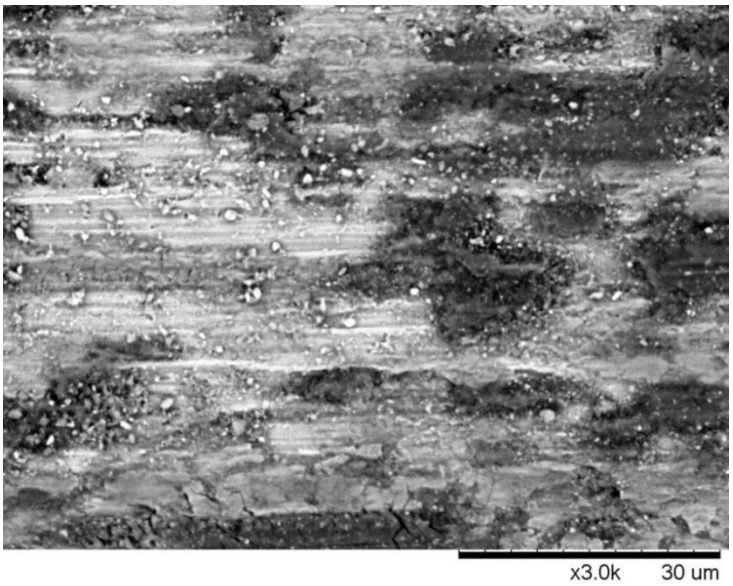

Figure 4.11 : Wear track image of as-received Cp-Titanium.

During adhesive wear, titanium and its alloys show an adhesive behavior called "stick-slip". This stick-slip behavior occurs because of the strong adhesion property of titanium. In the beginning of the wear test, the real contact area grows with ascending tangential force associated with junction growth. The surfaces of the specimen and the counterface (for example, Al_2O_3 ball) contact each other adhesively, which is why this is known as "stick" behavior. After that, if the applied force overcomes induces adhesive strength, the junction will be broken; thus this behavior between the surfaces is called "slip". If this "slip-stick" behavior is continuous, a wide fluctuation can be observed in the tracks of friction, as shown in Figure A.1. The reasons for titanium exhibiting a poor adhesive wear behavior are its reactivity and crystal structure. Moreover, electron structure, adhesion behavior, ductility, thermal conductivity and inadequacy of lubricants are the additional reasons for the low adhesive wear resistance of titanium and its alloys. Additionally, titanium and its alloys also have low abrasive and fretting wear resistances. Because of the low hardness values, the abrasive wear resistances of Ti and its alloys are low as well. During fretting wear, some wear mechanisms such as abrasive, adhesive and

oxidative wear can occur at the same time. Using surface treatments, changes nature of the titanium surface and thus solves these problems. With techniques like thermo-chemical processing, there is a compound layer of titanium with very high hardness values. In this way, while the tribological properties are enhanced, the mechanical features are enhanced as well [4-17].

Cp-Ti samples nitrided at 1120 and 1250 °C exhibited a wear mechanism different from the as-received Cp-Titanium as can be seen in Fig.4.12. On these nitrided samples wear progressed on the TiN layer so that shallow scratches were detected on the worn surfaces. No transferred material was identified on the counterface (Fig.4.13). In the case of the Cp-Ti samples nitrided at 950 °C, wear mechanism was almost identical with that of the as-received sample. This can be attributed to the TiN layer lacking sufficient thickness and the progress of wear on the NDZ. 2D profiles of the wear tracks formed on the nitrided Cp-Ti samples are presented in Figure A.2. For the samples nitrided at 950°C increase of nitriding time caused a reduction in the size of wear track in terms of width and depth. However for the samples nitrided at 1120 and 1250 °C smaller wear tracks were identified after nitriding for 7 hours.

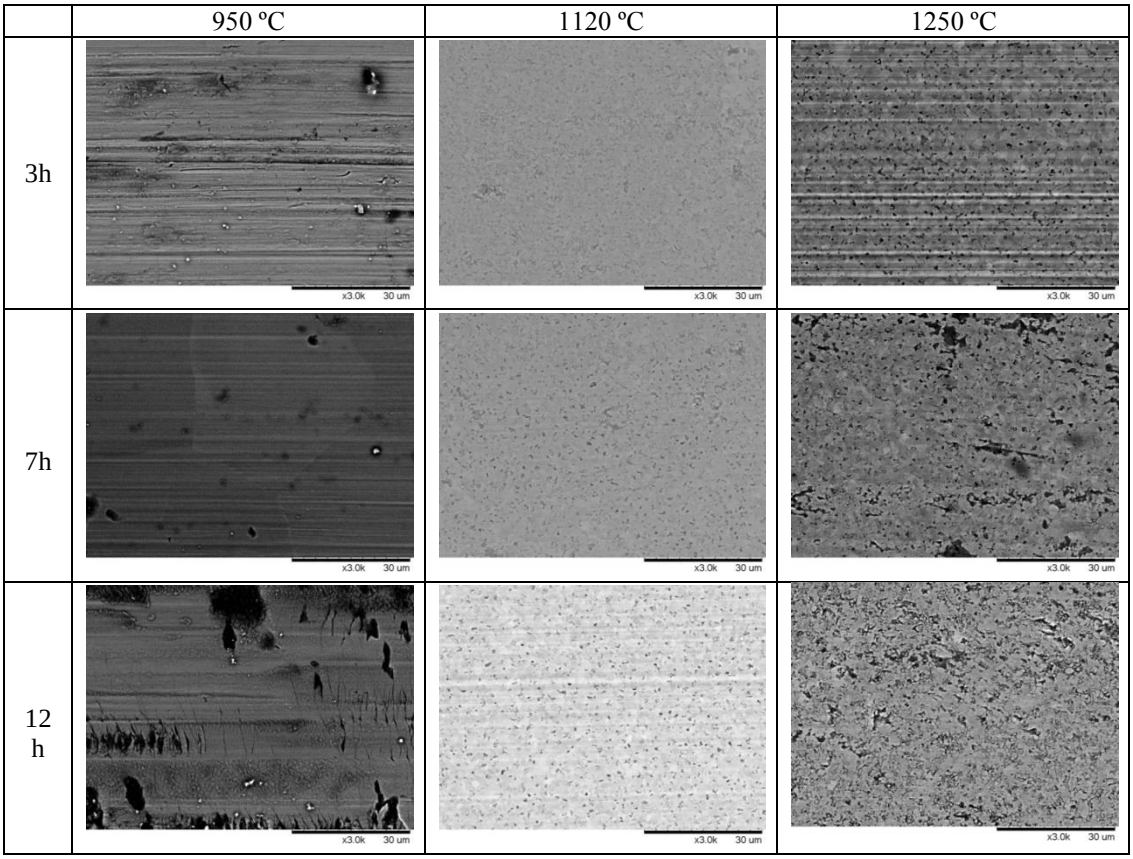

Figure 4.12 : SEM micrograph of the wear track formed on the surface of the nitrided Cp-Titanium.

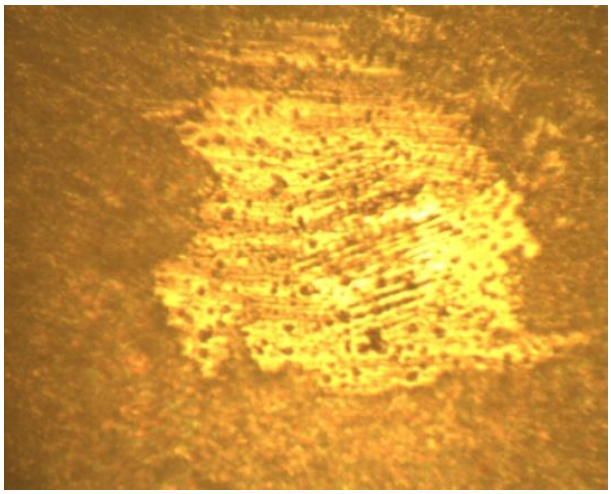

Figure 4.13 : LOM image of Al_2O_3 ball rubbed on Cp-Titanium nitrided at 1120 °C for 7 hours.

The friction coefficient (FC) curve of the as-received sample fluctuated in a very broad range and continuously increased, while nitrided sample's curves were very smooth and retained a constant value after an initial sudden increase. The high FC value of the as-received alloy (0.70) can be attributed to the severe wear taking place during the wear test. The mean values of the wear track areas are listed in Table 4.3.

Table 4.3 : Average wear track area (WT, μm^2) values and fricition coefficent (FC) values of nitrided and unnitrided Cp-Ti samples.

Cp-Ti Sample	Gas nitrided at 950 ^oC		Gas nitrided at 1120 ^oC		Gas nitrided at 1250 ^oC	
	WT	FC	WT	FC	WT	FC
3 H	3140	0.4	490	0.15	765	0.2
7 H	2826	0.5	392	0.25	400	0.25
12 H	863	0.6	647	0.325	686	0.45
Untreated	WT= 22365			FC= 0.7		

The relative wear resistances of the specimens were computed in Table 4.4. It should be noted that the wear resistance of the specimen with the highest value of wear track area is equal to one. In this study, the untreated specimen has the highest wear track area value, therefore its relative resistance has to be assumed as 1. These results show that the gas nitriding process increases the wear resistance of Cp-Titanium 4-grade around 57 times. The highest wear resistance values were observed for the specimens processed at 1120 ^oC for 7 hours.

Table 4.4 : Relative wear resistance values of the nitrided Cp-Titanium.

Cp-Ti Sample	Gas nitrided at 950 °C	Gas nitrided at 1120 °C	Gas nitrided at 1250 °C
3 H	7.12	45.64	29.23
7 H	7.91	57.05	55.91
12 H	25.01	34.56	32.60
Untreated	1		

4.2 Ti6Al4V

4.2.1 Microstructural features

The XRD patterns of the nitrided Ti6Al4V samples are given in Figure 4.14. A uniform, compact layer formed on the surface of the samples. Nitriding process done at 950 ºC for 3 hours induced less dark blue areas on the exposed surfaces in comparison to that of Cp-Titanium. α-Ti peaks appearing on the XRD pattern were related to local dark blue zones observed in samples nitrided at 950 ºC for 3 hours. With increasing nitriding time the entire surface of Ti6Al4V samples turned to golden color. At higher temperature and time (1120 ºC and 1250 ºC) only TiN peaks were detected on the XRD pattern (Figure 4.11 (b)). Although the examined Ti6Al4V alloy has α+β structure, no β-Ti peaks were identified on the XRD patterns.

High magnification SEM micrograph showing the cross sections of the nitrided samples, along with the result of EDX analysis are presented in Figure 4.15.Also line EDX of Ti, Al, V and N elements are shown in Figure 4.16. TiN, NDZ and IZ regions are shown in Figure 4.16. The high affinity of nitrogen to titanium encourages inward diffusion of the vanadium and niobium beneath the nitrided layers. The interfaces of TiN layer/IZ and IZ/NDZ exhibited an wavy morphology (Figure 4.15 (a-c)). The microstructure of the NDZ is very similar to the microstructure of the α-Ti. The SEM examination revealed that the microstructure of the NDZ is homogenous in terms of α-Ti. Unlike the TiN layer, the IZ was enriched by Al atoms (with some V) and sharp decrease was observed in N concentration (in comparison to what was found in the TiN layer, decreasing from ~50 at % to ~20 at %). Beneath the IZ, Al concentration dropped from ~20 at % to ~8 at %, while N concentration increased from ~20 at% to ~30 at%. At further depths, the NDZ concentration of N gradually decreased.

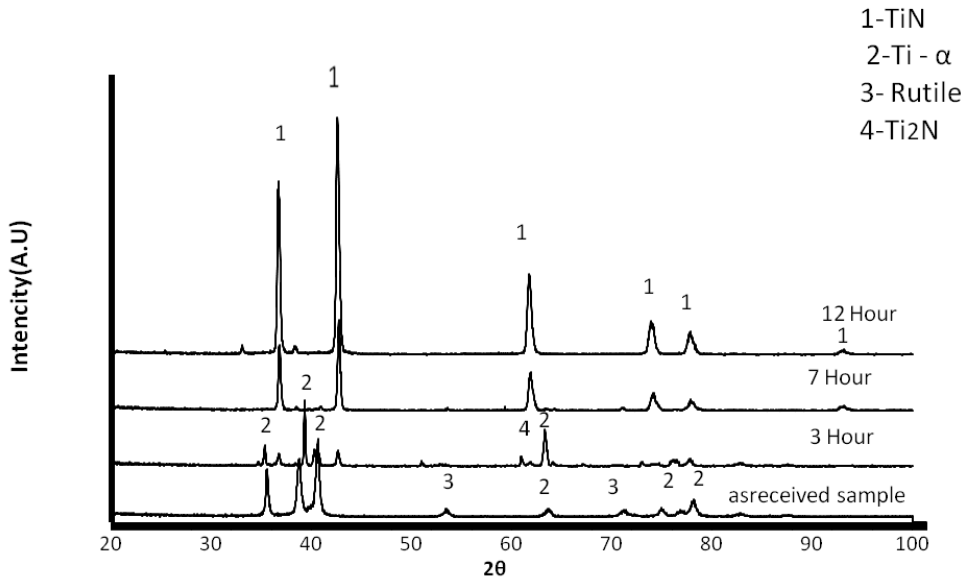

(a)

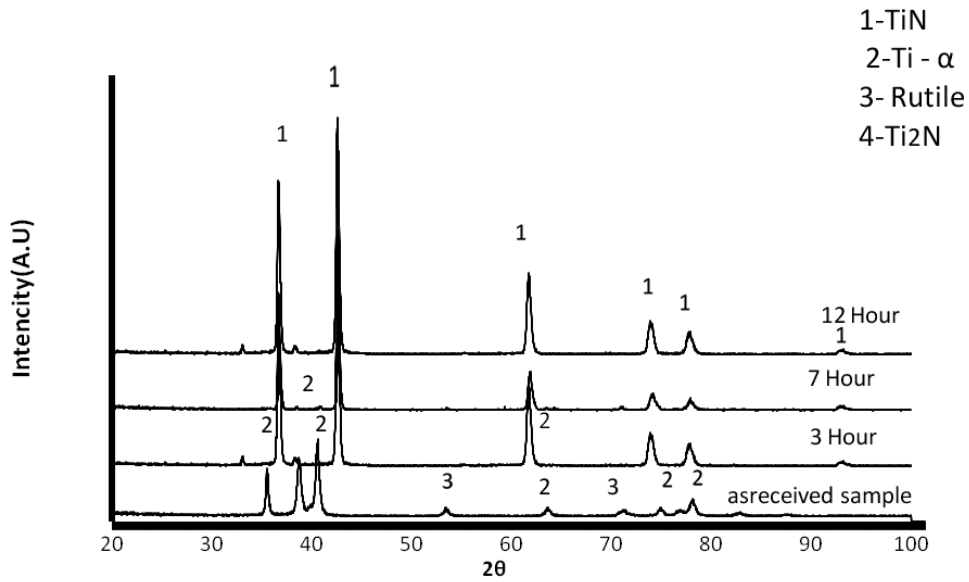

(b)

Figure 4.14 : XRD patterns of the Ti6Al4V samples nitrided at a) 950 ˚C and b) 1120 ˚C and 1250 ˚C .

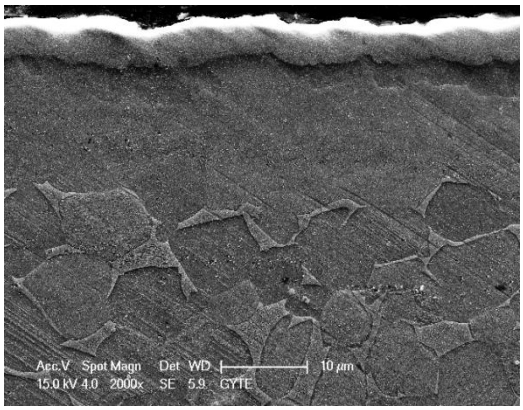

(a)

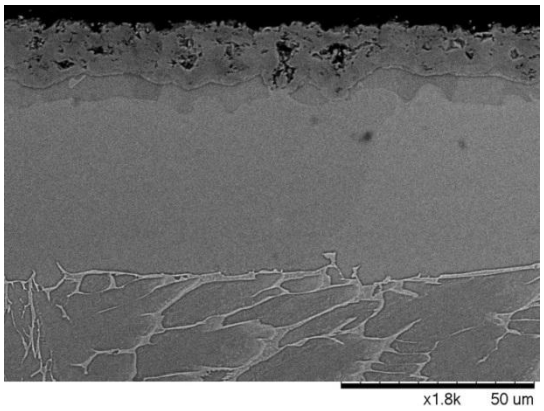

(b)

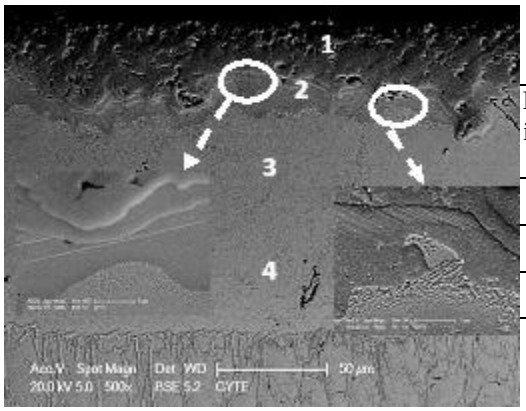

(c)

Numbers in Figure c	Location in Figure c	At. %			
		Ti	Al	V	N
1	TiN	61.14	0.44	0.10	36.93
2	IZ	56.37	20.08	2.41	21.14
3	NDZ	68.79	8.28	2.92	20.02
4	NDZ	18.22	8.62	2.74	18.22

Figure 4.15 : Cross-section SEM micrographs of the Ti6Al4V samples nitrided at a) 950 °C, b) 1120 °C, c) 1250 °C for 12h and d) EDX spot analysis of the main elements at different locations.

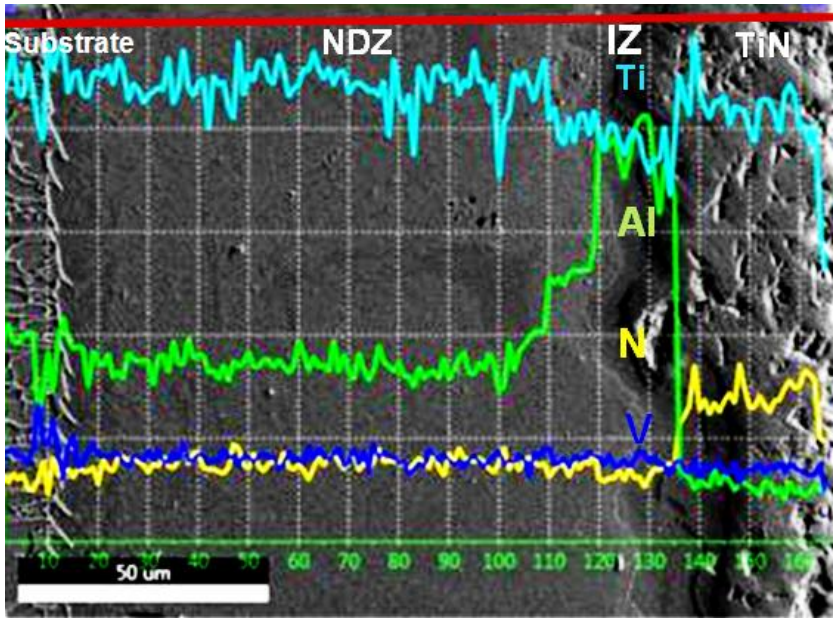

Figure 4.16 : Line scan analyses of Ti6Al4V showing distribution of the main elements after nitriding at 1250 °C for 12 hours.

According to the results of EDX analysis shown in Figure 4.15 the composition of the IZ is different from those of TiN and the NDZ. The TiN layer formed after nitriding at 1250 °C for duration of 12 hours mainly consisted of Ti and N with negligible amounts of Al and V. Unlike the TiN layer, the IZ was enriched by Al (with some V) and nitrogen concentration decreased towards the substrate. The line EDX of Ti, Al, V and N taken from the cross-section of nitrided Ti6Al4V showed high concentration of Al between TiN and NDZ after nitriding at 1250 °C for 12 hours.

The spot analysis and an X-ray elemental map analysis results presented in Figure 4.17 revealed that at 1250 °C the IZ has lower amounts of Ti and N contents in comparison to the TiN layer and NDZ.

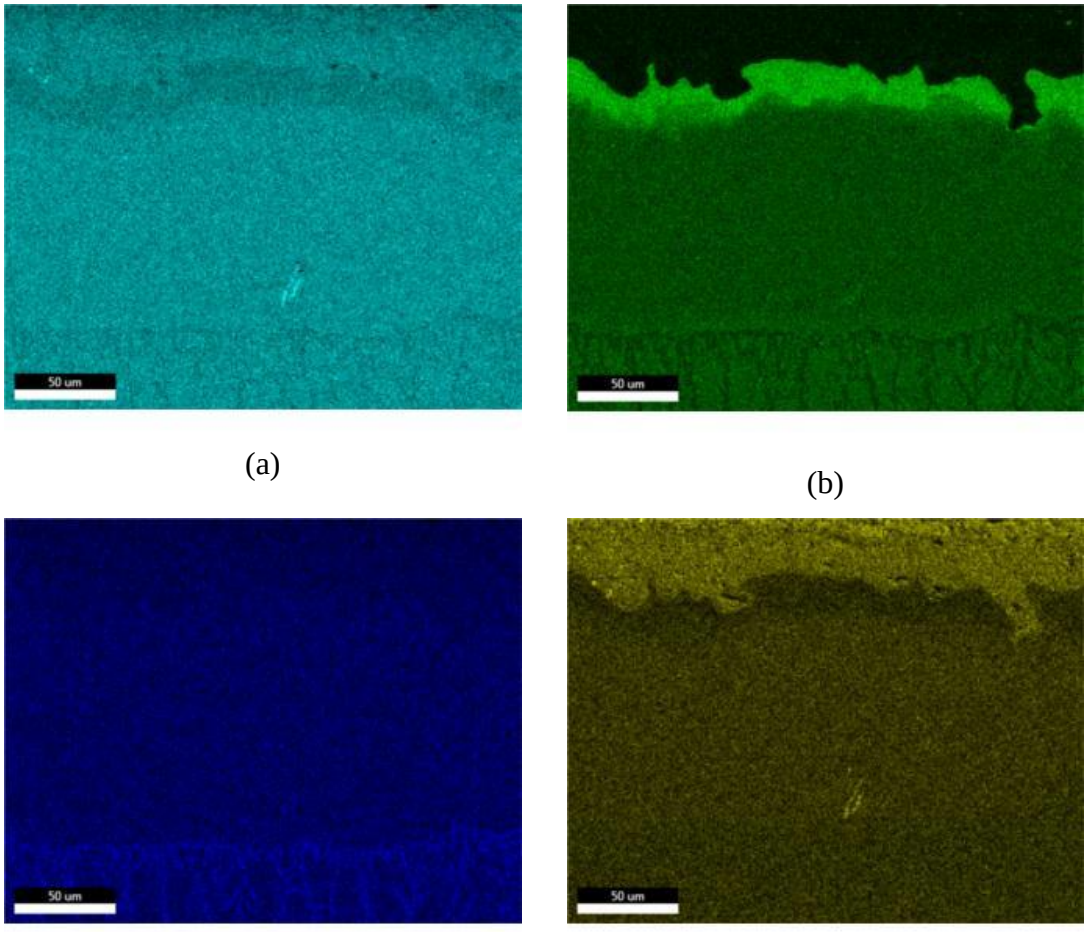

(a) (b)

(c) (d)

Figure 4.17 : X-ray elemental map analysis of the main elements after nitriding Ti6Al4V at 1250 °C for 12 h (a) titanium, (b) aluminum, (c) vanadium and (d) nitrogen.

4.2.2 Nitriding kinetics

4.2.2.3 Analyses of nitriding kinetic according to weight change

Weight changes of nitrided Ti6Al4V and related Arrhenius plot were are presented in Figure 4.18. The data listed in Table 4.5 and the Equation **(2.2)** indicated that gas nitriding of Ti6Al4V has a parabolic behaviour for the diffusion of nitrogen and activation energy was calculated as 118 kJ/mol.

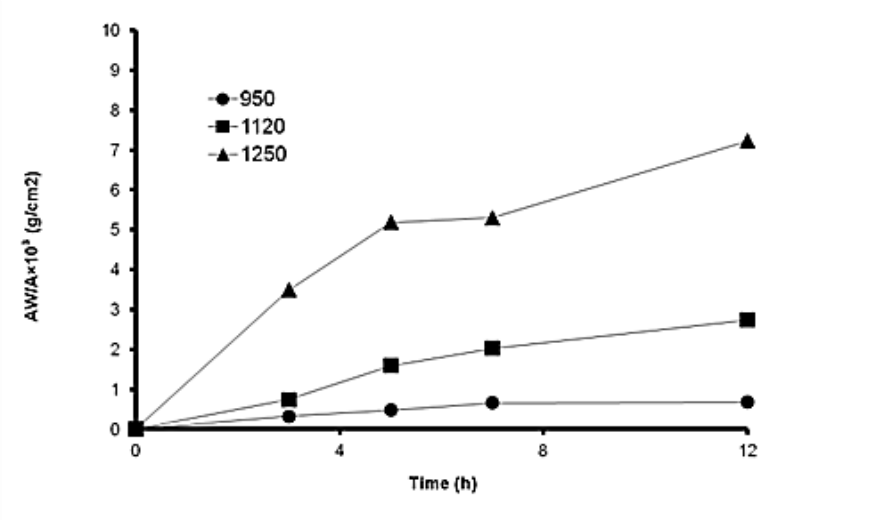

(a)

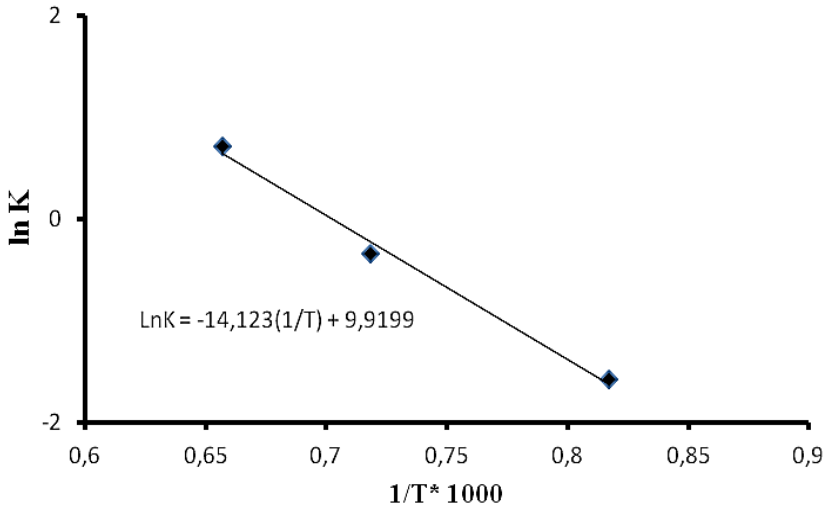

(b)

Figure 4.18 : a) Weight change of Ti6Al4V samples with respect to time and b) related Arrhenius plot.

Table 4.5 : Empirical equations derived from Figure 4.18 according to Equation (2.2).

	950 °C	1120 °C	1250 °C
Ti6Al4V	$\Delta m/S = 0.22 \times \sqrt{t}$	$\Delta m/S = 0.70 \times \sqrt{t}$	$\Delta m/S = 2.14 \times \sqrt{t}$

4.2.2.4 Analyses of nitriding kinetics according to cross-sectional examinations

The cross-sections of the nitrided Ti6Al4V samples were examined with LOM (Figure 4.19) to measure the thickness of the TiN and width of the NDZ and IZ with respect to processing parameters. Increasing nitriding temperature caused the structure to become irregular as seen in Figure 4.19. At temperature 950 ºC, the microstructure consisted of equiaxed α and β titanium grains. In the case of nitriding above transus temperature (1070 ºC), the microstructure was lamellar, which is typical for α+β Ti alloys slowly cooled from temperatures above β-transus [2]. At first glance, nitrogen-exposed surfaces can be generally characterized by a nitride layer and an underlying nitrogen diffusion zone (NDZ) as observed for Cp-Titanium. When the results of LOM analyses were investigated in details, a thin intermediate zone (IZ) can be seen at the upper sections of the NDZ in Figure 4.19.

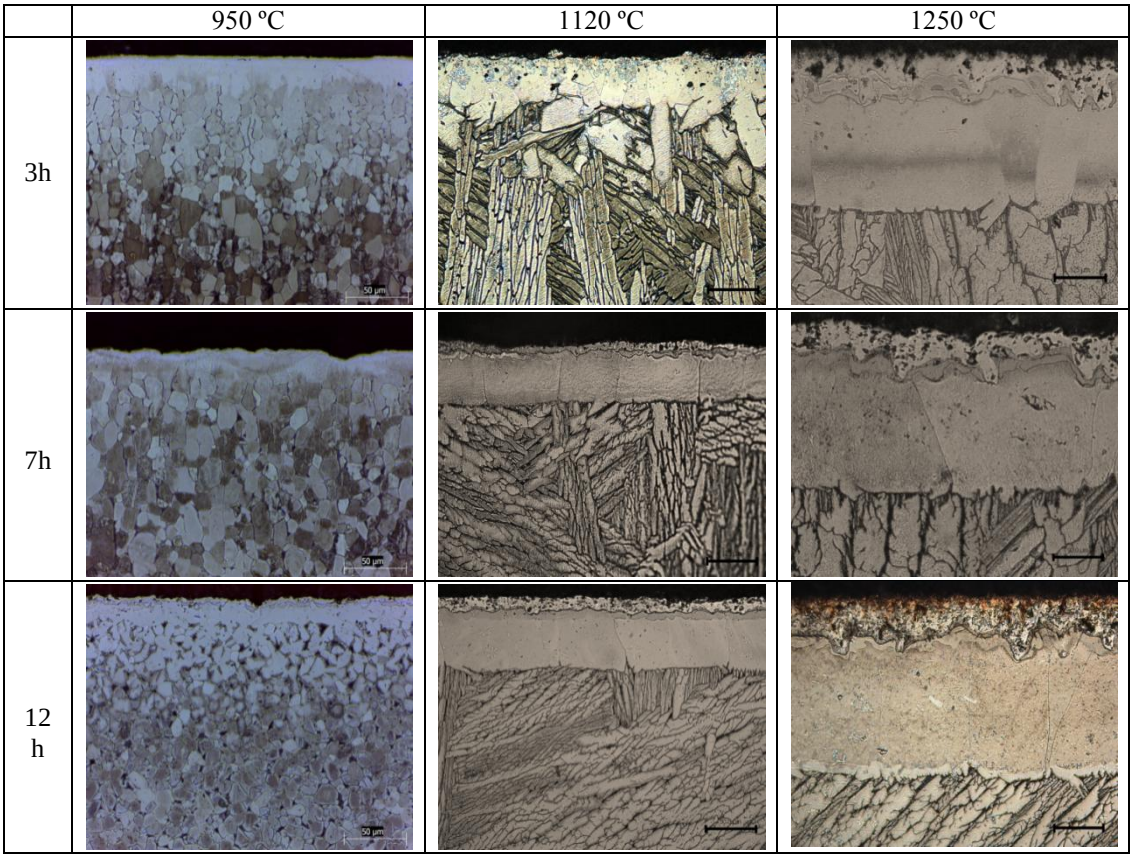

Figure 4.19 : The cross-section micrographs of the Ti6Al4V samples depending on the nitriding temperature and time.

The growth of nitride layers (X_{NL}) was linear with n = 1 as depicted in Figure 4.20 and X_{NL} growth is formulated in Table 4.6. Nitrogen diffusion zone expanded at higher nitriding temperature and for longer nitriding time. According to our

calculations the growth of nitride layer was linear and activation energy was calculated as 119 KJ/mol.

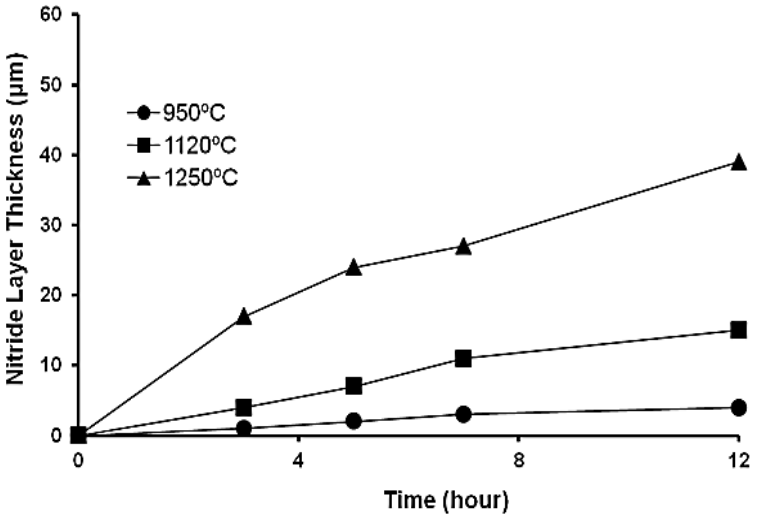

(a)

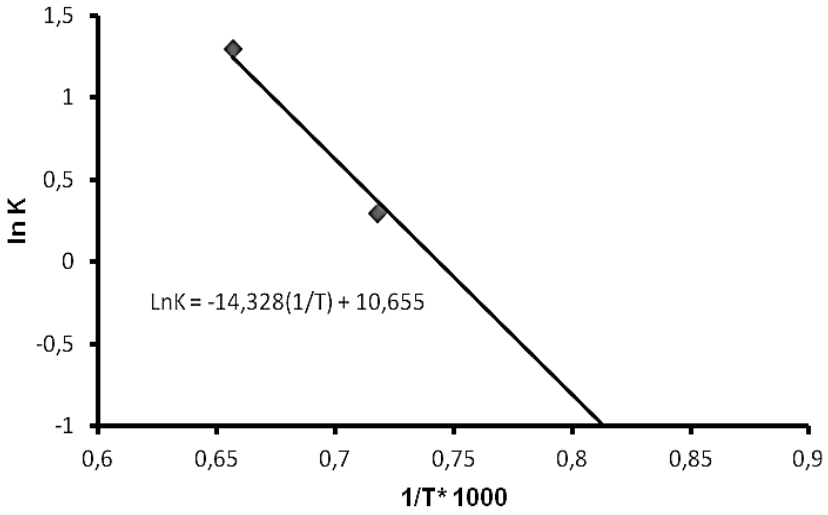

(b)

Figure 4.20 : a) The variation of thicknesses of titanium nitride layer on Ti6Al4V alloy with respect to nitriding temperature and time b) and related Arrhenius plot.

The growth of nitrogen diffusion zone was parabolic with n = 0.5 in Ti6Al4V as shown in Figure 4.21. The NDZ (X_{NDZ}) growth is formulated in Table 4.6 and activation energy was calculated as 90 KJ/mol.

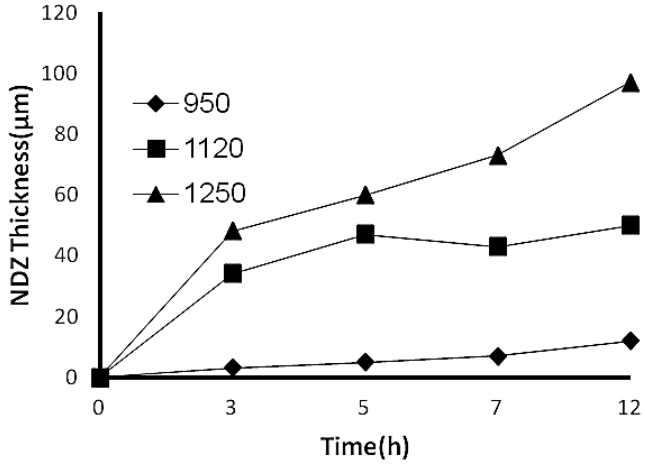

(a)

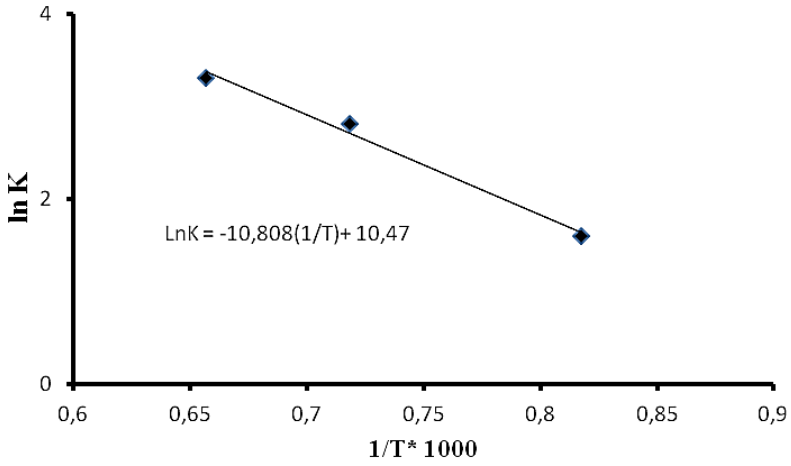

(b)

Figure 4.21 : a) The variation of thicknesses of NDZ layer of Ti6Al4V with respect to nitriding temperature and time b) and related Arrhenius plot.

Table 4.6 : Empirical equations derived from Figure 4.20 and Figure 4.21 according to Equation (2.4).

Materials	Layers	950°C	1120°C	1250°C
Ti6Al4V	Nitride Layer	X= 0.36×t	X = 1.34×t	X = 3.65×t
	Nitrogen Diffusion Zone	X= 4.97×√t	X= 16.58×√t	X= 22.50×√t

4.2.3 Case Depth Analyses

Figure 4.22 presents the results of the microhardness tests on the cross-sections of the nitrided Ti6Al4V as the case depth profile. On the cross section of the sample nitrided at 1250 °C for 12 h, the surface hardness was 2200 HV and the core hardness was 420 HV at a distance of about 140 µm from the surface. For samples

nitrided at 1120 °C for 12 h the surface hardness was measured as 2050 HV and total TiN and NDZ layer thickness was 70 µm. After processing at 950 ºC for 12 h surface hardness of the sample and total TiN and NDZ layer thickness were around 1600 HV and 30 µm, respectively.

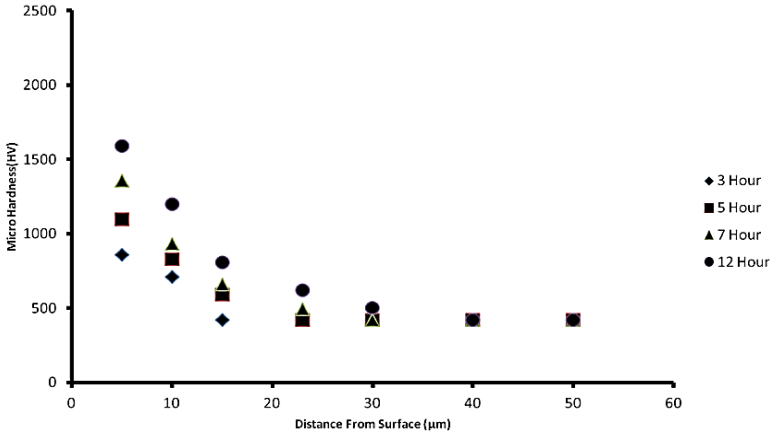

(a)

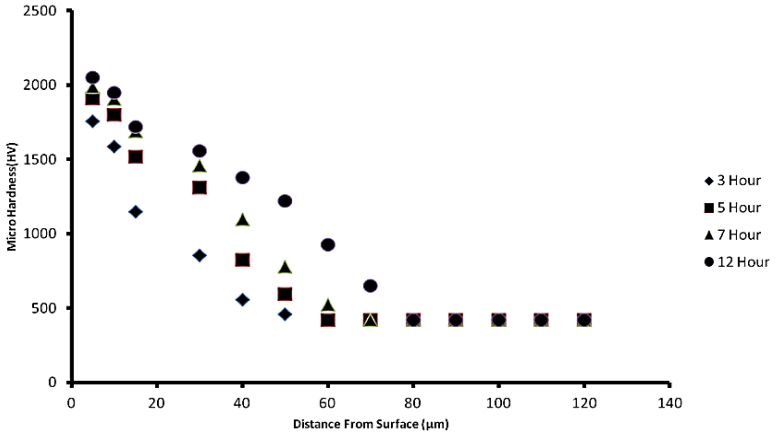

(b)

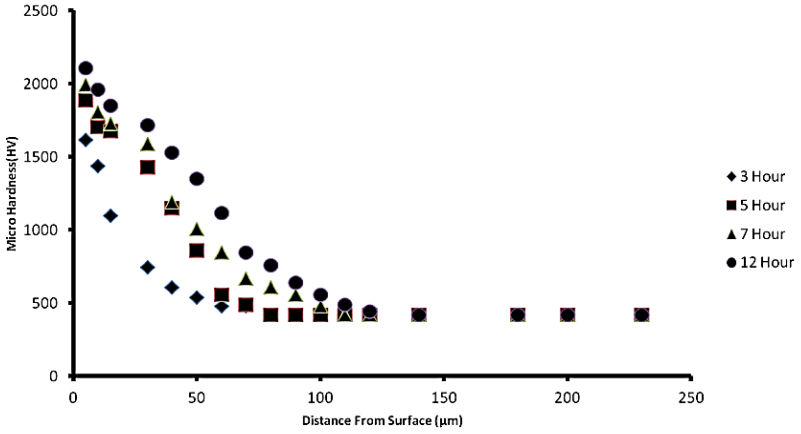

(c)

Figure 4.22 : Micro hardness tests results of nitrided Ti6Al4V at a) 950 °C, b) 1120 °C and c) 1250 °C.

Concerning the microstructure of the NDZ, the gradual decrease of hardness within the TiN and NDZ can be attributed to lower nitrogen concentration which continued to decrease close to the interior.

4.2.4 Adhesion Characteristics

As shown in Figure 4.23 with increasing time and temperature of nitriding process, the structure of the nitrided layers becomes porous and gradually loses its adherence to substrate. According to the RC test results, the layers nitrided at 950 ºC show better adhesion to the IZ and the NDZ.

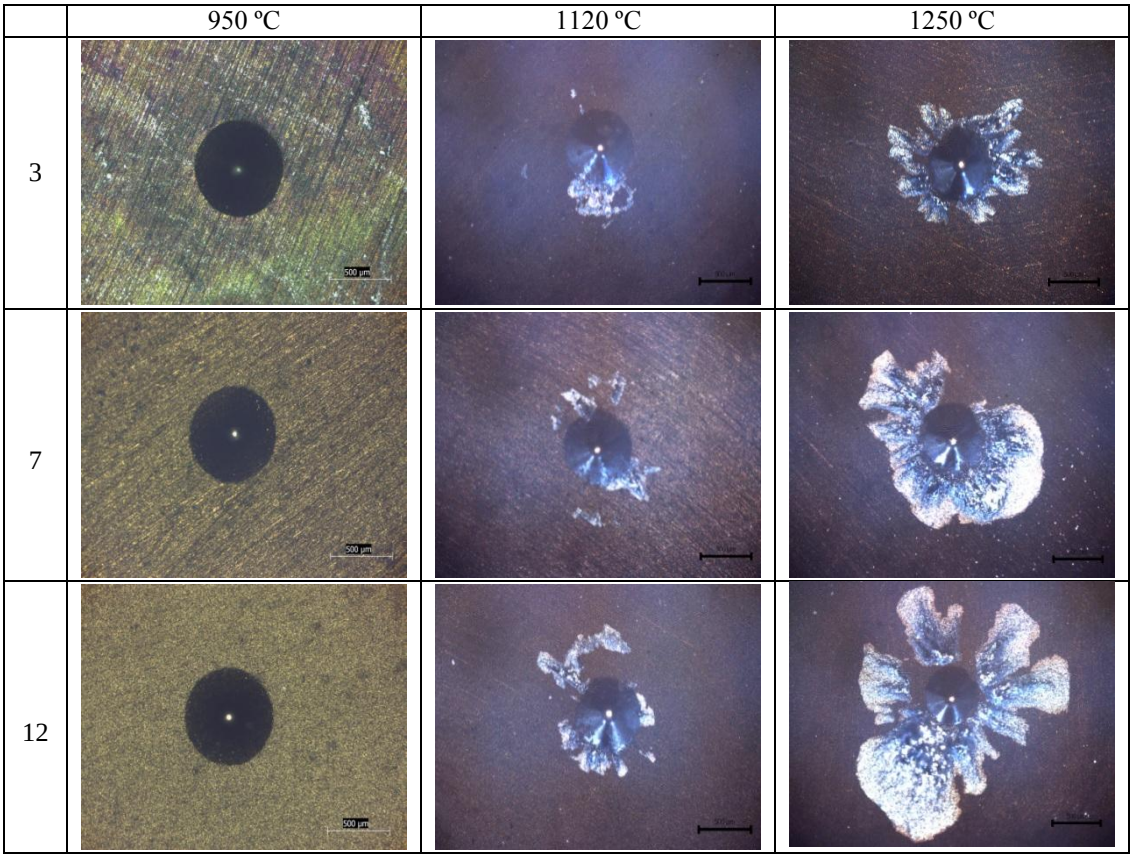

Figure 4.23 : RC test results of Ti6Al4V of nitrided samples at a) 950 °C, b) 1120 °C and c) 1250 °C.

4.2.5 Wear resistance

The worn surface morphology of the as-received Ti6Al4V sample in Figure 4.24 indicates severe plastic deformation along with grooves parallel to the sliding direction with the extensive ploughing and delamination. There usually were large quantities of wear debris on wear track of the as-received samples. Related friction coefficient and 2D-profile of wear track are presented in Figure A.3 and Figure A.4, respectively. Ti6Al4V alloy nitrided at the temperature 950 ^{o}C for 3 , 7 and 12 hours

exhibited very good wear resistance against sliding alumina ball and according SEM image in Figure 4.25 and 2D-profile in Figure A.4. wear track area was remarkably reduced .

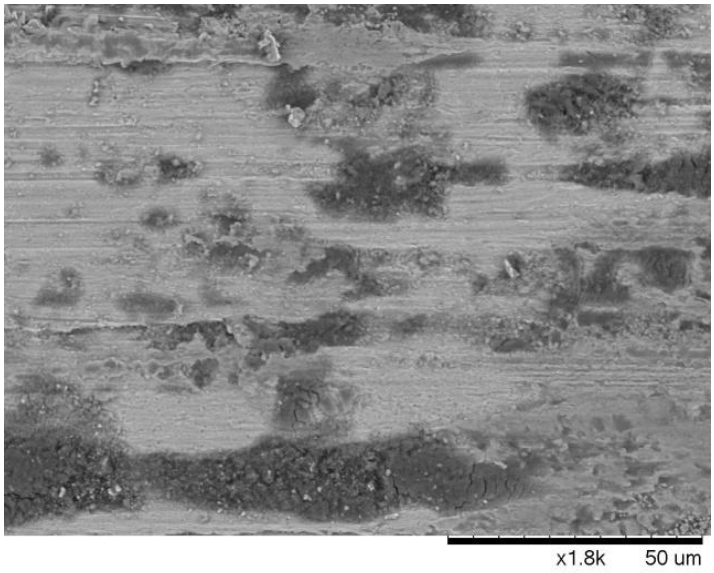

Figure 4.24 : As-received Ti6Al4V wear track SEM image.

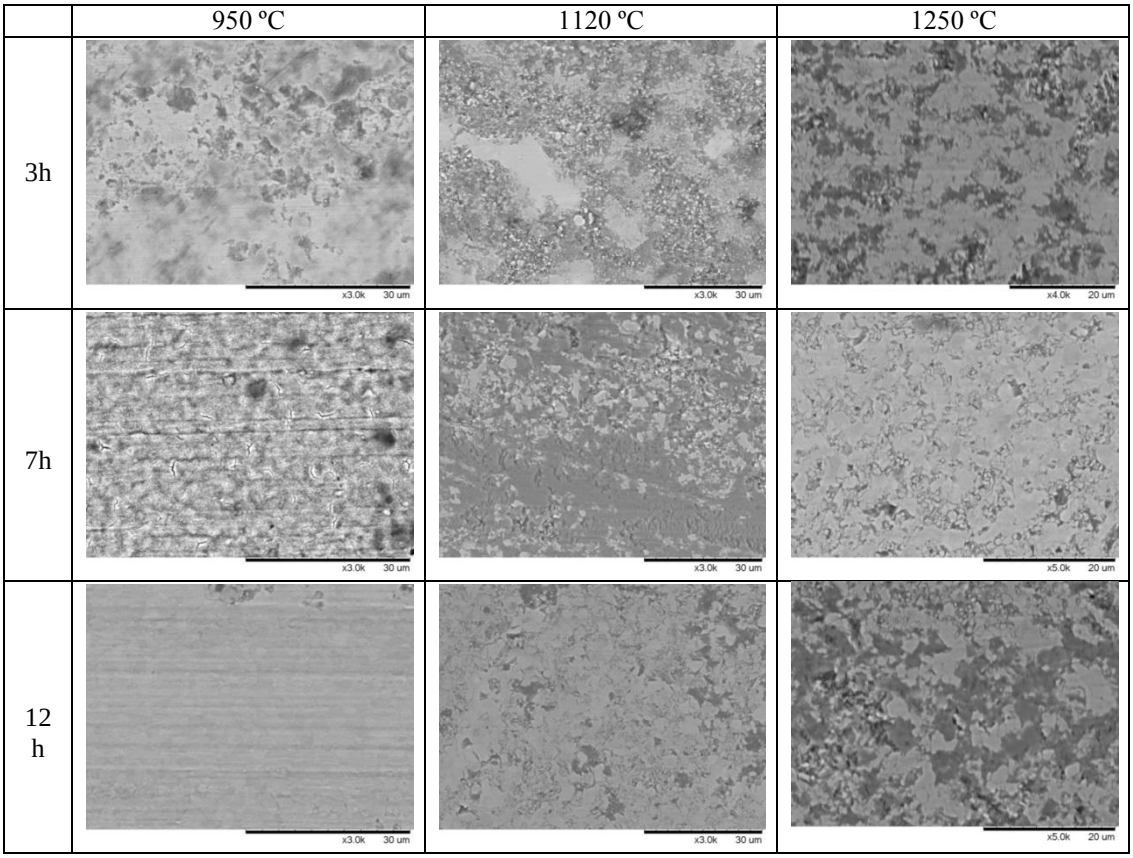

Figure 4.25 : SEM image of the wear track formed on the surface of the nitrided Ti6Al4V.

On the nitrided samples wear progressed only on the TiN. However, the minimum depth and width of the wear track was observed in the case of nitriding at 950 ºC for 3 hours. Shallow scratches were detected on the nitride layers due to abrasive wear and the sample surfaces were polished without any evidence of deformation, cracking, delamination or spalling.

Examination on the worn Al_2O_3 ball did not indicate the transfer of substrate materials to the balls. Adhered particles were not seen on the surface of the worn ball in the LOM image shown in Figure 4.26. In brief, tribological behaviour of nitrided Ti6Al4V was characterized by low coefficient of friction and slight wear of materials.

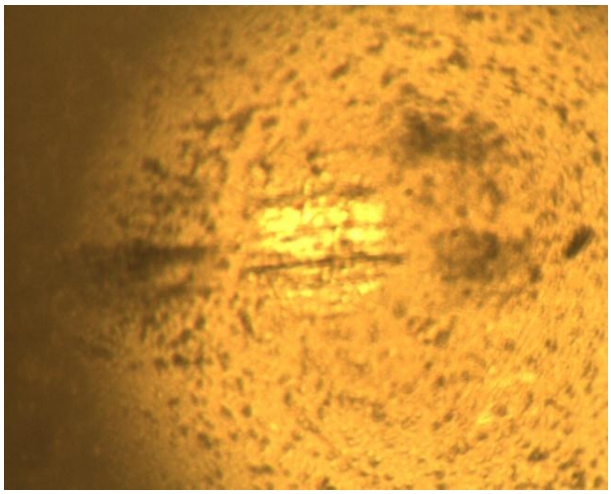

Figure 4.26 : LOM image of the Al_2O_3 ball rubbed on Ti6Al4V alloy nitrided at 1120 °C for 7 hours.

The numerical values of the average wear track areas (μm^2) of the each specimen and related friction coefficient (FC) are listed in Table 4.7 according to Figure A.3 and Figure A.4. The results of the wear tests in terms of relative wear rate (RWR) are shown in the Table 4.8. Wear test of the nitrided alloy exhibited considerably high RWR and low FC than the as-received sample in all nitriding conditions. These results show that the gas nitriding process increases the wear resistance of Ti6Al4V and the highest wear resistance was obtained after nitriding at 950 ^oC for 3 hours.

Table 4.7 : Average wear track area values of the nitrited and unnitrided Ti6Al4V samples.

Ti6Al4V4 Sample	Gas nitrided at 950^{o} C		Gas nitrided at 1120^{o} C		Gas nitrided at 1250^{o} C	
	WT	FC	WT	FC	WT	FC
3 H	47	0.18	58	0.20	149	0.19
7 H	49	0.18	471	0.20	153	0.22
12 H	294	0.20	942	0.35	314	0.35
Untreated	WT= 13089		FC= 0.50			

Table 4.8 : Relative wear resistance values of the Ti6Al4V nitrided samples.

Ti6Al4V Sample	Gas nitrided at 950 °C	Gas nitrided at 1120 °C	Gas nitrided at 1250 °C
3 H	278	267	44.52
7 H	225	27.78	13.89
12 H	87.84	85.54	41.68
Untreated	1		

4.3 Ti6Al7Nb

4.3.1 Microstructural features

The nitriding process resulted in the surface appearances of the Ti6Al7Nb samples with a color change from metallic grey to golden (the characteristic color of TiN). The XRD patterns of the samples nitrided at 950 °C for 3, 7 and 12 hours are shown in Figure 4.27. In the case of the sample nitrided at 950 °C for 3 hours, α-Ti, Ti_2N and TiN peaks detected. Like XRD pattern obtained during analyses of nitrided Ti6Al4V at 950 °C for 7 and 12 hours, the peaks of rutile (a form of titanium oxide) did not appear on the XRD pattern of nitrided Ti6Al7Nb and only TiN peaks were observed. XRD analysis revealed that the surfaces of the samples nitrided at 1120 and 1250 °C were completely coated with TiN layer in all test duration, Figure 4.27.

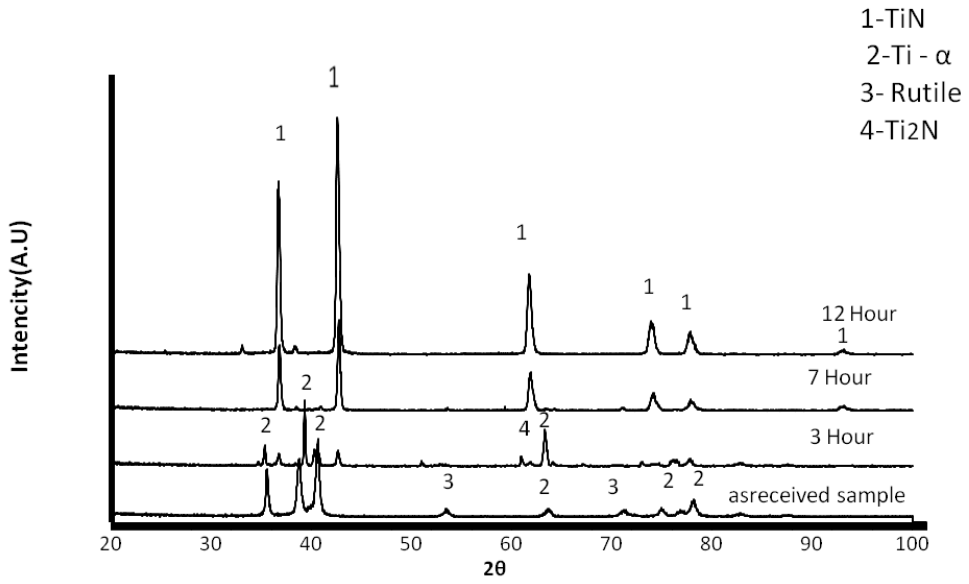

(a)

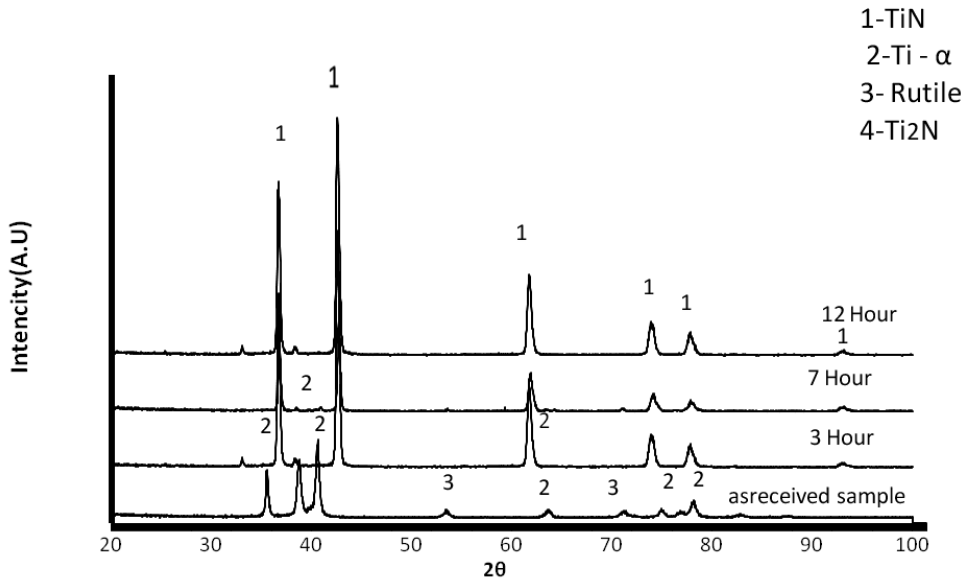

(b)

Figure 4.27 : XRD patterns of the Ti6Al7Nb samples nitrided a) at 950 ^{o}C b) at 1120 ^{o}C and 1250 ^{o}C.

In order to make a detailed characterization of the nitrogen exposed surfaces, SEM imaging and EDX examinations were conducted on the cross-sections as shown in Figure 4.28. The interfaces of TiN layer/IZ and IZ/NDZ exhibited wavy morphology (Figure 4.28, (a-c)). At the maximum temperature of the present study (1250 °C) nitriding induced variation of the IZ width from a few micrometers to about 20 μm as observed for Ti6Al4V alloy.

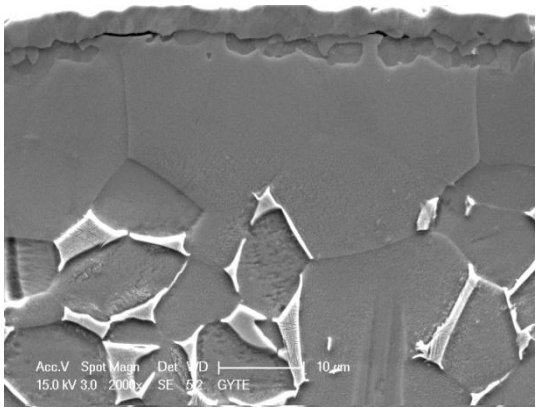

(a)

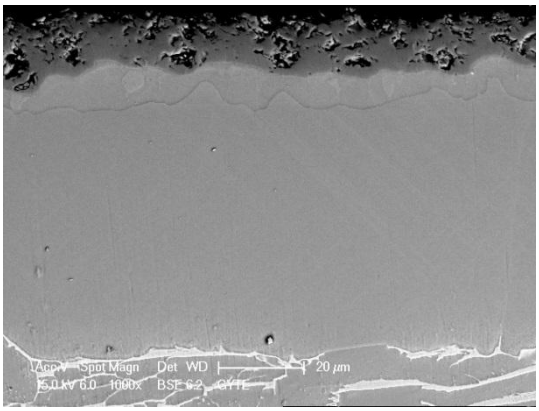

(b)

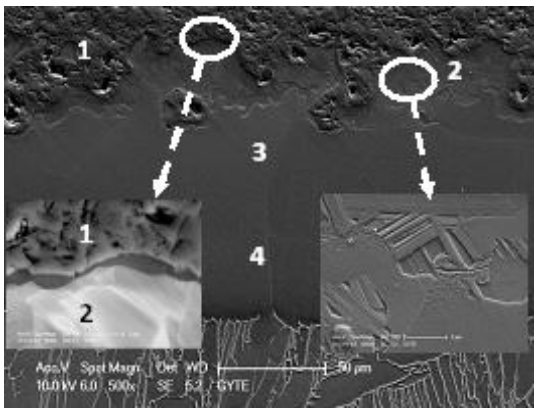

(c)

Numbers in Figure c	Location in Figure c	At. %			
		Ti	Al	Nb	N
1	TiN	45.22	0.85	0.36	53.57
2	IZ	54.86	21.01	2.86	21.28
3	NDZ	60.29	7.79	1.38	30.55
4	NDZ	66.36	8.61	1.68	23.35

Figure 4.28 : Cross-section SEM micrographs of the samples Ti6Al7Nb nitrided at a) 950 °C, b) 1120 °C, c) 1250 °C for 12 h and d) EDX spot analysis of the main elements at different locations.

The distribution of the main elements on the cross-sections of the nitrided samples of the examined alloys (Ti, Al, Nb and N) is determined by X-ray elemental maps and line scan profiles shown in Figure 4.29 and 4.30 respectively. X-ray elemental map analysis conducted on the sample nitrided at 1250 °C confirmed the results of the spot analysis indicating that the IZ was mainly enriched with Al (and with some Nb), while its Ti and N contents were lower than the TiN layer and the NDZ. When the TiN layer is examined carefully, small Al and/or Nb enriched islands observed. It should be noted that there were very few Nb enriched islands when compared to the number of Al enriched ones, while higher Nb concentration was detected mostly at the grain boundaries of the substrate.

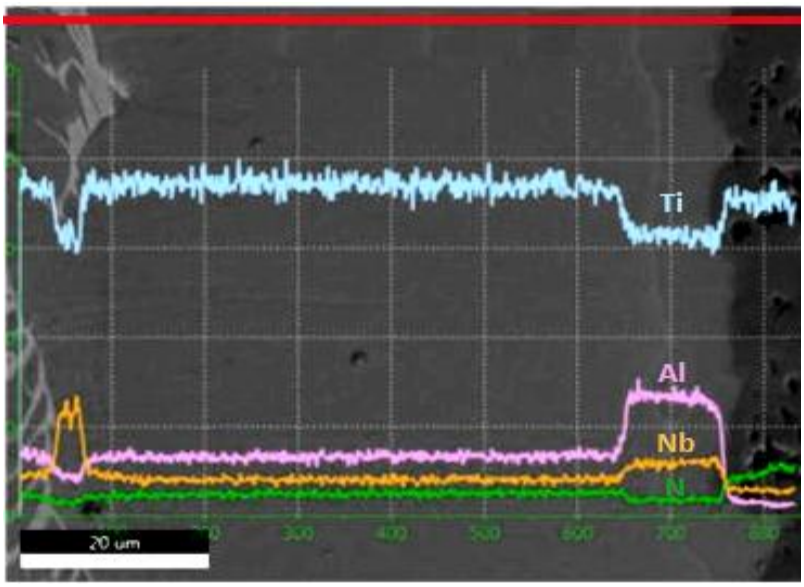

Figure 4.29 : Line scan analysis of Ti6Al7Nb showing distribution of the main elements after nitriding at 1120°C for 12 hours.

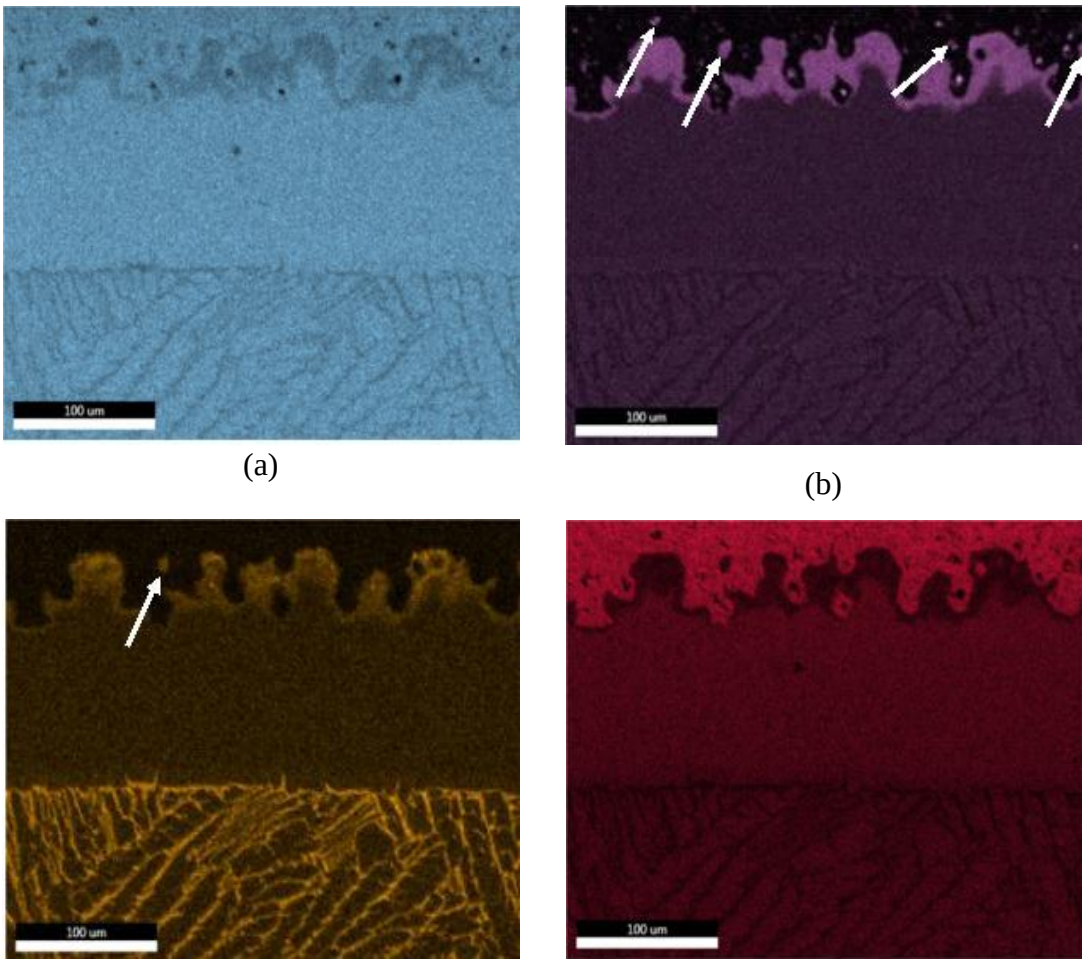

(a) (b)

(c) (d)

Figure 4.30 : X-ray elemental map analysis of the Ti6Al7Nb after nitriding at 1250 °C for 12 h (a) titanium, (b) aluminum, (c) niobium and (d) nitrogen (arrows show aluminum and niobium rich islands in the titanium nitride layer).

Similar to the nitriding temperature of 1250 °C, redistribution of the main elements during nitriding at 1120 °C induced relatively high Al and Nb concentrations in IZ while there was a decrease in Ti and N concentrations.

4.3.2 Nitriding Kinetics

4.3.2.5 Analyses of nitriding kinetic according to weight change

The weight changes of the Ti6Al7Nb samples shown in Figure 4.31 exhibited the parabolic diffusion kinetics of nitrogen and Q value calculated according to Arrhenius equation is determined as 117 kJ/mol which has almost the valuefound for Ti6Al4V.

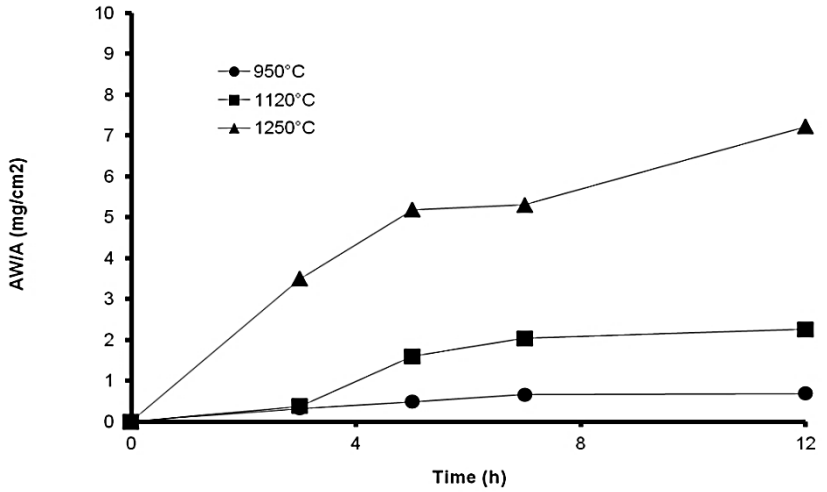

(a)

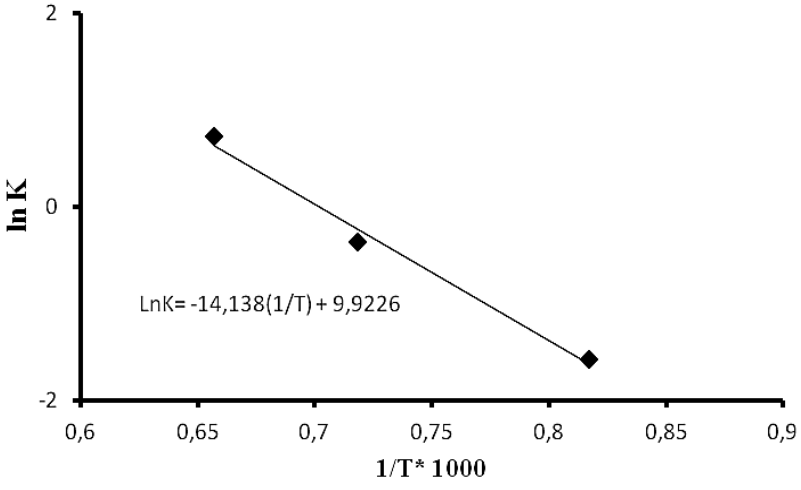

(b)

Figure 4.31 : The variation of weight of nitrided Ti6Al7Nb with respect to nitriding temperature and time b) and related Arrhenius plot.

Table 4.9 : Empirical equations derived from Figure 3.22 according to Equation (1.2).

	950 °C	1120 °C	1250 °C
Ti6Al7Nb	$\Delta m/S = 0.21 \times \sqrt{t}$	$\Delta m/S = 0.69 \times \sqrt{t}$	$\Delta m/S = 2.06 \times \sqrt{t}$

4.3.2.6 Analyses of nitriding kinetic according to cross-sectional examination

The cross-sectional LOM micrographs of the nitrided samples are shown in Figure 4.32. The results are the same as observed for Ti6Al4V alloy, with three zones in cross-section image (TiN, IZ and NDZ). The NDZ appeared with coarse-grained single-phase microstructures. Detection of α-Ti peaks on the XRD patterns along with the TiN peaks confirmed that NDZ has α-Ti structure. The grains of the Ti6Al7Nb alloy at 950 ºC temperature consisted of equiaxed α and β titanium. The grain size grew and showed columnar structure with respect to increasing time at nitriding temperature of 1120 ºC and 1250 ºC.

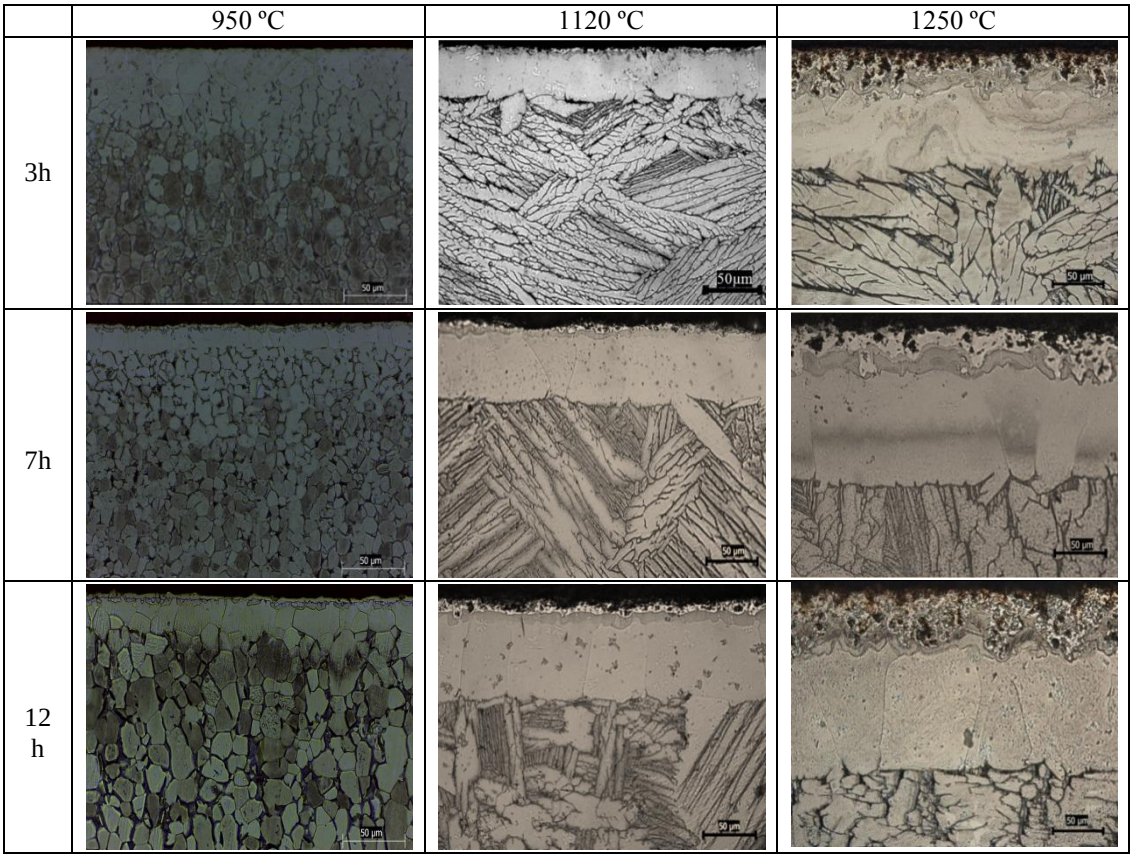

Figure 4.32 : The cross-section micrographs of the Ti6Al7Nb samples depending on the nitriding temperature and time.

The changes in the thickness of titanium nitride layer with respect to nitriding time are shown in the Figure 4.33 and formulated in Table 4.10. The nitride layer growth

was linear and yielded Q values of 114 kJ/mol. NDZ layer depth variations measured on the cross sections of nitride Ti6Al7Nb samples are plotted in the Figure 4.34. The growth of NDZ layer in Ti6Al7Nb was parabolic as calculated in Table 4.10 and Q value was calculated as 92 kJ/mol.

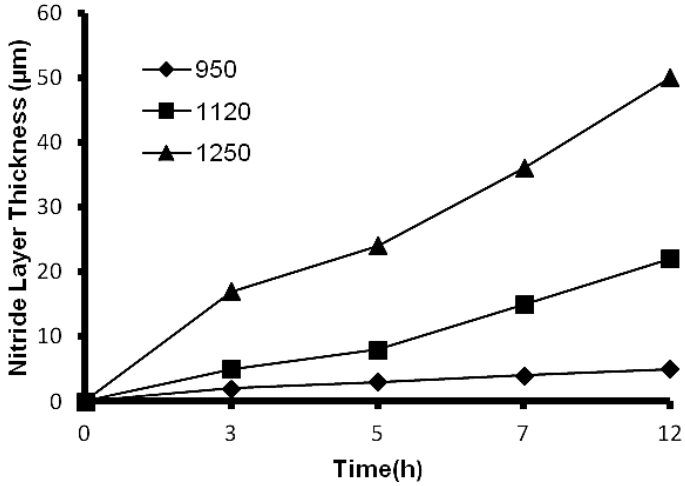

(a)

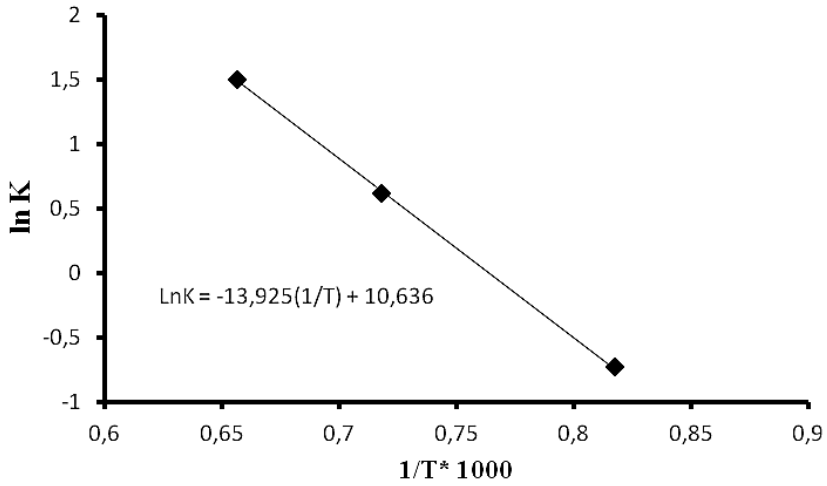

(b)

Figure 4.33 : a) The variation of thicknesses of titanium nitride layer of Ti6Al7Nb with respect to nitriding temperature and time b) and related Arrhenius plot.

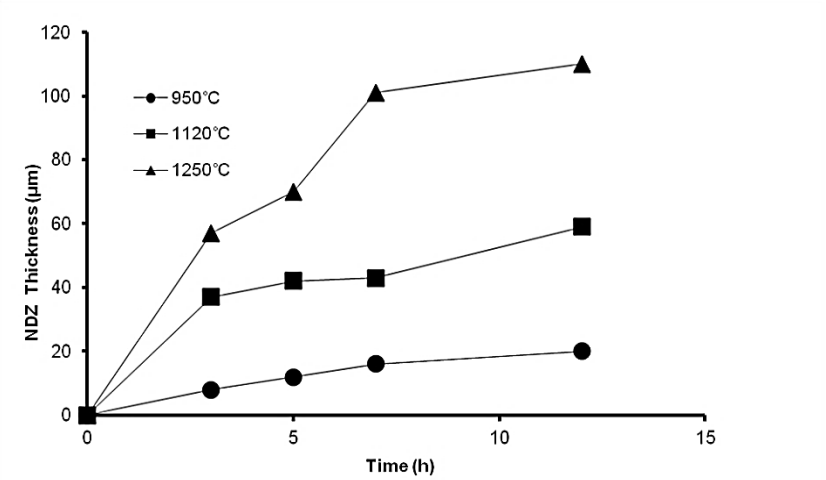

(a)

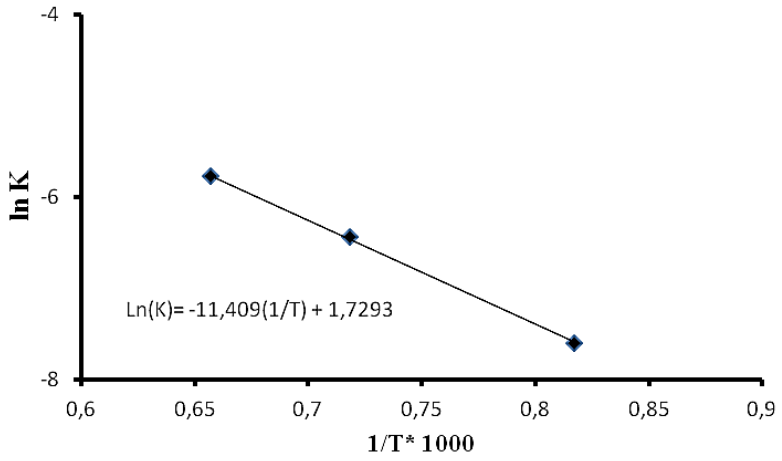

(b)

Figure 4.34 : a) The variation of thicknesses of NDZ layer of Ti6Al7Nb with respect to nitriding temperature and time b) and related Arrhenius plot.

Table 4.10 : Empirical equations derived from Figure 4.33 and Figure 4.34 according to Equation (1.4).

Materials	Layers	950°C	1120°C	1250°C
Ti6Al7Nb	Nitride Layer	X= 0.48×t	X = 1.87×t	X = 4.51×t
	Nitrogen Diffusion Zone	X= 5.64×√t	X= 17.63×√t	X= 33.46×√t

4.3.3 Case Depth Analyses

Figure 4.35 presents the results of the microhardness tests conducted on the cross-sections of the nitrided Ti6Al7Nb as the case depth profile. On the cross section of

the sample nitrided at 1250 °C for 12 h, the surface hardness dropped from 2400 HV to 420 HV

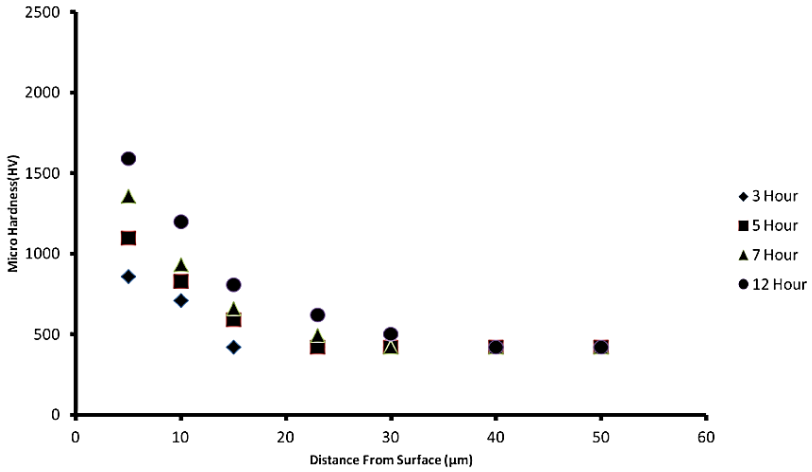

(a)

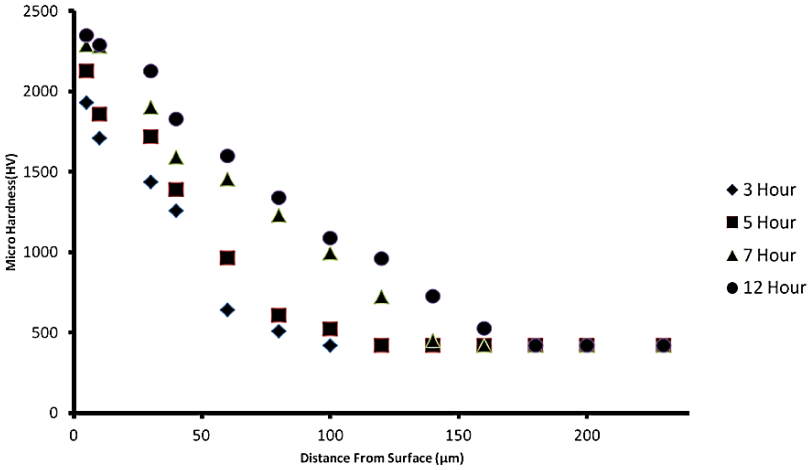

(b)

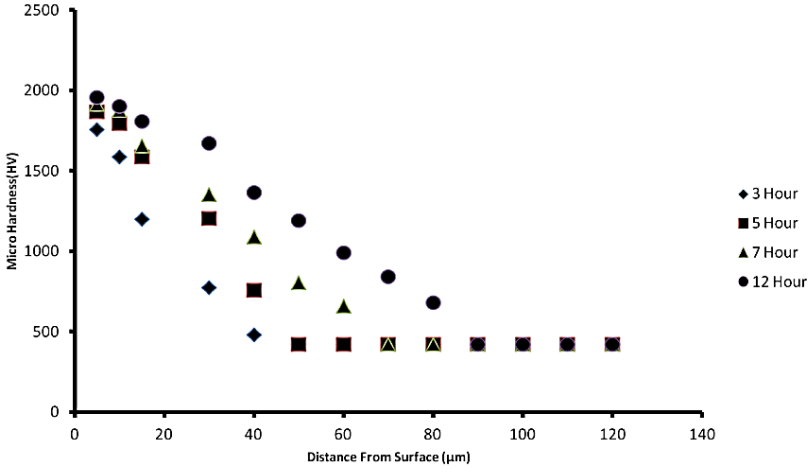

(c)

Figure 4.35 : Case depth profile of the nitrided Ti6Al7Nb at a) 950 ºC, b) 1120 ºC and c) 1250 ºC (Hardness measurements were made under indentation load of 50 g).

in the core, at a maximum distance of about 160 μm from the surface. For samples nitrided at 1120 °C for 12 h the surface hardness measured as 2000 HV and total TiN and NDZ layer thickness was 83 μm. After nitriding at 950 ºC for 12 h, surface hardness of sample and total TiN and NDZ layer thickness were around 1650 HV and 27 μm respectively.

4.3.4 Adhesion Characteristics

Similar to the Ti6Al4V, the nitriding over transus temperature resulted in development of irregular and coarse grain in the microstructure and rough surface. As shown in Figure 4.36 the nitride layers formed at 950 ºC showed better adhesion (with less cracked and delaminated regions) on the surface as compared to 1120 and 1250 ºC. With increasing nitiriding time and temperature area of the cracked and delaminated regions increased.

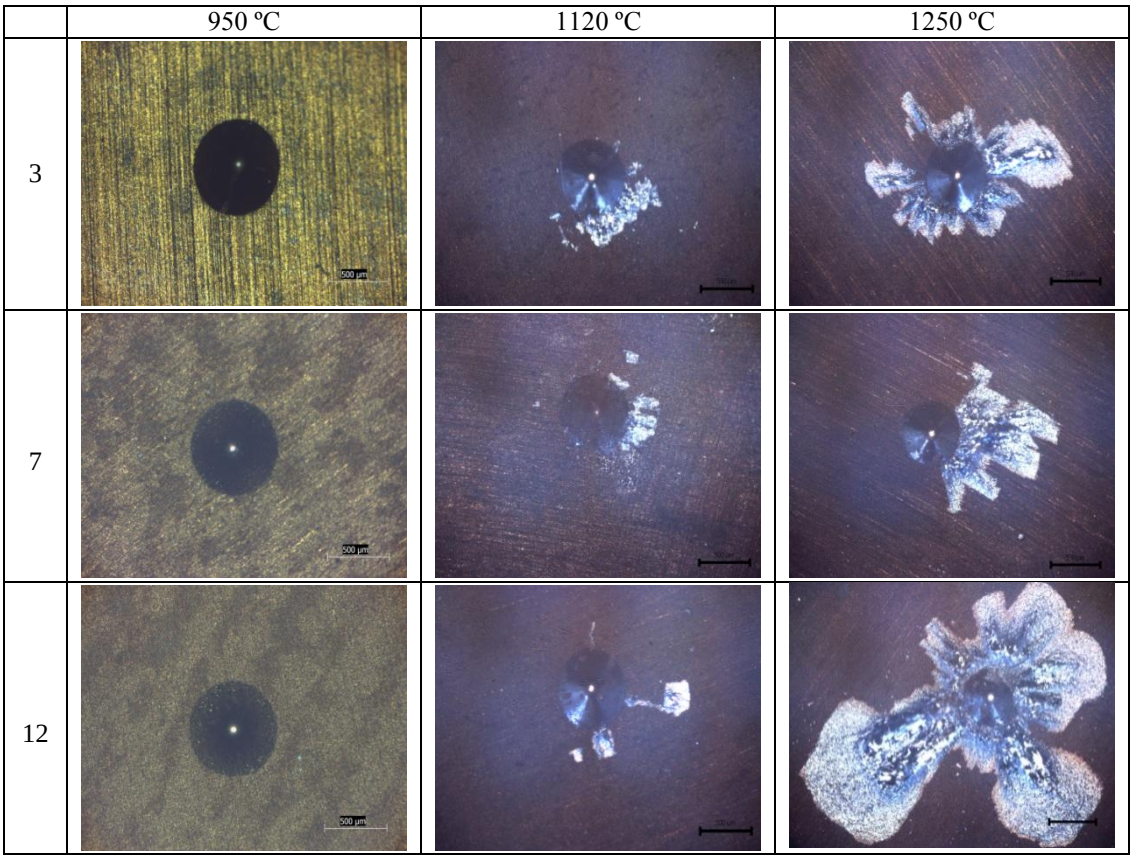

Figure 4.36 : RC test results of Ti6Al4Nb samples nitrided at a) 950 °C, b) 1120 °C and c) 1250 °C.

4.4 Wear Resistance

Figure 4.37 presents SEM micrographs of the worn surface of the as-received Ti6Al7Nb samples. The dominant wear mechanism was severe abrasive and adhesive wear under the normal load of 7 N. The friction coefficient of as-received sample under 7 N normal load exhibited significant fluctuation and stopped machine due to the friction force threshold of the load cell attached to the wear testing equipment.

The nitrided Ti6Al7Nb was slightly worn without any evidence of deformation and cracking. Extremely tiny scratches were detected within the wear tracks. For all of the samples, the wear occurred only on the nitride layer and did not penetrate through the diffusion zone. The friction curve was very smooth and retained at a constant level. The SEM images of the wear tracks are presented in Figure 4.38. LOM image of rubbing Al_2O_3 ball shown in Figure 4.39 demonstrated negligible mass transfer from the surface of the nitrided sample, similar to the one obtained for Ti6Al4V. The FC values (obtained from friction coefficient curves presented in Figure A.5) of the as-received and nitrided samples were determined as 0.6 and 0.2 , respectively as shown in Table 4.11, similar to the one obtained for Ti6Al4V.

The 2-D profiles of the wear tracks are shown in Figure A.6. The calculated wear track area is presented in Table 4.11. The depth and width of the wear track increased with increasing nitriding time and temperature. Although nitriding time of 12 h yielded the highest hardness level, it exhibited widest wear track area compared to the TiN layer formed in shorter nitriding time. The values of RWR and friction coefficient (FC) are shown in the Table 4.12.

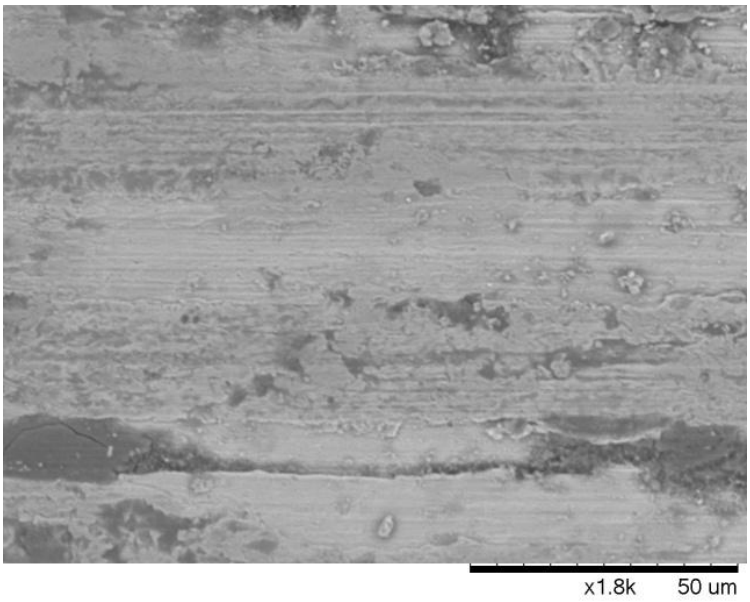

Figure 4.37 : Wear track image of as-received Ti6Al7Nb.

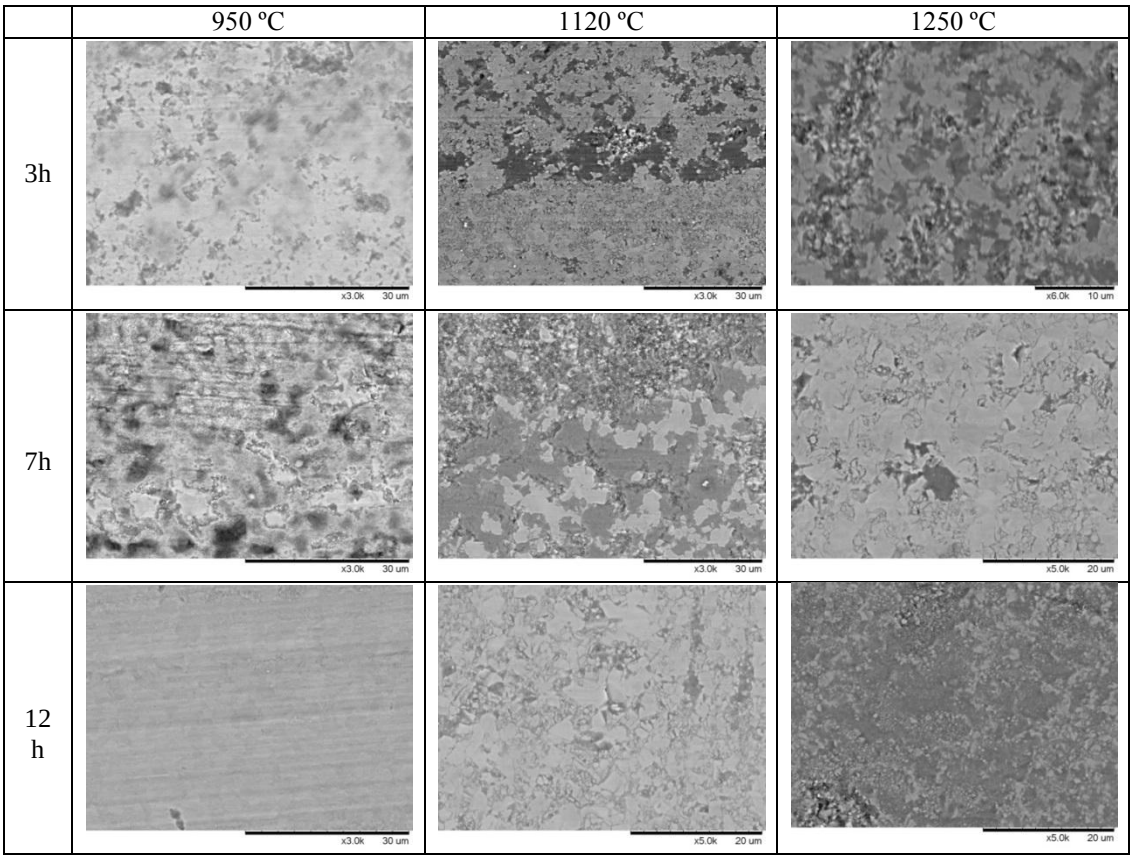

Figure 4.38 : SEM micrograph of the wear trackd formed on the surface of the nitrided Ti6Al7Nb samples.

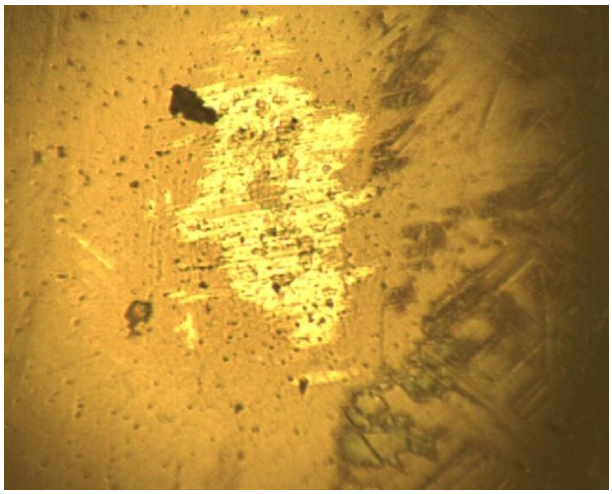

Figure 4.39 : LOM image of Al_2O_3 ball rubbed on Ti6Al7Nb alloy nitrided at 1120 °C for 7 hours.

Table 4.11 : Average wear track area values of the nitrided and untreated Ti6Al4V samples.

Ti6Al7Nb Sample	Gas nitrided at 950^o C		Gas nitrided at 1120^o C		Gas nitrided at 1250^o C	
	WT	FC	WT	FC	WT	FC
3 H	42	0.20	157	0.15	262	0.17
7 H	137	0.20	262	0.28	392	0.22
12 H	323	0.20	392	0.50	431	0.35
Untreated	WT= 16956			FC= 0.60		

Table 4.12 : Relative wear resistance values of the nitrided Ti6Al7Nb samples.

Ti6Al7Nb Sample	Gas nitrided at 950 °C	Gas nitrided at 1120 °C	Gas nitrided at 1250 °C
3 H	403	123	52.49
7 H	108	64.70	43.20
12 H	64.70	43.25	39.34
Untreated	1		

The samples nitrided at 950 ^{o}C showed better wear performance than the ones nitrided at 1120 and 1250 ^{o}C. The specimen nitrided for 3 hours at 950 ^{o}C exhibited higher wear resistance (approximately 400 times) than the other specimens.

5. DISCUSSION

The structural changes that took place on the nitrogen exposed surfaces of titanium during nitriding can be interpreted with the guidance of the Ti-N binary phase diagram [27, 47-51]. At the early stages of gas nitriding in the α-Ti phase field, introduction of nitrogen forms interstitial solid solution of α-Ti phase at the surface. As the concentration of the dissolved nitrogen increases, β-Ti starts to transform into α-Ti. When the fast diffusion ability of N along grain boundaries is considered, α-Ti nucleation is more likely at the grain boundaries of β-Ti. In the Ti-N binary phase diagram, there is a nitrogen concentration range where α- and β-Ti phases are in equilibrium within a certain range under isothermal conditions. Longer nitriding durations provide further enrichment of the surface with nitrogen and lead to full transformation of β-Ti to α-Ti constituting the NDZ. Inward diffusion of nitrogen was coupled with grain boundary sweeping towards the core, so that α-Ti grains tend to grow to the size of the NDZ, which can be characterized by the texture of α-Ti solid solution [50-56].

Enrichment of β-Ti by nitrogen encourages it to transform into α-Ti and therefore contribute to the broadening of the NDZ. According to the Ti-N binary phase diagram, α-Ti can dissolve at a maximum of 23 at.% N and excess nitrogen introduced during nitriding causes the generation of titanium nitride layer in the form of TiN (over 1050 °C) or Ti_2N (below 1050 °C). Standard free energy calculations made by using Fact Sage software in Figure 5.1 indicate that titanium nitride (i.e.Ti_2N and TiN) formation is more favorable than the nitrides of alloying elelments such as Al , V and Nb (i.e. AlN, VN NbN and Nb_2N) under the employed nitriding conditions. Manova et al. who studied nitrogen ion implantation in titanium, reported that starting the implantation at room temperature leads to simultaneous formation of TiN and Ti_2N but the growth rate of TiN is faster than Ti_2N, so that processing at temperatures above 700 ^{o}C induces the transformation of Ti_2N to TiN [17, 57]. Berberich et al who implanted nitrogen in a Ti6Al4V alloy observed Ti_2N formation beneath the TiN layer at higher temperatures as a consequence of nitrogen

diffusion [12, 58]. Strarosvetsky et al also detected Ti_2N beneath the TiN layer of titanium and Ti6Al4V alloy nitrided by powder immersion reaction assisted coating process [59-60]. Nakai et.al, Manhabosco et al and Lee et al observed a nitride layer composed of an outer TiN and an inner Ti_2N layers on Ti6Al4V alloy after gas nitriding [21, 24, 26]. In the light of these studies, we can suppose that the dark colored thin layer appearing just beneath the TiN layer is Ti_2N (Figure 4.28). Where the nitriding temperature of 1250 °C is concerned, Ti-N binary phase diagram dictates the formation of Ti_2N layer beneath the TiN layer as a result of local decomposition of TiN during cooling. In addition, according to the Ti-N binary phase diagram, formation of Ti_2N can accompany the growth of the nitride layer at nitriding temperatures lower than 1050 °C.

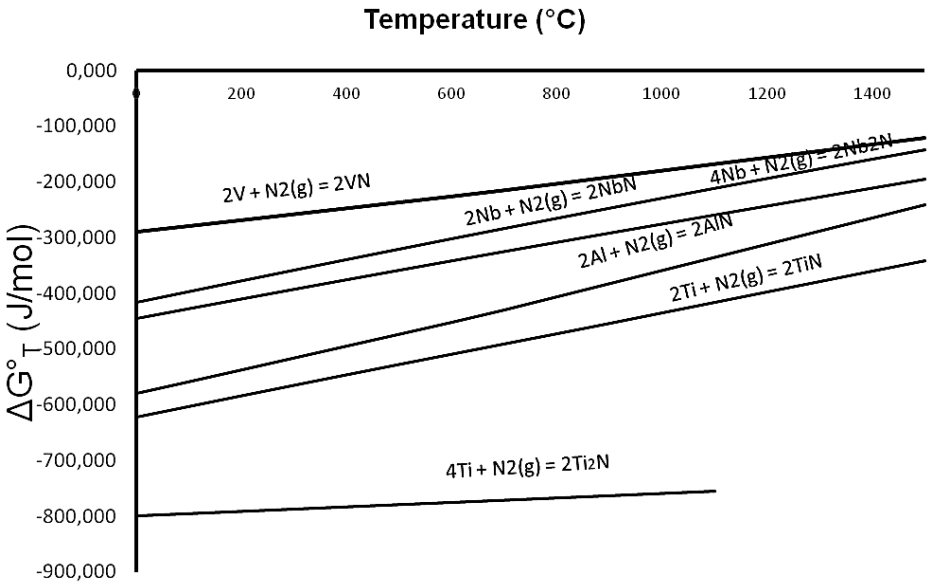

Figure 5.1 : Standard free energies for nitrides of titanium, aluminum and niobium.

As a result of stronger chemical affinity of Ti to N, Al, Nb and V were not involved in the process of nitride formation and were expelled from the nitride layer to form an Al (with some Nb or V) which enriched the IZ. In this respect, the porous nature of the nitride layer can be attributed to the generation of Kirkendall porosities which formed by depletion of Al along with Nb or V [1, 61-63]. The increase of the nitriding temperature not only increased the imperfectness within the nitride layer but also induced more heterogeneity and wavy morphology for the IZ at Ti6Al4V and Ti6Al7Nb but this morphology was not observed for Cp-Titanium and border between Nitride layer and NDZ was straight line. Thus, the thick sections of the nitride layer (in the form of spike) were consistent with the shallow sections of the

IZ. This suggests alloying elements expelled from the nitride layer segregate to the sides of growing spikes and finally cause local broadening of the IZ. The encircling of the thick sections of the IZ by the growing nitride spikes resulted in generation of Al (and some Nb or V) rich islands within the TiN layer. When the β-Ti stabilizing effect of V/Nb along with its limited solubility in α-Ti are taken into consideration, growth of the NDZ was coupled with migration of Nb/V towards to substrate, so that IZ became mainly enriched with Al while the concentration of Nb/V in the substrate increased . Diffusion of α-Ti stabilizing elements (such as Nb/V) towards the core after generation of NDZ on the nitrogen exposed surfaces has also been reported previously [25, 64-65].

The nitrided aluminum has a well-known property to form a very densely packed thin alumina layer on the surface, which is very difficult to be penetrated by oxygen and nitrogen. In other words, it has very low diffusivity to substitutional and interstitial elements. The inner-diffusion of nitrogen is retarded by the alumina layer, and further nitriding can therefore be delayed [53, 66-68].

Since the growth of the nitride layer was locally retarded at broad sections of the IZ, it is suggested that diffusion of Al in α-Ti plays a crucial role on growth kinetics of the nitride layer. For the nitriding temperatures employed in this study, the growth of the nitride layer on Ti6Al4V and Ti6Al7Nb were down easily in lower temperature in comparing of Cp-Titanium as a result of retarding manner of IZ. The expelled aluminum which delayed diffusion of nitrogen towards the core of the sample causes an increase in nitrogen concentration at the surface in TiN layer. To compare the same TiN layer in Cp-Titanium and Ti6Al4V and Ti6Al7Nb, we have to induce higher temperatures at longer periods of time to Cp-Titanium samples which it causes the growth of grains, cavity and porosity size inside the nitride layers and decrease mechanical property of Cp-Titanium samples. In this research growth activation energy of nitride layer and diffusion layer for Cp-Ti by thickness variation method was obtained 145 and 65 KJ/mol, respectively.

It is reported that diffusion activation energy values of N in β-Ti and α-Ti vary between 101-140 KJ/mol and 185-240 KJ/mol, respectively [68]. Therefore it is obvious that while the growth of the NDZ was controlled by diffusion of N in β-Ti, the growth of TiN layer was controlled by diffusion of N in α-Ti.

Also growth activation energy of nitride layer for Ti6Al4V and Ti6Al7Nb by thickness variation method was obtained 119 and 114 KJ/mol, respectively.

Our finding is accordance with the diffusion values of Al in Ti in open literature which was reported 115 KJ/mol [68-70]. This indicates that growth of the nitride layer was more likely to be controlled by diffusion of Al in β-Ti. It has been reported that [10, 11, 67] redistribution and coagulation of Al on the nitrogen exposed surfaces tend to form Ti_3Al as a TiAl intermetallic phase beneath the nitride layer. Since the ~20 at % Al concentration of IZ falls into α-Ti + Ti_3Al phase field in Ti-Al binary phase diagram, it is suggested that precipitation of Ti_3Al on α-Ti during cooling in the furnace (from nitriding temperature) favored lamellar morphology in IZ. On the other hand, when the nitrogen concentration (~20 at%) of the IZ is considered along with Al concentration, a possibility for precipitation of Ti_3AlN [29,30] from N supersaturated Ti_3Al for lamellar morphology can also be supposed. An age hardening effect of the c-$Ti_{1-x}Al_xN$ metastable phase can be observed above 700°C, which is an important and preferred feature for a hard coating operated at elevated temperature. A thermal activated phase separation, called spinodal decomposition, causes the formation of fine Ti- and Al-rich domains (around few nanometers in diameter) distributed within the matrix. The domains can be considered as c-$Ti_{1-x}Al_xN$ phase but with low and high x value respectively and their lattice are usually perfectly coherent through the matrix. The lattice parameter difference between TiN (a = 4.242) and AlN (a = 4.045) in their rock-salt cubic structure introduces the coherent strains in the lattice, working as obstacles to the movement of dislocations. Further increase of the temperature increases the separation of TiN and AlN, in other words, it depletes the Al and Ti from the Ti- and Al-rich domains. Hexagonal phase h-AlN starts to nucleate and grow from Al-rich domains (c-AlN) until all the metastable phase transforms into c-TiN and h-AlN phases [66-69]. It should be noted that no extra attempt has been made in this study to identify the phase structure of IZ. When the results of the nitriding kinetics are of concern, higher activation energies for nitrogen diffusion in titanium alloys as compared with Cp-Titanium can be associated with accumulation of Al at IZ, which tend to restrict further diffusion of nitrogen. Based on the above results and discussions, changes in the surface of Titanium and its alloy during gas nitriding in β-Ti phase field can be summarized in three sequential stages (Figure 5.2):

Stage 1: Introduction of N atoms first forms solid solution of β-Ti at the surface of the alloy (Figure 5.2.a).

Stage 2: As the surface is enriched by N, β-Ti transforms to α-Ti forming the NDZ, whose grains tend to grow towards the substrate (Figure 5.2.b).

Stage 3: When the N concentration of α-Ti becomes high enough, TiN layer with metallic golden color forms over all of samples. In the case of titanium alloys (Ti6Al4V and Ti6Al7Nb) growth of the nitride layer is coupled with accumulation of Al (with some V/Nb) beneath it as the IZ (Figure 5.2.c).

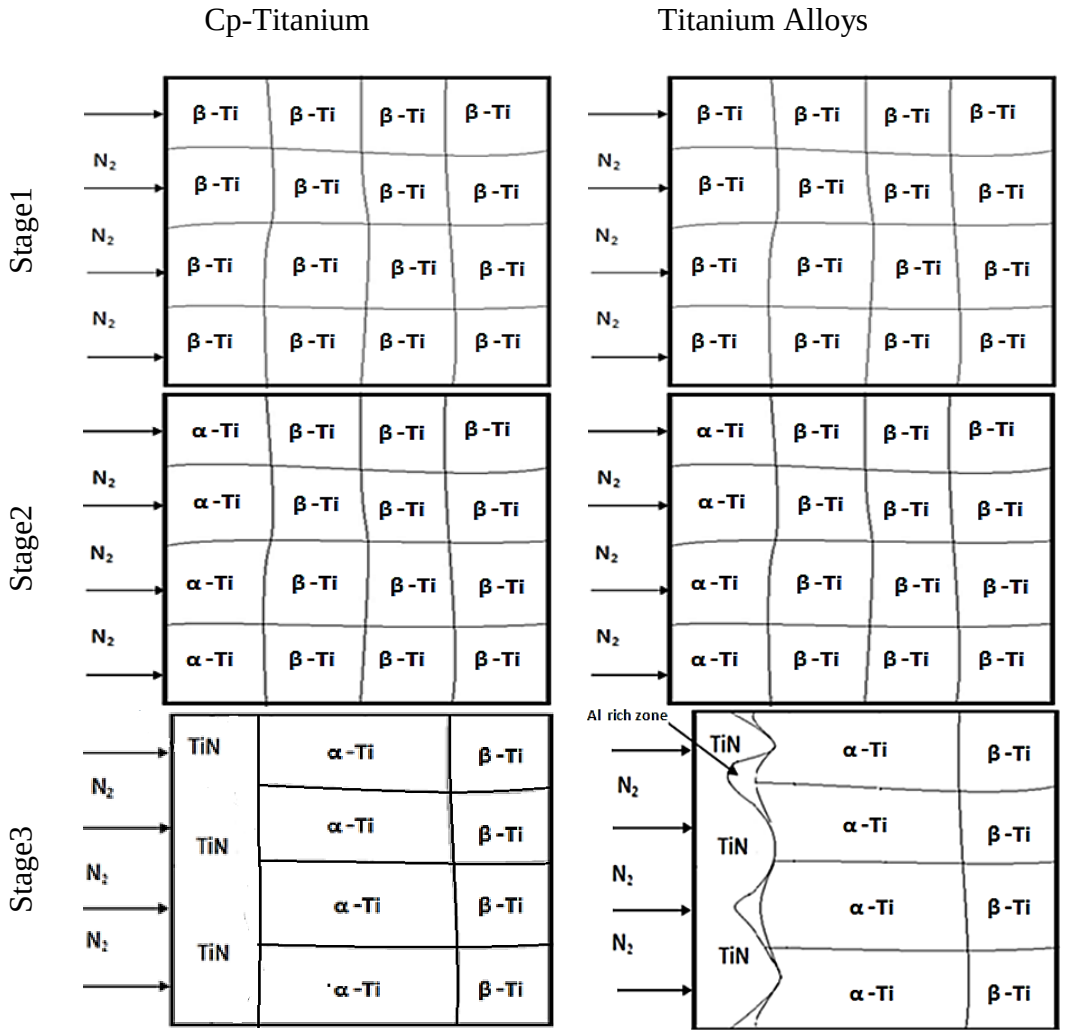

Figure 5.2 : Schematics of layered structure formation at the nitrogen exposed surfaces of Cp-Titanium and Titanium alloys (Ti6Al4V and Ti6Al7Nb).

Hardness measurements revealed remarkable hardening on the nitrogen exposed surfaces as compared to the substrate. The hardness of the TiN layer was measured around 2500 HV, which is five times as high as that of the substrate 450HV.

Dissolution of nitrogen atom in the NDZ promoted higher hardness than the substrate beneath the TiN layer. In the NDZ reduction of hardness towards the substrate can be associated with lower concentration of nitrogen atoms at higher depths. It is should be noted that hardening in the NDZ imposed gradual decrease of hardness towards the substrate and therefore provide extra resistance to the TiN layer under mechanical contact. However, generation of thicker TiN layer with wider NDZ tended to reduce the adhesion characteristic leading extensive spalling and failure during Rockwell C adhesion tests. Therefore, to enhance the wear resistance of the nitrogen exposed surfaces, it is necessary to consider the adhesion characteristics of the TiN layer. In this respect superior wear resistance was obtained from the titanium alloys nitrided at 950 °C. Since low temperatures (i.e. 950 °C) did not promote TiN layer formation, optimum nitriding parameters for enhancing wear resistance of Cp-Ti were determined as 1120 °C for 7 h.

.

6. CONCLUSIONS AND RECOMMENDATIONS

In this study, nitriding behavior of Cp-Titanium grade 4, Ti6Al4V and Ti6Al7Nb alloy at 950, 1120, and 1250 ^{o}C for 3, 7and 12 hours in nitrogen gas atmosphere has been investigated. The results of experiments can be summarized as follows:

1- Nitrogen exposed surfaces of Cp-Ti and titanium alloys exhibited multilayer structure. For Cp-Ti samples the surface was consisted of TiN layer and NDZ. Unlike Cp-Titanium growth of nitride layer over Ti6Al4V and Ti6Al7Nb is coupled with accumulation of Al (with some V/Nb) beneath it as the IZ, which is the result of expelling of main alloying elements from nitride layer towards to substrate. Accumulation of Al at IZ, restricts future diffusion of nitrogen. Therefore higher activation energies for nitrigen diffuision are obtained from titanium alloys as compared with Cp-Titanium.

2- As a general trend higher nitrding temperature and times lead to thicker and porous TiN with a deeper case depth. In this respect adhesion performance of TiN layer tended to be reduced with increasing processing temperature and time. For titanium alloys nitriding temperature of 950 C provided better adhesion for TiN layer in comparison to the nitride layers formed at 1120 and 1250 ºC. TiN layer formation was not promoted at 950 C for Cp-Ti, while TiN layer formed at 1120 C exhibited better adhesion characteristics as compared to the layer developed at 1250 C.

3-The hardness and the case depth of the nitrogen exposed surfaces increased with increasing processing time and temperature. The hardness of the TiN layer was measured about 2500 HV, which is five times as high as that of the substrate hardness (around 290-450 HV). On the cross section of nitride samples hardness gradually decreased upon formation of NDZ.

4-Covering of the surfaces of examined samples with TiN layer imposed resistance against rubbing action of the alumina ball by inducing better performance as compared to the as-received samples. However adhesion characteristics of TiN layer played crucial role on the wear performance of the nitrogen exposed surfaces. In this

respect optimum nitriding parameters were determined as 950 C/3 hours for titanium alloys and 1120 C/7 hours for Cp-Ti.

REFERENCES

[1] **Leyens, C., Peters, M.** (2003). *Titanium and titanium alloys: Fundamentals and Applications*, p. 7-19, Wiley-VCH, Weinheim.

[2] **Lütjering, G. and Williams, J.C.** (2007). *Titanium*, second ed., p. 1-14, Springer, Berlin Heidelberg.

[3] **Zhang, S., Zhu, W**. (1993). TiN coating of tool steels, *Journal of Materials Processing Technology*, *39*, 165-177.

[4] **Zhecheva, A., Sha, W., Malinov, S., Long, A**. (2005). Enhancing the microstructure and properties of titanium alloys through nitriding and other surface engineering methods. *Surface Coatings & Technology*, *200*, 2192-2207.

[5] **Bunshah, R.F.** (2001). Handbook of Hard Coatings, Deposition Technologies, Properties and Applications, p. 247-273, Noyes Publications, Park Ridge, New Jersey.

[6] **Holmberg, K. and Matthews, A.** (2005). Chapter 7: Tribology of Engineered Surfaces, in *Wear: Materials, Mechanisms and Practice*, p. 32-45, Eds. G. W. Stachowiak, John Wiley & Sons Ltd., England.

[7] **Jaffee, R. I., Promisel, N. E.** (1970). *The Science, Technology and Application of Titanium*, p. 1-55, Pergamon Press, Oxford, UK.

[8] **Jaffee R. I. and Burte H. M.** (1973). *Titanium Science and Technology*, Plenum Press, New York, USA.

[9] **Williams J. C. and Belov A. F.** (1982). *Titanium and Titanium Alloys*, Plenum Press, New York, USA.

[10] **Kimura, H. and Izumi, O.** (1980). *Titanium '80, Science and Technology*, AIME Publication, Warrendale, USA.

[11] **Lütjering, G., Zwicker, U., Bunk, W.** (1985). *Titanium, Science and Technology*, p. 267-286, DGM Publication, Oberursel, Germany.

[12] **Lacombe, P., Tricot, R., Beranger, G.** (1988). Titanium and applications, *Sixth World Conference on Titanium*, Les Editionsde Physique, Les Ulis, France.

[13] **Froes, F. H., Caplan, I. L.** (1993). Titanium '92, Science and Technology, *TMS conference*, Warrendale, USA.

[14] **Blenkinsop, P. A., Evans, W. J., Flower, H. M., (EDS).** (1996). *Titanium '95, Science and Technology*, p. 1944-1950, The University Press, Cambridge, UK.

[15] **Gorynin I. V., Ushkov S. S.**, (EDS). (2000). *Titanium '99, Science and Technology*, p. 254-263, CRISM, St. Petersburg, Russia.

[16] **Lütjering, G., Albrecht, J.** (2004). *Ti-2003, Science and Technology*, p. 35-38, Wiley-VCH, Weinheim, Germany.

[17] **Niinomi, M., Maruyama, K., Ikeda, M., Hagiwara, M., Akiyama, S.** (2007). Preparation of hydrogen storage Ti-V-Cr alloy from the oxide mixture in $CaCl_2$, *Proceedings of the 11th World Conference on Titanium*, The Japan Institute of Metals, Sendai, Japan.

[18] **Pye, D.,** (2006). Nitriding Techniques, Ferritic Nitrocarburizing, and Austenitic Nitrocarburizing Techniques and Methods, *Steel heat treatment: Metallurgy and Technologies, Second Edition*. p. 477-510, Taylor & Frances Group, Portland, Oregon, USA.

[19] **Knerr, C.H., Rose, T.C., Filkowski, J.H., O'Brien, J.M., Goodman, D.**(1991). Gas nitriding of Steels, Liquid Nitriding of Steels, Plama (Ion) Nitriding of Steels, *ASM Hanbook Vol 4: Heat Treating, tenth edition*. p. 903-923, ASM International, Ohio, USA.

[20] **Schwartz, M.** (2010). New Innovative Heat Treating Processes, *Innovations in materials manufacturing, Fabrication, and Environmental Safety*, p. 495-499. CRC Press, Florida, USA.

[21] **Korwin, M.J., Morawski, C.D., Tymowski, G.J., Liliental, W.K**. (2004). Design of Nitrided and Nitrocarburized Materials, *Handbook of Metallurgical Process Design*, p. 548-578, Marcel Dekker, New York, USA.

[22] **Beer, O.** (2006). Plasma Assisted Heat Treating Processes of Bearing Components, *Journal of ASTM International. 3*, March. ASTM International.

[23] **Pohrelyuk, I., Fedirko, V.** (2012). Chemico-Thermal Treatment of Titanium Alloys-Nitriding**,** Titanium Alloys-Towards Achieving Enhanced Properties for Diversified Applications, p115-139, Ed. Nurul Amin A.K.M., InTech Publication, Croatia.

[24] **Zhecheva, A., Malinov, S., Katzarov, I., & Sha, W.** (2006). Modelling of kinetics of nitriding titanium alloys. *Surface Engineering*, *22*, 452–454.

[25] **Guleryuz, H., Cimenoglu, H.** (2005). Surface modification of a Ti–6Al–4V alloy by thermal oxidation, *Surface and Coating Technology, 192*, 164-170.

[26] **Massalski, T.B., Okomoto, H., Subramanian, P.R., Kacprzak, L.** (1990). Binary Alloys Phase Diagrams, 2nd Edition, ASM International, Material Park, USA.

[27] **Sha, W., Haji, MA., Mohamed, A., Wu, X., Siliang, B., Zhecheva, A.** (2008). X-ray diffraction, optical microscopy, and microhardness studies of gas nitrided titanium alloys and titanium aluminide, *Materials Characterization*, *59*, 229-240.

[28] **Birkholz, M., Ehwald, K.E., Wolansky, D., Costina, I., Baristyran-Kaynak, C., Fröhlich, M., Beyer, H., Kapp, A., Lisdat, F.** (2010). Corrosion-resistant metal layers from a CMOS process for bioelectronic applications, *Surface and Coating Technology*, *204*, 2055–2059.

[29] **Zhecheva, A., Malinov, S.,Sha, W.** (2005). Microstructure and microhardness of gas nitrided surface layers in Ti–8Al–1Mo–1V and Ti–10V–2Fe–3Al alloys, *Surface Engineering*, *21*, 269-278.

[30] **Boyer, R., Welsh, G., Collings, E.W.** (1994). *Materials Properties Handbook—Titanium Alloys*, ASM International, Materials Park, USA.

[31] **Collings, E.W.** (1984). *The Physical Metallurgy of Titanium Alloys*, American Society for Metals, USA.

[32] **Shashkov, D.P., Vinogradov, A.V., Polohov, V.N.** (1981). Nitriding kinetics and wear resistance of titanium alloys, *Metally*, *6*, 172-177.

[33] **Shibata, H., Tokaji, K., Ogava, T., Hori, C.** (1994). The Effect of Gas Nitriding on Fatigue Behavior in Titanium-Alloys, *International Journal of Fatigue*, *16*, 370-376.

[64] **Monova, D., Gerlach, J.W., Neumann, H., Assmann, W., Mandl, S**. (2006). Phase formation in Ti after high fluence/high temperature nitrogen implantation, *Nuclear Instruments and Methods in Physics Research Section B, 242*, 282-284.

[65] **Berberich, F., Matz, W., Richter, E., Schell, N.** (2011). In situ study of phase transformation at elevated temperature and correlated mechanical degradation of nitrogen implanted Ti-6Al-4V alloys, Biannual Report 1999/2000, Project-Group ESRF-Beamline, Germany.

[34] **Maksimovich, G.G., Pogrelyuk, I. N., Fedirko, V.N.** (1986). Structure formation in nitrided layers of titanium alloys, *Metal Science and Heat Treatment*, *28*, 393-397.

[35] **Williams, J. C., Belov, A. F.** (1982). *Titanium and Titanium Alloys*, p. 124-135, Plenum Press, New York,USA.

[36] **Bomberger, H. B., Froes, F. H., Morton, P. H.** (1985). Titanium Technology: Present Status and Future Trends, *TDA Conference*, Dayton, USA.

[37] **Seagle, S. R.** (1996). The state of the USA titanium industry in 1995, *Materials Science and Engineering A*, *213*, 1-7.

[38] **Gorynin, I. V.** (1993). Titanium ‘92, Science and Technology, *TMS Conference*, Warrendale, USA.

[39] **Yamada, M.** (1996). An overview on the development of titanium alloys for non-aerospace application in Japan, *Materials Science and Engineering A, 213*, p. 8-15.

[40] **Boyer, R. R.** (1980). Design properties of a high-strength titanium alloy: Ti-10V-2Fe-3Al, *Journal of Metals, March*, 61-62.

[41] **Combres, Y., Champin, B**. (1996). *Titanium ‘95, Science and Technology*, p. 11-25, The University Press, Cambridge, UK,.

[42] **Schutz, R. W., Watkins, H. B.** (1998). Recent developments in titanium alloy application in the energy industry, *Materials Science and Engineering A, 243*, p. 305-315.

[43] **Bhushan, B., Gupta, B.K.** (1991). *Handbook of Tribology*, p.98-102, McGraw-Hill, Inc., New York, USA.

[44] **Kimura, H., Izumi, O**. (1985). *Titanium '80, Science and Technology*, p. 115-118, AIME Publication, Warrendale, USA.

[45] **Barsoum, M.W., Brodkin, D., El-Raghy, T.** (1997). Layered machinable ceramics for high temperature applications, *Scripta Materialia*. *36***,** 535-541.

[46] **Zabinski, J.S., Voevodin, A.A.** (1998). Recent development in the design, deposition and processing of hard coating, *Journal of Vacuum Science and Technology A, 16***,** 1890-1900.

[47] **Procopio, A.T., El-Raghy, T., Barsoum, M.W.** (2000). Synthesis of Ti4AlN3 and Phase Equilibria in the Ti-Al-N System, *Metallurgical and Materials Transactions A, 31***,** 373-378.

[48] **Armigliato, A.,Valdre, G.** (1987). Analytical electron microscopy of Al/TiN contact on silicon for application to very large scale integrated device, *Journal of Applied Physics, 61***,** 390-396.

[49] **Birkholz, M., & Genzel, C.** (2006). Residual Stress Analysis. In *Thin Film Analysis by X-Ray Scattering*, p. 239–295, Weinheim, FRG: Wiley-VCH Verlag GmbH & Co. KGaA.

[50] **Roquiny, F. Bodart, G. Terwagne**.(1999). Colour control of titanium nitride coatings produced by reactive magnetron sputtering at temperature less than 100°C, *Surface and Coatings Technology, 116-119,* 278-283.

[51] **Niyomsoan, S., Grant, W., Olson, D., & Mishra, B.** (2002). Variation of color in titanium and zirconium nitride decorative thin films. *Thin Solid Films*, *415*, 187–194.

[52] **McIntyre, D., Greene, J.E., Hakansson, G., Sundgren, J.E, Münz, W.D.** (1990). Oxidation of metastable single-phase polycrystalline $Ti_{0.5}Al_{0.5}N$ films – kinetics and mechanism, *Journal of Applied Physics*, **67**, 1542-1553.

[53] **Desmaison, J., Lefort, P., Billy, M.** (1979). Oxidation of titanium nitride in oxygen: Behavior of $TiN_{0.83}$ and $TiN_{0.79}$ plates, *Oxidation of Metals*. *13***,** 203-222.

[54] **Münz, W.D.** (1986). Titanium aluminum nitride films: A new alternative to TiN coatings, *Journal of Vacuum Science and Technology A*, **4**, 2712-2718.

[55] **Mayhofer, P.H., Music, D., Schneider, J.M.** (2006). Energetic balance and kinetics for the decomposition of supersaturated $Ti_{1-x}Al_xN$, *Acta Materialia, 55*, 1441-1446.

[56] **Chen, H-Y. and Lu, F-H., (2005).** Oxidation behaviorof titanium nitride films, *Vacuum science and Technology A, 23*, 1006-1010.

[57] **Ohnuma, H., Nihira, N., Mitsuo, A., Toyoda, K., Kubota, K., Aizawa, T.** (2004). Effect of aluminum concentration on friction and wear properties of titanium aluminum nitride films, *Surface and Coatings Technology*, **177-178,** 623-626.

[58] **Rovere, F., Music, D., Ershov, S., Baben, M., Fuss, H.G., Mayrhofer, P.H., Schneider, J.M.** (2010). Experimental and computational study on the

phase stability of Al-containing cubic transition metal nitrides, *Journal of Physics D: Applied Physics*, *43*, 1-11.

[59] **Adibi, F., Petrov, I., Greene J.E., Hultman, Sundgren, J.E.** (1993). Effects of high-flux low-energy (20-100 eV) ion irradiation during deposition on the microstructure and preferred orientation of Ti0.5Al0.5N alloys grown by ultra-high-vacuum reactive magnetron sputtering, *Journal of Applied Physic*s, *73*, 8580-8585.

[60] **Kutschej, P. H. Mayrhofer, M. Kathrein, P. Polcik, R. Tessadri, C. Mitterer.** (2005). Structure, mechanical and tribological properties of sputtered $Ti_{1-x}Al_xN$ coatings with $0.5 \leq x \leq 0.75$, S*urface & Coatings Technology*, *200***,** 2358-2365.

[61] **Porter, D.A., Easterling, K.E.** (1992). *Phase Transformations in Metals and Alloys, 2nd ed.*, p.105-136, Chapman & Hall, London, UK.

[62] **Chung Chuan, Lai.** Growth and Phase Stability of Titanium Aluminum Nitride Deposited by High Power Impulse Magnetron Sputtering, *Master Thesis*, Department of Physics, Chemistry and Biology, Linkoping University.

[63] **Bird, R.B., Stewart, W.E., Lightfoot, E.N**. (1977).*Transport Phenomena*, p. 204-217, John Wiley & sons, New York.

[64] **Berg, H.C.** (1977). *Random Walks in Biology*, p. 28-34, Princeton University Press, USA.

[65] **Nakai, M., Niinomi, M., Akahori, T., Ohtsu, N., Nishimura, H., Toda, H., Fukui, H., Ogawa, M.** (2008). Surface hardening of biomedical Ti–29Nb–13Ta–4.6Zr and Ti–6Al–4V ELI by gas nitriding, *Materials Science and Engineering A*, *486*, 193-201.

[66] **Lee, D.B., Pohrelyuk, I., Yaskiv, O., Lee, J.C.**(2012). Gas nitriding and subsequent oxidation of Ti-6Al- 4V alloys, Nanoscale Research Letter, **7**, 1-5.

[67] **Paransky, Y., Gotman, I., Gutmanas, E.Y.,**(2000). Reactive phase formation at AlN–Ti and AlN–TiAl interfaces, *Materials Science and Engineering A*, *277*, 83-94.

[68] **Mehrer, H.** (1990). *Diffusion in Solids Metals and Alloys*, p. 320-580, Springer-Verlag, Berlin.

[69] **Zhao, B., Sun, J., Sheng Wu, J., Xin Yuan, Z.** (2002). Gas nitriding behavior of TiAl based alloys in an ammonia atmosphere, *Scripta Materialia*, *46*, 581-586.

[70] **Wilson, S., Alpas, A.T.** (1989). TiN coating wear mechanisms in dry sliding contact against high speed steel, *Surface and Coatings Technology*, *108– 109*, 369-376.

APPENDICES

APPENDIX A : Recorded friction coefficient curves and 2-D profiles of the wear tracks of examined coatings.

APPENDIX A

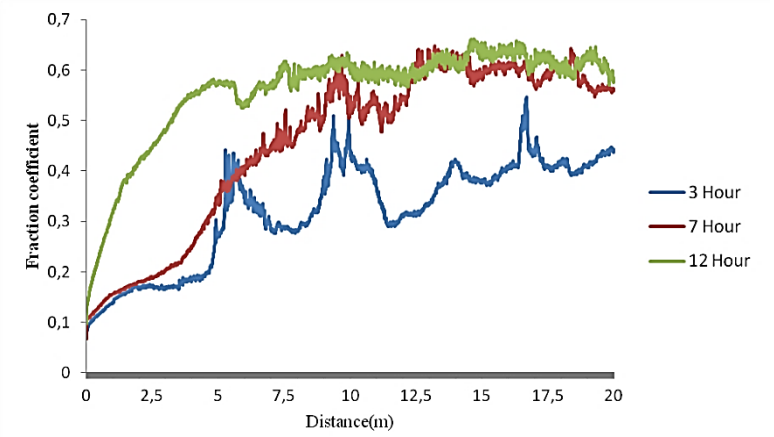

(a)

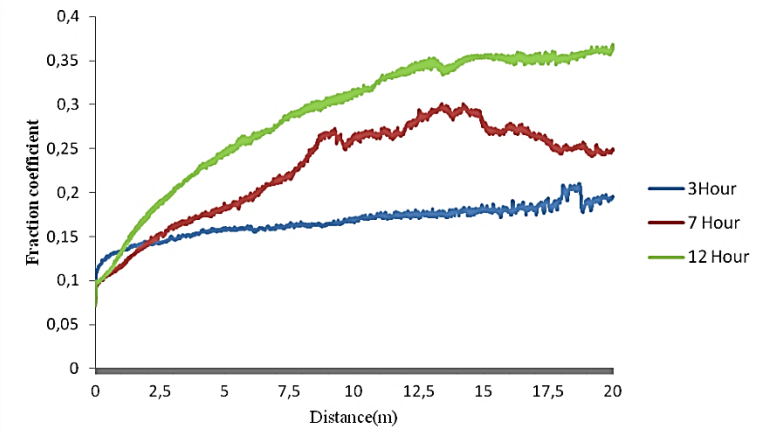

(b)

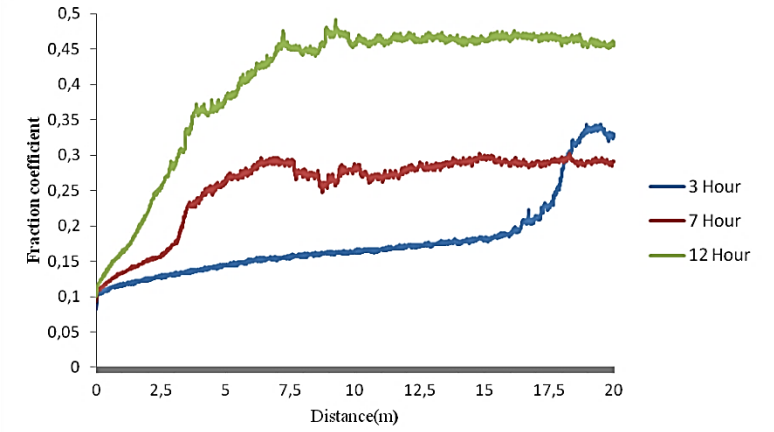

(c)

Figure A.1 : The friction curves of Cp-Titaniumsamples tested at a) 950 ºC, b) 1120 ºC and c) 1250 ºC.

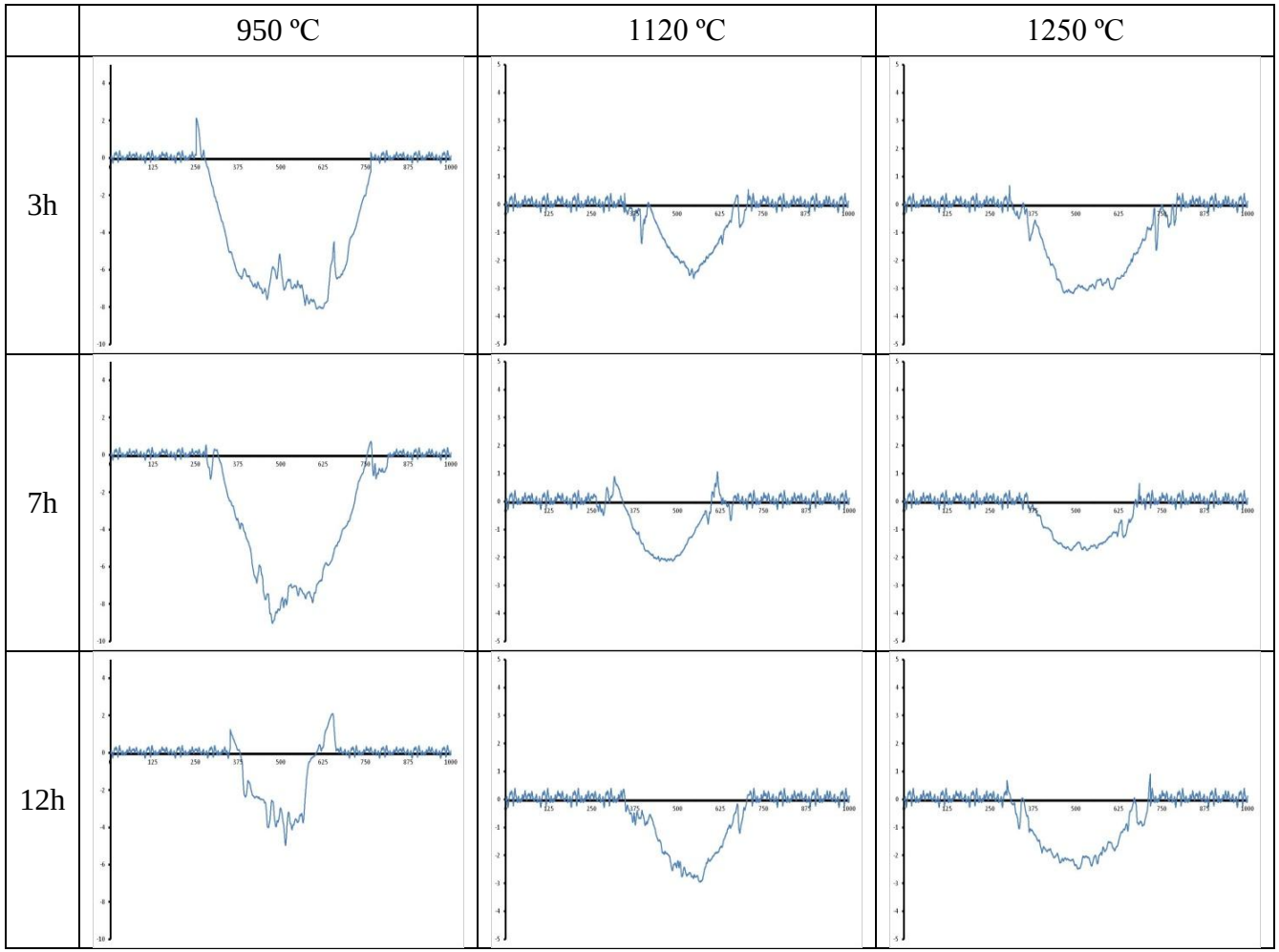

Figure A.2 : 2-D profiles of the wear tracks formed on the surfaces of the nitrided CP-titanium.

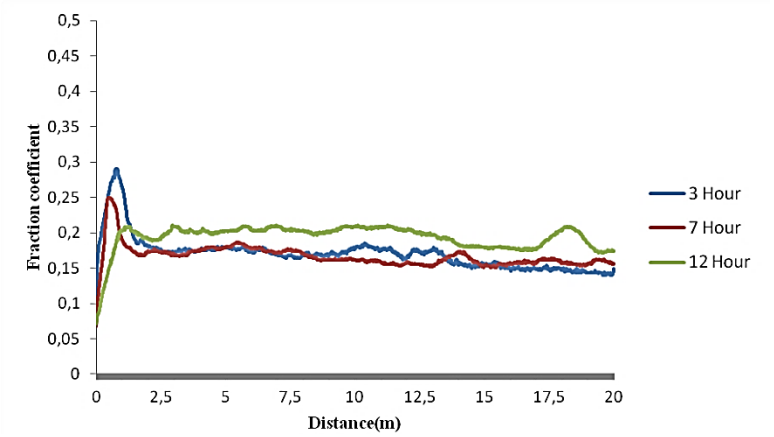

(a)

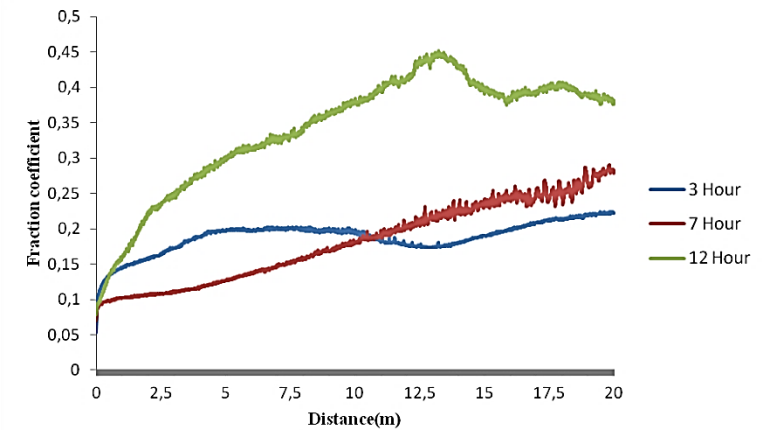

(b)

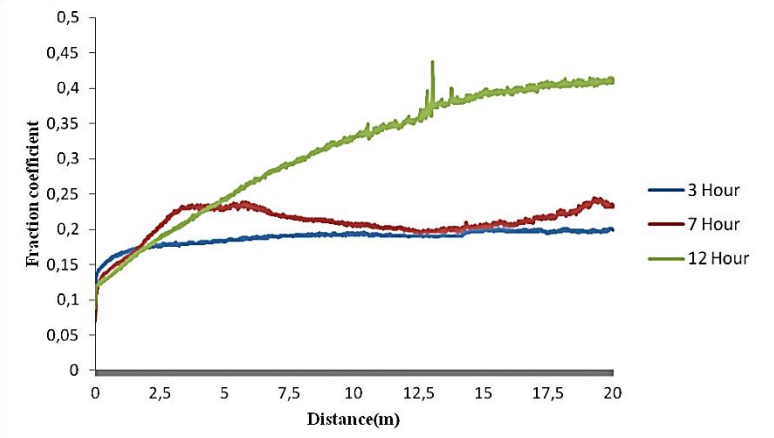

(c)

Figure A.3 : The friction curves of Ti6Al4V samples tested at a) 950 ºC, b) 1120 ºC and c) 1250 ºC.

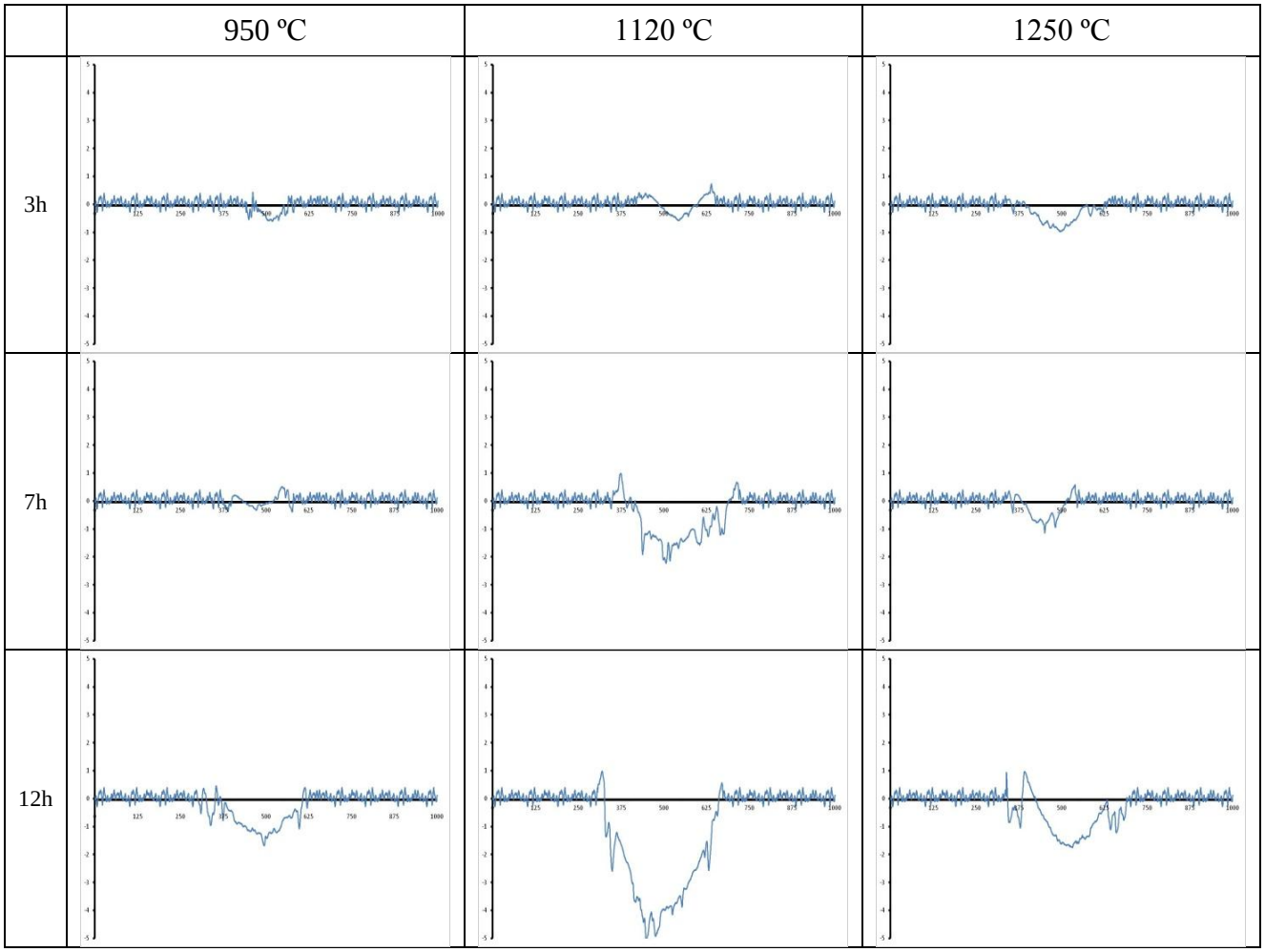

Figure A.4 : 2-D profiles of the wear tracks formed on the surfaces of the nitrided Ti6Al4V.

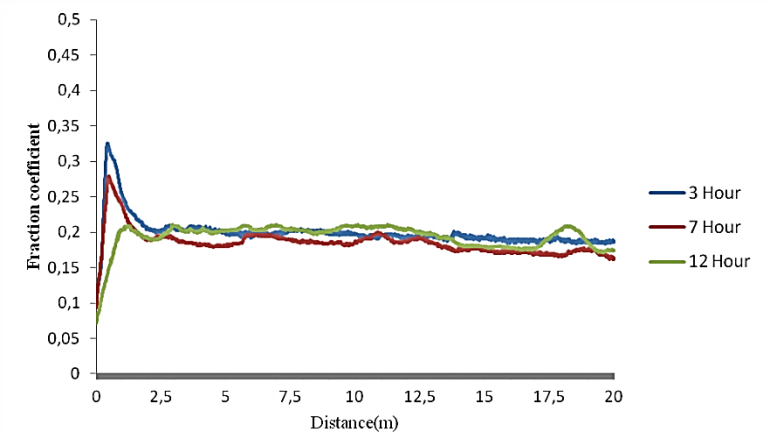

(a)

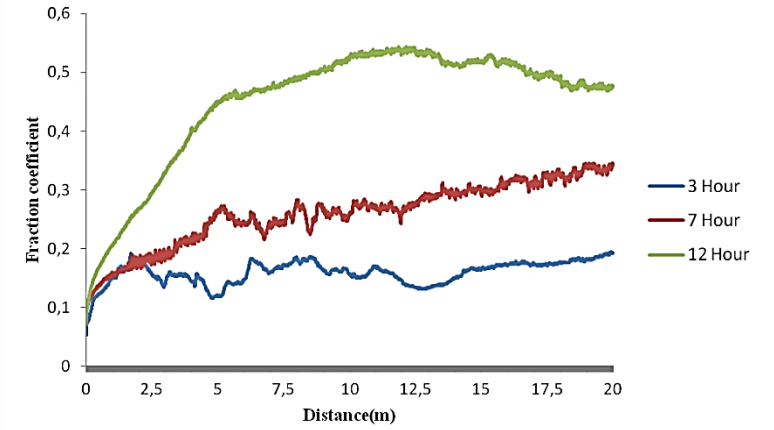

(b)

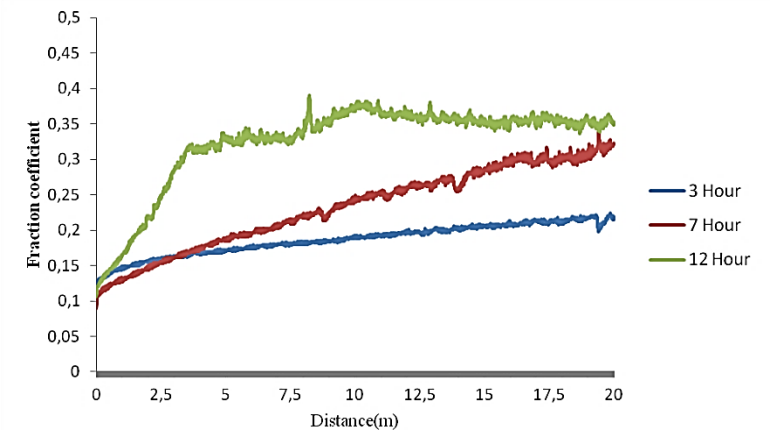

(c)

Figure A.5 : The friction curves of Ti6Al7Nb samples tested at a) 950 ºC, b) 1120 ºC and c) 1250 ºC.

	950 ºC	1120 ºC	1250 ºC
3h	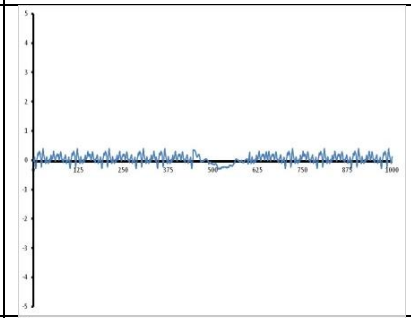	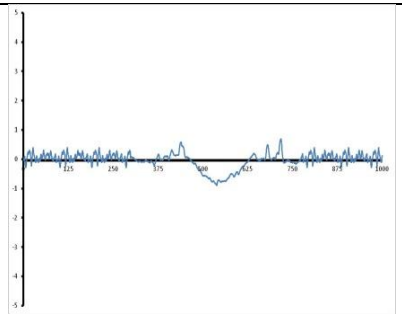	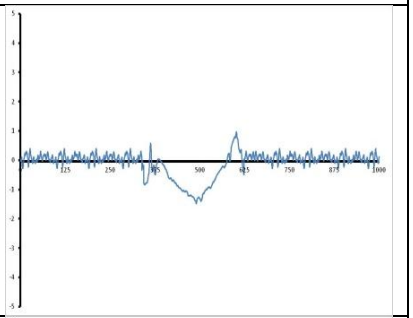
7h	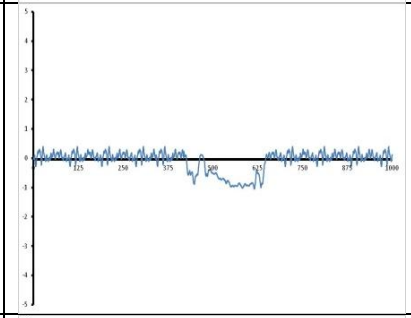	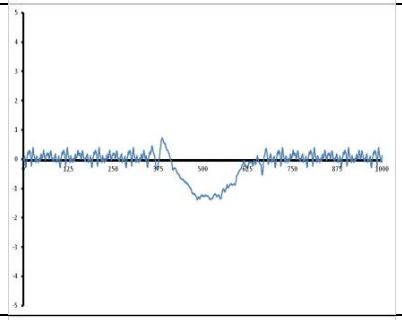	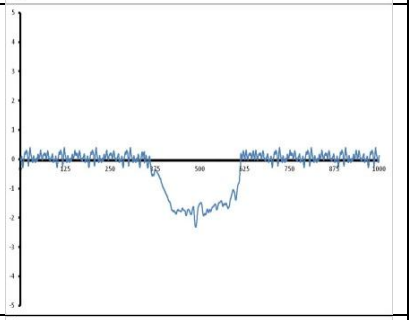
12h	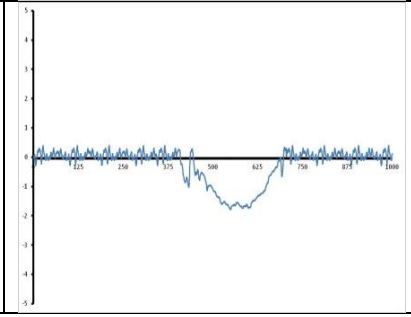	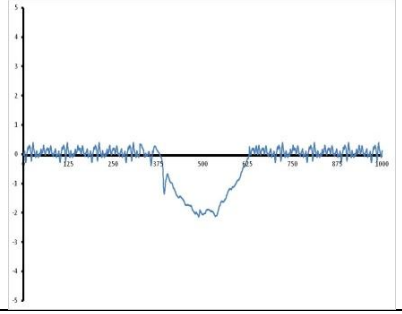	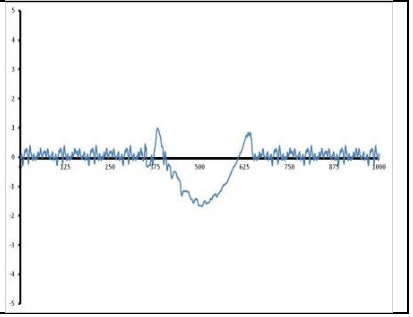

Figure A.6 : 2-D profiles of the wear tracks formed on the surfaces of the nitrided Ti6Al7Nb.

CURRICULUM VITAE

Name Surname: Farid Siyahjani

Place and Date of Birth: Tabriz, 25 August 1980

E-Mail: farid.siyahjani@yahoo.com

Address: Metallurgical and Materials Engineering Department
Chemical and Metallurgy Faculty
ITU Ayazaga Campus, Maslak 34469
Istanbul

B.Sc.: 1998-2002
Esfahan Azad University
Materials Science and Metallurgical Engineering

M.Sc.: 2003-2006
Science and Technology University of the Tehran
Materials Science and Metallurgical Engineering

PUBLICATIONS, PRESENTATIONS AND PATENTS ON THE THESIS:

Journal Articles (Covered by SCI)

- **Siyahjani, F.,** Atar, E. and Cimenoglu, H., (2015). Structural Changes Imposed by Gas Nitriding on The Surface of Ti6Al7Nb Alloy", *Metal Science and Heat Treatment*, Accepted Manuscript.

Journal Articles (Covered by other indices)

- Güleryüz, H., Atar, E., **Seahjani F.** and Çimenoğlu, H., (2015). An Overview On Surface Hardening of Titanium Alloys By Diffusion of Interstitial Atoms, *Diffusion Foundations,* Vol.4, 103-116.
- Ipekci, M., **Siyahjani, F.,** and Cimenoglu, H., (2013). Thermochemical Nitriding of Commercial Purity Titanium, *Defect and Diffusion Forum,* Vols. 334-335, 117-121.

- **Siyahjani, F.,** and Cimenoglu, H., (2012). Characteristics and Wear Performance of Nitrided Ti6Al4V, *Defect and Diffusion Forum,* Vols. 326-328, 494-497.
- **Siyahjani, F.,** and Cimenoglu, H., (2011). Nitriding of Cp Titanium, Defect *and Diffusion Forum,* Vols. 312-315, 1010-1014.